

FACIES TYPES AND DEPOSITIONAL ENVIRONMENTS OF A MORPHOLOGICALLY DIVERSE CARBONATE PLATFORM: A CASE STUDY FROM THE MUSCHELKALK (MIDDLE TRIASSIC) OF UPPER SILESIA, SOUTHERN POLAND

Michał MATYSIK

Institute of Geological Sciences, Jagiellonian University, Oleandry 2a, 30-063 Kraków, Poland

*Present address: Natural History Museum, University of Copenhagen, Øster Voldgade 5–7, DK-1350 Copenhagen K,
Denmark; e-mail: ma4tys@interia.pl*

Matysik, M., 2016. Facies types and depositional environments of a morphologically diverse carbonate platform: a case study from the Muschelkalk (Middle Triassic) of Upper Silesia, southern Poland. *Annales Societatis Geologorum Poloniae*, 86: 119–164.

Abstract: The detailed sedimentological study of the 150-m-thick Muschelkalk succession, deposited on a small (~200 by 80 km), morphologically diverse Upper Silesian carbonate platform during four major marine-transgressive pulses of the Tethys Ocean, enhanced the understanding of the depositional history, palaeogeography, and facies distribution. A total of thirty-five lithofacies types were identified, described and interpreted in terms of depositional settings. These different lithofacies represent various shallow-marine environments along the platform transect, from peritidal to offshore areas. The vertical and lateral organization of the lithofacies delineated was caused by the interplay of platform morphology, third-order eustasy and the long-term tectonic evolution of the area. Accordingly, the carbonate system studied is a good example of the influence of large-scale processes on the facies architecture of carbonate platforms. In general, all of the four Transgressive Systems Tracts are characterized by similarity in lithofacies composition and vertical succession and by minor lateral change, indicating only limited influence of the three large-scale factors mentioned on lithofacies development and distribution during transgressions. In contrast, each of the four associated Highstand Systems Tracts comprises an individual (unique) lithofacies assemblage displaying substantial regional and local variation, which indicates that the filling of accommodation space during highstands strongly depended on the extrinsic processes.

Key words: Lithofacies assemblage; depositional sequence; sabkha-tidal flat-lagoon environment; shoreface-offshore environment; Central Europe.

Manuscript received 18 November 2014, accepted 4 June 2016

INTRODUCTION

The Upper Silesia region in southern Poland is one of several places in Europe, where the Middle Triassic marine deposits, termed Muschelkalk, are well-exposed over a wide area. The region is widely regarded as the most distal and open-marine part of the homoclinal carbonate-siliciclastic ramp that encompassed the entire Germanic (European) Basin in Middle Triassic time (e.g., Aigner, 1985; Aigner and Bachmann, 1992; Knaust, 1997; Götz, 2004; Götz and Lenhardt, 2011). However, in fact, the Upper Silesia region formed a submarine threshold, separating the Germanic Basin from the Tethys Ocean (Szulc, 2000). The region itself sloped westward and was bounded to the west and east by Variscan Massifs. Because of this palaeogeographic and palaeotopographic setting, the region should be considered as an independent, attached platform, character-

ized by a distinctive assemblage of lithofacies and depositional environments.

Although sedimentological investigations of the Upper Silesian Muschelkalk carbonates already were initiated in the second half of the 19th century (Eck, 1865), up to now no author has described the lithofacies types and discussed in detail their distribution and depositional setting. The majority of studies were focused either on the lithostratigraphical classification of Muschelkalk deposits (e.g., Assmann, 1913, 1944; Siedlecki, 1948, 1952; Śliwiński, 1961; Pawłowska, 1979; Bodzioch, 1997b; Niedźwiedzki, 2000; Kowal-Linka, 2008, 2009), or some specific sedimentological aspect, such as the development of crumpled limestone fabric (Bogacz *et al.*, 1968; Bodzioch, 1985), the origins of intraformational conglomerates (Chudzikiewicz,

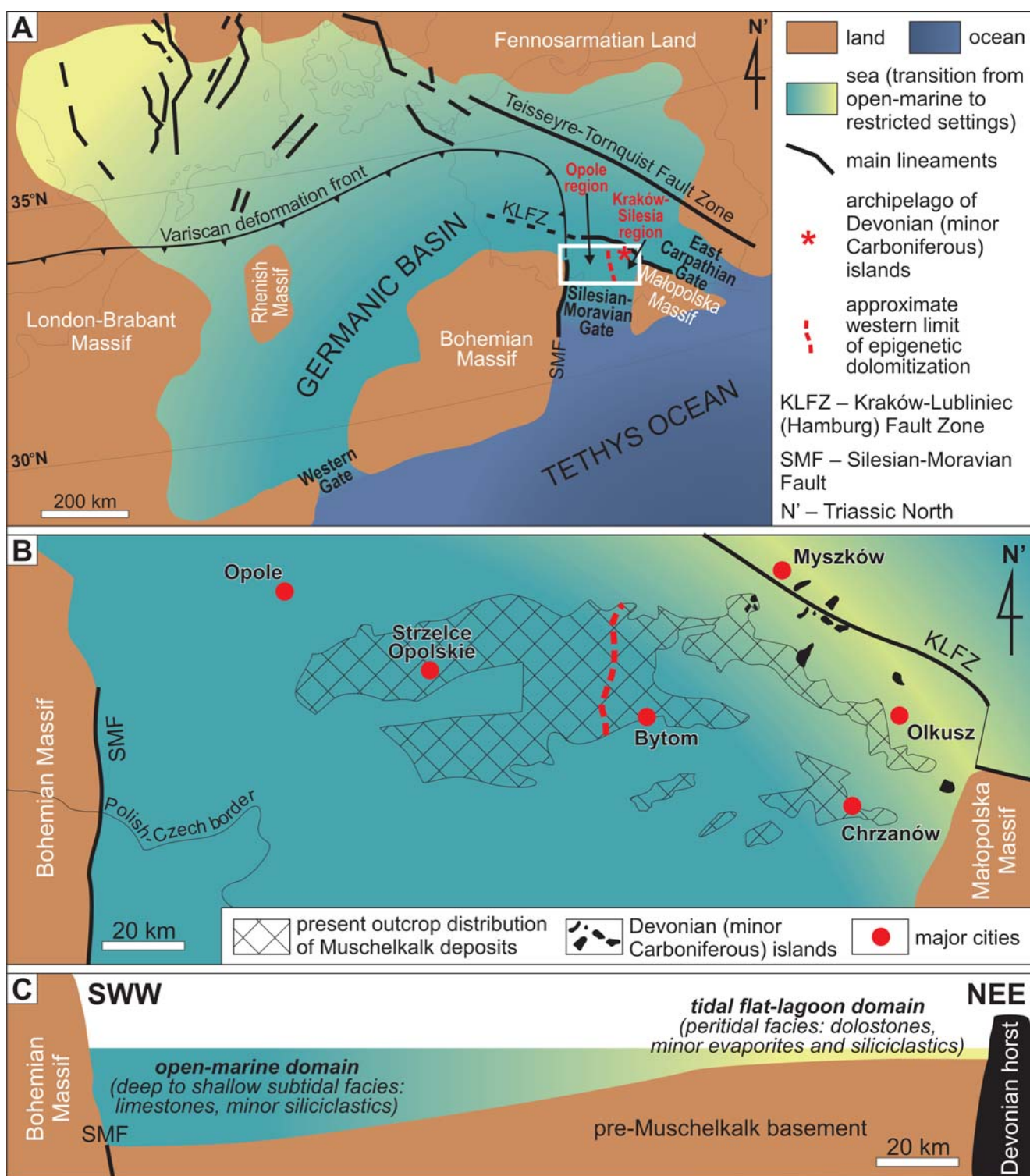


Fig. 1. Palaeogeographic setting of the Upper Silesia region in the Middle Triassic. **A.** Position of the Upper Silesia region (white rectangle) within the Germanic Basin. The three gates that connected the Germanic Basin with the Tethys Ocean were active at different times. The Silesian-Moravian Gate was generally open throughout the entire Anisian–Ladinian time span, but it began to close already in the Illyrian. Map modified from Szulc (2000) and Narkiewicz and Szulc (2004). **B.** Palaeogeographic reconstruction of the northern outlet of the Silesian-Moravian Gate, framed to the west by the Bohemian Massif and to the east by the Małopolska Massif and an archipelago of Palaeozoic islands – the location of islands is taken from Wyczółkowski (1971, 1982). The Muschelkalk deposits are eroded to the south and covered by the Jurassic and Cretaceous strata to the north and west. **C.** Regional schematic cross-section of the Upper Silesian carbonate platform, showing the transition from the restricted-marine to the open-marine domain.

1975) and brachiopod shell accumulations (Dżułyński and Kubicz, 1975; Bodzioch, 1985), and the environmental controls on sponge-coral bioherms and biostromes (Bodzioch, 1989; Szulc, 2000; Matysik, 2010; Morycowa and Szulc, 2010). A general characterization of the basic lithofacies types of selected lithostratigraphic units was given by Chudzikiewicz (1982), Pawłowska (1985) and Myszkowska (1992). Recently, Matysik (2014) provided an extensive discussion of the lithofacies architecture of the epigenetically dolomitized Muschelkalk strata.

This paper presents a detailed (bed-by-bed) sedimentological analysis of the Muschelkalk formations exposed in all existing outcrops. The main objective of this paper is to reconstruct the variety and distribution of lithofacies and depositional environments over the Upper Silesian carbonate platform in the Middle Triassic and to discuss the influence of third-order eustasy, platform morphology and the long-term tectonic evolution of the area on their distribution.

GEOLOGICAL SETTING

Palaeogeography

In Middle Triassic time, the Germanic Basin or northern Peri-Tethys area was situated at subtropical latitudes (Ziegler, 1990; Nawrocki and Szulc, 2000). The overall hot and arid climate favoured carbonate and evaporitic sedimentation. The basin was generally enclosed by several extensive massifs consolidated in the Precambrian, Caledonian and Variscan orogeneses, whereas communication with the Tethys Ocean was provided by three narrow, submeridional, fault-controlled depressions, known as the East Carpathian Gate, the Silesian-Moravian Gate and the Western (Burgundy) Gate (Fig. 1A). This semi-closed configuration determined the specific distribution of palaeoenvironments and facies throughout the Germanic Basin; normal-marine settings, dominating near the gates were gradually replaced by more restricted environments toward the basin margins (Szulc, 2000). The three gates opened and closed diachronically because of the westward relocation of the Tethys spreading centre. Consequently, the main communication pathways between the Tethys and the Germanic Basin in the Anisian led through the Silesian-Moravian and East Carpathian gates, while the situation was reversed in the Ladinian when the Western (Burgundy) Gate became active (Szulc, 2000). The Upper Silesia region was located at the northern mouth of the Silesian-Moravian Gate where it formed a distinct elevated element of submarine topography, stretching between the Bohemian Massif to the west and the Małopolska Massif to the east (Szulc, 2000; Fig. 1B).

The morphology of the Upper Silesia threshold was differentiated, both on regional and local scales, and it basically reflected the Variscan structural framework (Wyczółkowski, 1971, 1982) and syndepositional tectonic block movements (Szulc, 1989, 1993, 2000; Matysik, 2012). The area generally dipped to the west which resulted in a gradient of depositional environments along an E–W transect (Fig. 1C). As a consequence, its western part (the Opole region) was dominated by subtidal facies even during high-

stands (Szulc, 2000), whereas its eastern part (the Kraków–Silesia region) temporarily entered into the inter- and supratidal zone (Pawłowska and Szuwarzyński, 1979; Pawłowska, 1982, 1985; Myszkowska, 1992; Matysik, 2014). Local highs and lows modified this simple facies pattern, producing a complex facies mosaic over the entire region (Wyczółkowski, 1971, 1982; Myszkowska, 1992; Matysik, 2012, 2014). Moreover, the northeastern part of the region was attached to an archipelago of several isolated cliff-edged islands, mainly composed of Middle Devonian dolostones (with minor Lower Carboniferous limestones and dolostones; Fig. 1A, B). The island geometry and the distance to neighbouring islands controlled the water circulation pattern within the archipelago which in turn strongly influenced the local facies distribution (Matysik, 2012, 2014). In addition, intensive erosion of the cliff walls generated a large number of silt- to boulder-sized rock fragments, most of which were deposited up to 50 m from the island margins (Alexandrowicz, 1971; Wyczółkowski, 1971, 1982; Matysik, 2012; Matysik and Surmik, 2016).

Stratigraphy

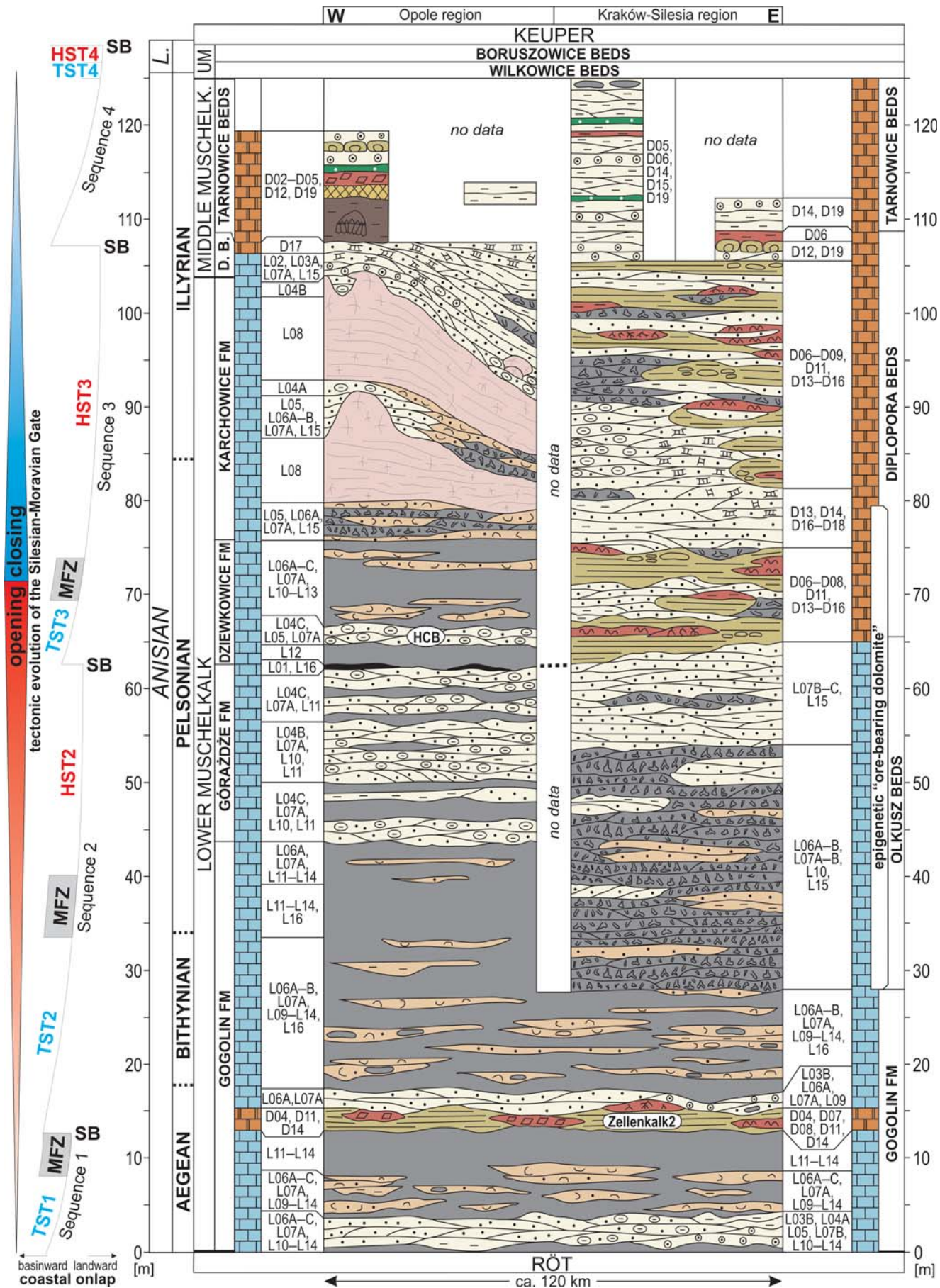
The Muschelkalk succession of the Upper Silesia, 150 m thick, displays marked vertical and lateral lithofacies variation (Fig. 2) which basically reflects: 1) a long-term tectonic evolution (opening-closing trend) of the Silesian-Moravian Gate, controlling the subsidence of the entire platform; 2) third-order transgressive-regressive eustatic pulses; and 3) differentiated antecedent topography (Wyczółkowski, 1971, 1982; Szulc, 2000; Matysik, 2012, 2014). On the basis of this variation, the succession is divided into nine lithostratigraphic formations (Assmann, 1944; Śliwiński, 1961) that together represent four depositional sequences (Szulc, 2000; Matysik, 2012, 2014). A combination of sequence boundaries, systems tracts and several marker beds permits accurate and reliable correlation within the succession (Fig. 2).

It is noteworthy that the Lower–Middle Muschelkalk deposits of the eastern Upper Silesia were replaced epigenetically by “ore-bearing dolomite” (Fig. 2). This dolomite is commonly, but mistakenly treated as a lithostratigraphic unit (see Matysik, 2014, and references cited therein).

The sequence stratigraphic framework discussed correlates well with the more universal scheme of Alpine stratigraphy by means of magnetostratigraphy (Nawrocki and Szulc, 2000) as well as conodont, ammonoid and crinoid biostratigraphy (Assmann, 1944; Zawidzka, 1975; Haggorn and Głuchowski, 1993; Kaim and Niedźwiedzki, 1999; Narkiewicz and Szulc, 2004). For the Middle Muschelkalk, devoid of these index-fossils, green algal zonation has been proposed by Kotański (1994, 2013).

MATERIALS AND METHODS

Fieldwork was carried out in 83 quarries, scattered over an area of 150 by 50 km. Each section was sampled and logged bed by bed, giving a total measured stratigraphic thickness of approximately 2.3 km. For the poorly exposed formations of the upper Muschelkalk succession (Tarno-



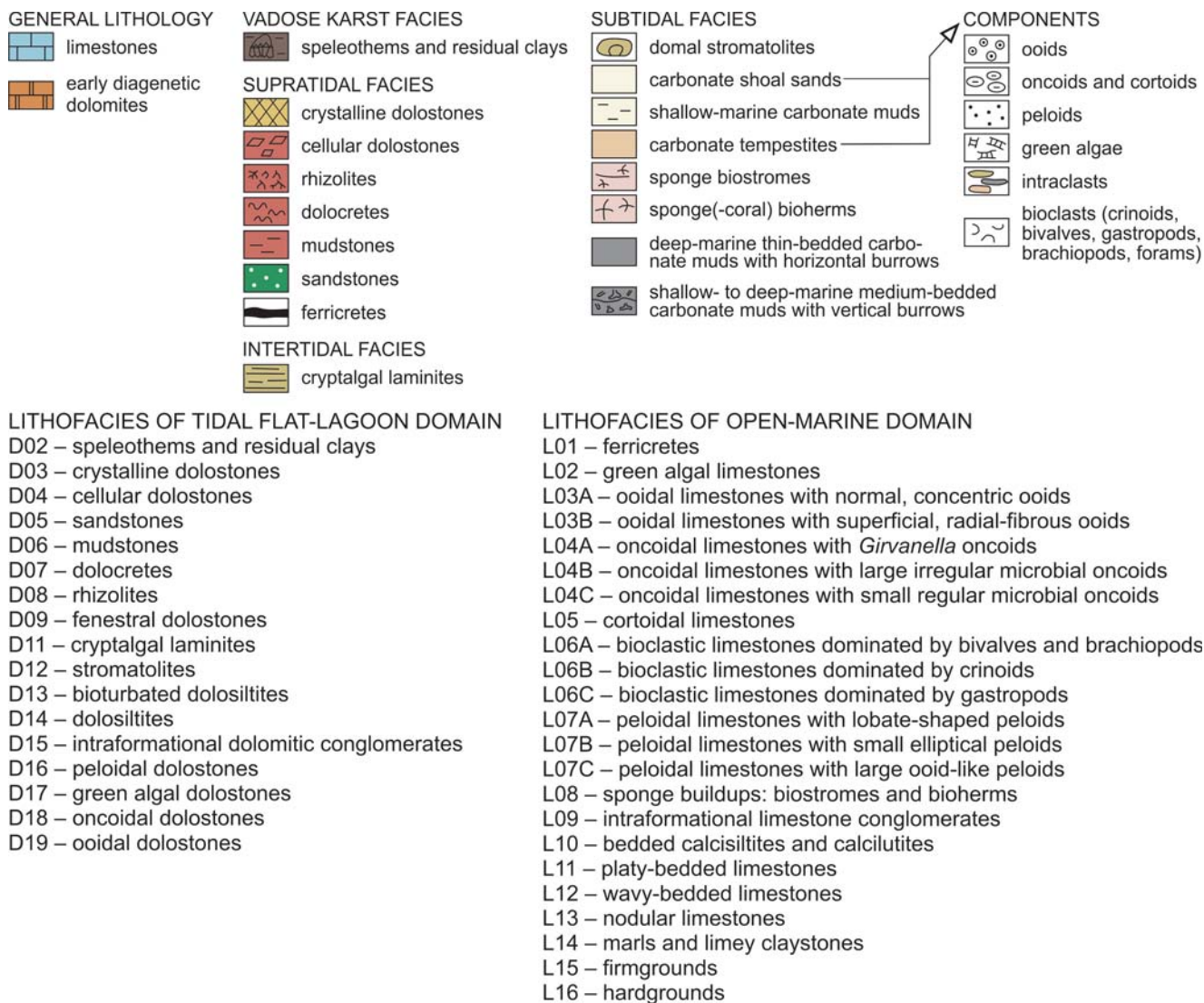


Fig. 2. Generalized stratigraphic section for the Muschelkalk of the Opole region and the Kraków–Silesia region, showing thickness, overall lithological character, provisional formation names, range of epigenetic dolomitization, and distribution of lithofacies types distinguished. The transition between the eastern Kraków–Silesia region and the western Opole region is not studied because of the lack of outcrops. Two marked correlation horizons are depicted: Hauptcrinoidenbank (HCB) and Zellenkalk2. L. – Ladinian; UM – Upper Muschelkalk; D. B. – Diplopora Beds; TST – Transgressive Systems Tract; HST – Highstand Systems Tract; MFZ – Maximum Flooding Zone; SB – Sequence Boundary. Scheme modified from Matysik (2014), sequence stratigraphy framework after Szulc (2000) supplemented by Matysik (2014), lithostratigraphy after Assmann (1913, 1944) and Siedlecki (1948, 1952) with later changes and formalization by Śliwiński (1961), Myszkowska (1992), Bodzioch (1997b), Niedźwiedzki (2000), Szulc (2000), Kowal-Linka (2008) and Matysik (2014).

wice, Wilkowice and Boruszowice beds), loose hand specimens collected from meadows and private properties were examined. All of the 2,600 samples collected were slabbed and investigated with a hand lens. A petrographic microscope was used for the microfacies analysis of 900 thin sections.

A major obstacle to be overcome in this study was the advanced secondary dolomitization which obliterated some original rock properties of the lower and middle Muschelkalk deposits of the Kraków–Silesia region (Fig. 2). Typically, the microtexture had undergone extensive to complete recrystallization, whereas the macrofabric, grain size and sedimentary structures remained unaltered; this was adequate for reconstruction of the depositional history of this so-called “Ore-Bearing Dolomite”.

The lithofacies types were defined on the basis of the macrotextural properties, while microscopic observations were used only for more detailed characterization of the macrofabric. This procedure permitted the creation of a consistent and clear classification of all the material examined (both epigenetically dolomitized and undolomitized). The textures and features produced by the epigenetic dolomitization were not included in this classification. This means that the epigenetically dolomitized lithologies were classified, as if the dolomitization never had taken place.

The allochthonous carbonates were described according to the Dunham's (1962) classification, expanded by Embry and Klovan (1971) and Wright (1992), whereas the microbial carbonates were classified according to the Grey's

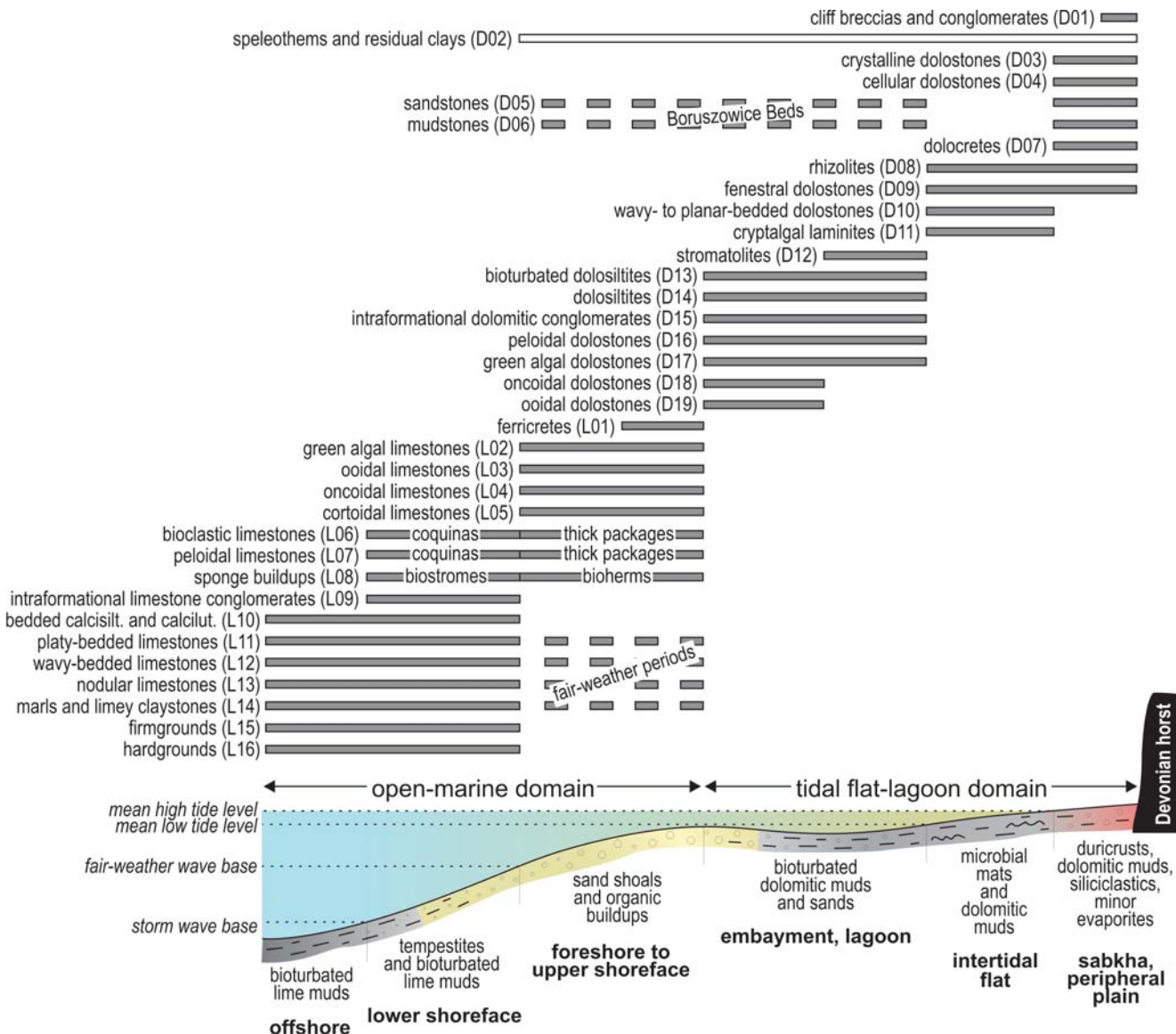


Fig. 3. Distribution of lithofacies and depositional environments along a generalized transect across the Upper Silesian carbonate platform. Speleothems and residual clays (D02) developed within caves and cavities formed as a result of meteoric dissolution of various lithofacies.

(1989) handbook. Many descriptive terms used in this paper follow the usage by Flügel (2010).

LITHOFACIES TYPES AND THEIR DEPOSITIONAL SETTING

The Muschelkalk succession of Upper Silesia is predominantly composed of limestones and early diagenetic dolostones (Fig. 2), which basically represent an open-marine domain and a tidal flat-lagoon (restricted) domain, respectively. Evaporites or evaporite vestiges are extremely rare and always are associated with particular dolomitic lithofacies. Siliciclastics usually are intercalated in the various carbonate deposits, with the exception of the siliciclastics-dominated Boruszowice Beds. As the evaporitic and siliciclastic lithofacies are generally uncommon in the Muschelkalk investigated, they were included in the dolo-

stone and limestone category, depending on whether they had been formed within the dolostone or limestone marine domain. In the dolostone domain, nineteen lithofacies types (D01–D19) were delineated, in the limestone domain sixteen types (L01–L16). They are listed below generally from the shallowest (proximal) setting to the deepest (distal). The lateral and vertical relationships between these lithofacies are shown in a diagrammatic platform cross-section (Fig. 3), two schematic, three-dimensional reconstructions of the depositional system (Fig. 4), and two generalized lithostratigraphic columns (Figs 5, 6). The main characteristics of these lithofacies are summarized in Tables 1 and 2.

Cliff breccias and conglomerates (D01)

Characteristics

The cliff breccias (sporadically conglomerates) are composed of lithoclasts of black Devonian (Givetian) dolo-

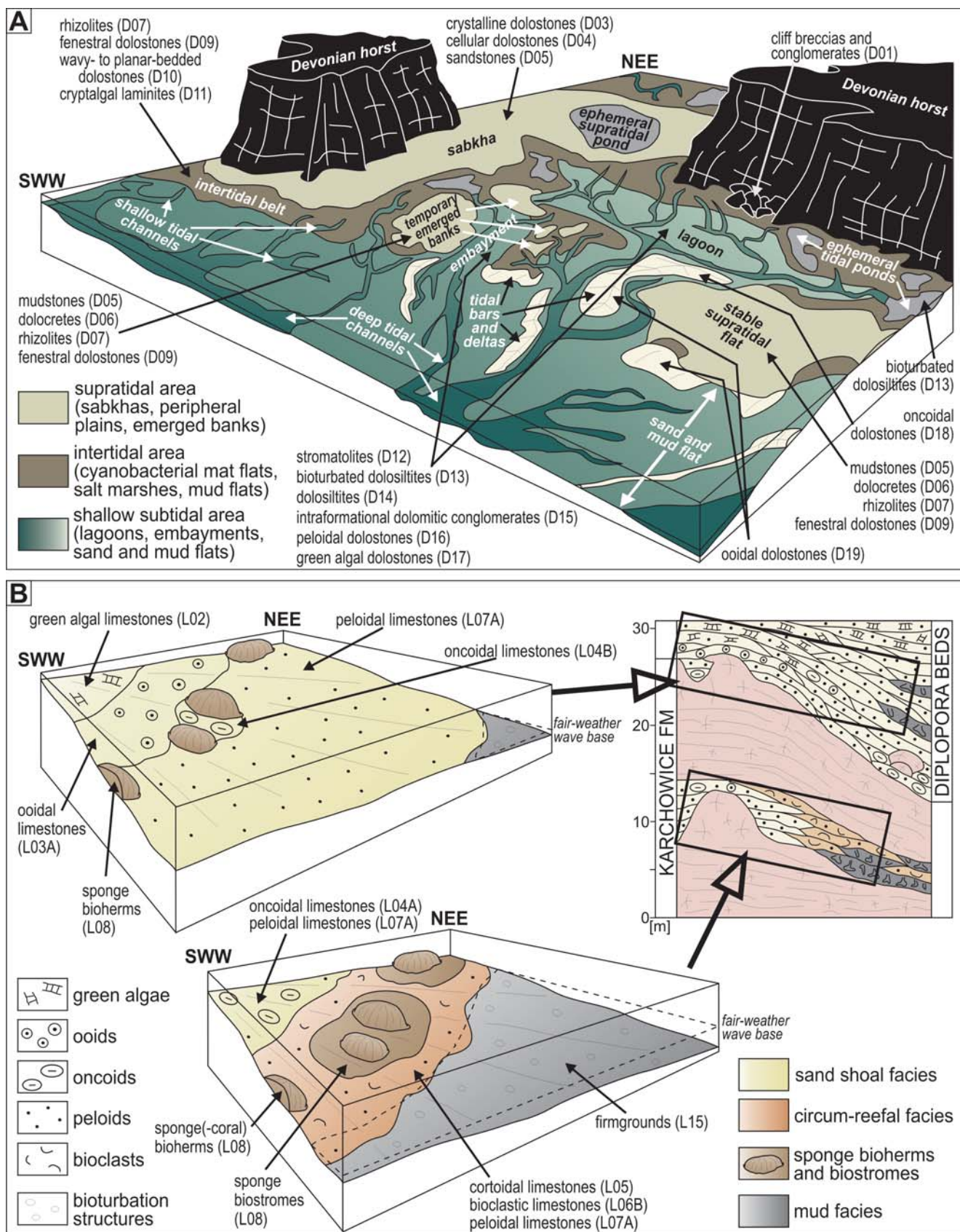


Fig. 4. Hypothetical three-dimensional reconstruction of the tidal flat-lagoon system attached to the Devonian islands (A) and of the reefal complex (B).

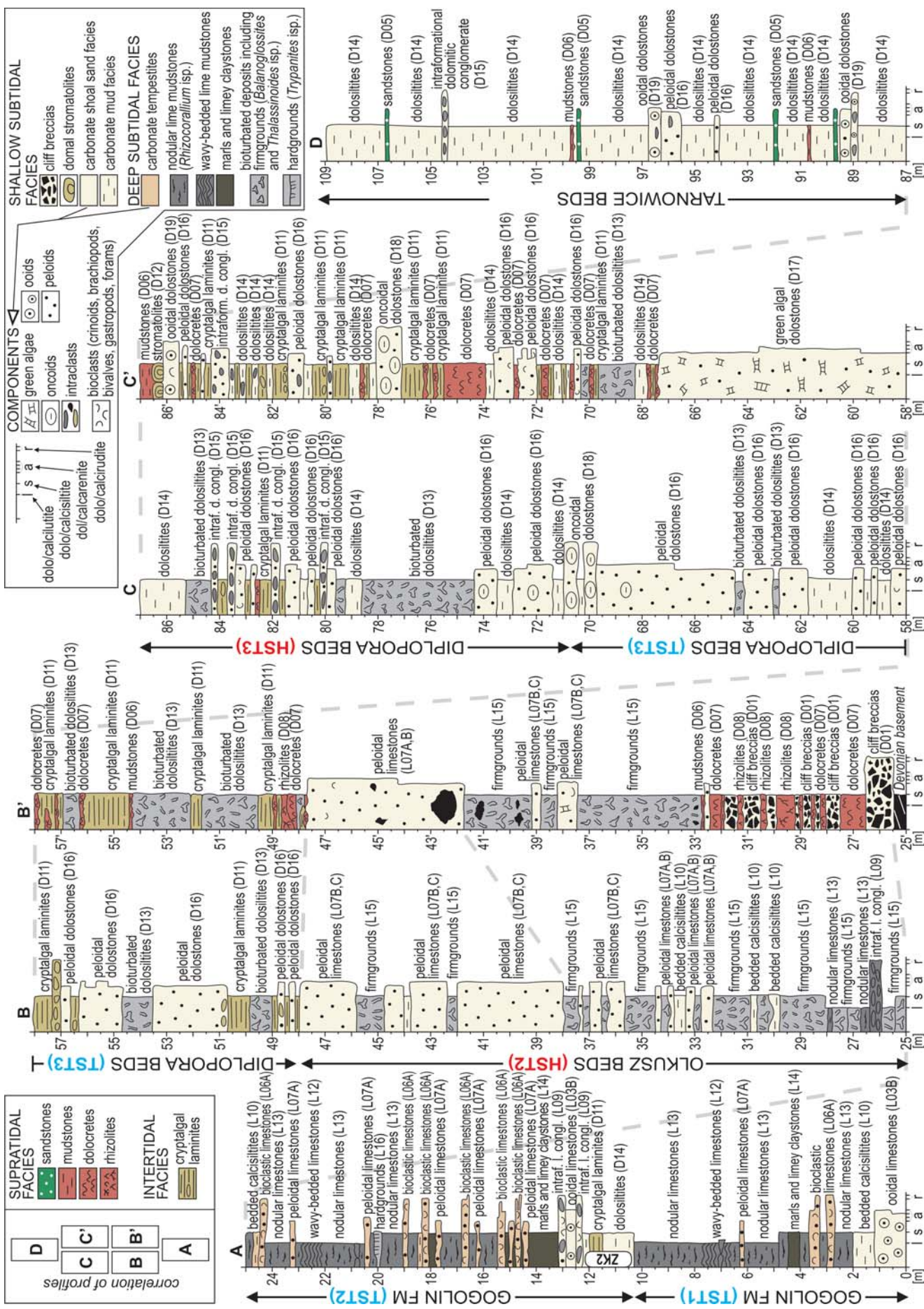


Fig. 5. Complete lithostratigraphic columns for the Lower and Middle Muschelkalk of the Kraków-Silesia region compiled from several most representative sections. Note that between the 25th and 87th m, the column splits into two laterally equivalent profiles; profile with thickness given with an apostrophe (e.g., 25', 26', 27' etc.) shows Muschelkalk succession within the archipelago of Devonian islands, and profile with thickness given without an apostrophe (e.g., 25, 26, 27 etc.) represents the area off the archipelago. 0–25 m – Plaza Quarry, 25–64 m – Żelatowa Quarry, 64–87 m – Pomorzany Zn-Pb mine, 25'–47.5' m – Stare Gliny Quarry, 47.5'–67.5' m – GZD Quarry, 67.5'–87' m – Libiąż Quarry, 87–109 m – Blachówka Quarry. Letters (A, B, B', C, C', D, D' and E) clarify the correlation of logs. Abbreviations: ZK2 – Zellenkalk2 (correlation horizon); TST – Transgressive Systems Tract; HST – Highstand Systems Tract; LST – Lowstand Systems Tract; intraf. d. congл. – intraformational dolomitic conglomerates; intraf. l. congл. – intraformational limestone conglomerates.

stones, cemented in a Middle Triassic matrix (Fig. 7). Although the overall size of lithoclasts gradually increases towards an island margin, all breccias and conglomerates are very poorly sorted and contain mixed millimetre- to centimetre-sized, randomly oriented lithoclasts (Fig. 7B). The breccias deposited at the foot of steep cliffs comprise additionally decimetre- to metre-sized boulders.

The matrix is predominantly composed of: 1) yellow dolosiltites (Fig. 7C, D); 2) bioclastic wackestones- packstones (Fig. 7E); or 3) green dolosiltites, containing lithoclasts and peloids made up of dense aphanitic or clotted-micropeloidal automicrite (Fig. 7F). Sporadically, the Devonian lithoclasts are cemented by gypsum/anhydrite (Fig. 7G).

The cliff breccias and conglomerates intertongue with other lithofacies of the Olkusz and Diplopora beds (Figs 4A, 5). They form either separate, large (metre-thick and decametre-long), pinching-out bodies, attached to the island margins (Fig. 7A), or pass laterally within one bed into other lithofacies, listed below. Single surrounded centimetre-sized lithoclasts are found in the strata situated hundreds of metres away from the island margins. One such lithoclast was found in deposits 7 km distant from the closest known Devonian island. Extremely rarely, metre-sized boulders occur 200 m from the island margin.

Environment

Various types of matrix indicate that the lithoclasts were deposited in marine or continental settings, depending on island morphology and sea-level position. The transport of rock fragments was generally short or almost absent, as evidenced by very poor sorting and rounding of lithoclasts.

Speleothems and residual clays (D02)

Characteristics

The speleothems are bulbous in shape (Fig. 8A) and typically display a thickly laminated mesotexture, composed of palisade calcite crystals with characteristic triangle tips (Fig. 8B). However, locally centimetre-sized dripstone cements are also present (Fig. 8C). The

speleothems are enveloped in red-tan residual clays (Fig. 8A). Both speleothems and clays occur in the Tarnowice Beds of the Opole region (Figs 2, 6).

Environment

The speleothems unequivocally were precipitated in cavities and small caves, created owing to the meteoric dissolution of the carbonates and evaporites of the Tarnowice Beds, while the clays are interpreted as being a residuum after the removal of evaporitic-carbonate material. The general environmental context strongly indicates that the sub-aerial weathering was related to a third-order sea-level drop at the end of the Anisian (sequence 3; Fig. 2).

Crystalline dolostones (D03)

Characteristics

Equidimensional rhombohedral or anhedral dolomite crystals reach up to 1 cm in size and overgrow each other in various directions (Fig. 8D, E). The crystals are commonly distributed throughout a layer without any pattern. Nevertheless, locally the parallel or small-scale cross-lamination of a precursor deposit is preserved. The crystalline dolostones were found to occur solely in the Tarnowice Beds of the Opole region (Figs 2, 5).

Environment

Locally preserved lamination implies that the crystals are replacive. The formation of crystalline dolomitic fabric required large quantities of magnesium-rich brine, which might have been released during evaporite diagenesis (Warren, 1991). The replacement might have taken place during early diagenesis, in which case the crystalline dolostones might represent a sabkha (Figs 3, 4A).

Cellular dolostones (= Rauchwacke; D04)

Characteristics

These are yellow-orange dololutites and dolosiltites, comprising numerous centimetre-sized cavities (Fig. 8F), millimetre-sized calcite/dolomite pseudomorphs after sulphates and halite (Fig. 8G, H), and sporadic silt-sized quartz grains. Some dolostones underwent dedolomitization. The cellular dolostones occur in the Zellenkalk2 of the Gogolin Formation as well as in the Tarnowice Beds of the Opole region (Figs 2, 5, 6), where they locally contain selenite crystals that are vertically upright, up to 30 cm high (Worobiec and Szulc, 2012).

Environment

The characteristic fabric might have been formed owing to the leaching of evaporitic minerals, transformation of calcite to dolomite (e.g., Chilingar and Terry, 1964) and/or dedolomitization (e.g., Evamy, 1967). This deposit may represent a sabkha environment (Figs 3, 4A), as indicated by the association of evaporites, dolomitic mud and siliciclastic material (Warren, 2006). Similar fabrics, but of Early Triassic age, have been interpreted by Bodzioch and Kwiatkowski (1992) as the deposits of ephemeral ponds on supratidal plains, occasionally filled with sea water. However, in

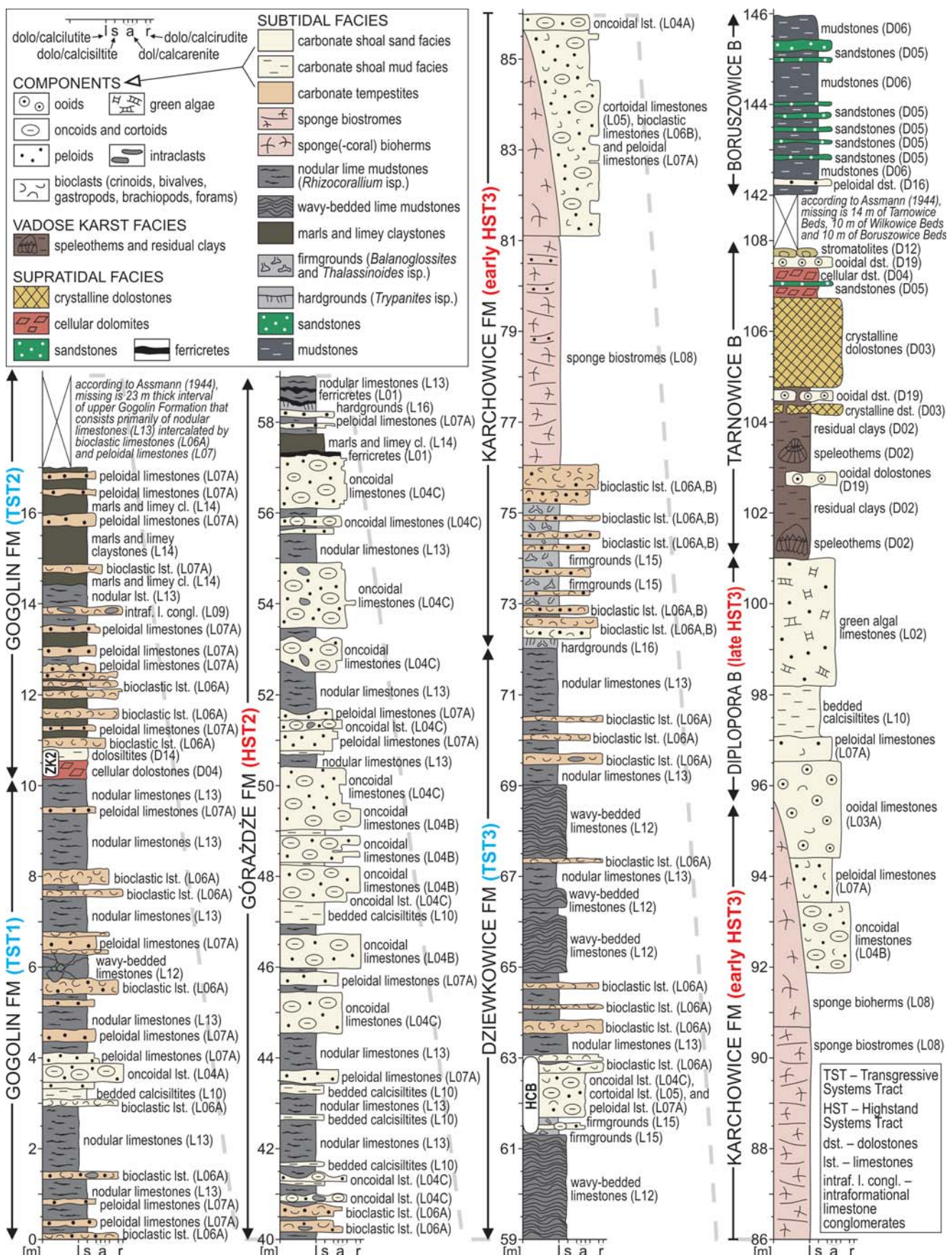


Fig. 6. Almost complete lithostratigraphic column for the Muschelkalk of the Opole region compiled from five most representative sections. 0–17 m – Mikołów Quarry, 40–72 m – Strzelce Opolskie Quarry, 72–86 m – Tarnów Opolski Quarry, 86–108 m – Kamień Śląski Quarry, 142–146 m – Laryszów clay pit. Correlation horizons: ZK2 – Zellenkalk2, HCB – Hauptcrinoidenbank.

Table 1

Summary of principal characteristics of dolomitic lithofacies and their environmental interpretation

Lithofacies type	Lithological characteristics	Environment/process
Cliff breccias and conglomerates (D01)	Lithoclasts of black Devonian dolostones cemented in a Middle Triassic dolosiltite matrix (minor sulphates); clasts randomly oriented, mostly angular, and very poorly sorted.	Marine or continental settings at the foot of Palaeozoic islands.
Speleothems and residual clays (D02)	Bulbous, thickly laminated forms composed of palisade calcite; local dripstone cements; occur within reddish residual clay.	Dissolution cavities.
Crystalline dolostones (D03)	Overgrown, equidimensional, rhombohedral or anhedral dolomite crystals up to 1 cm in size; parallel or cross-lamination of a precursor deposit locally preserved.	Early dolomitization in a sabkha due to influx of Mg-rich brines.
Cellular dolostones (= Rauchwacke) (D04)	Fine-grained dolostones with numerous centimetre-sized cavities; common carbonate pseudomorphs after sulphates and halite; locally selenite crystals and admixed quartz grains; dedolomitization present.	Diagenetic changes within evaporite-bearing carbonates in a sabkha.
Sandstones (D05)	Subrounded quartz grains (0.01–0.20 mm across) embedded in micrite, microspar or poikilotopic calcite cement; common planar bedding and ripple or low-angle cross-bedding.	Supratidal to shallow marine coastal areas.
Mudstones (D06)	Laminated deposits composed of silt-sized quartz grains and muscovite flakes floating in a carbonate mud; occur either as thin caps over subaerially weathered surfaces or thick subtidal units.	Supratidal to shallow marine coastal areas.
Dolocretes (D07)	Commonly fine-grained nodular dolostones composed of alomicrite or microspar; less abundantly massive dolostones with peloids and clasts of aphanitic or clotted automicrite enclosed in alomicrite or microspar; occur as thin caps over subaerially weathered surfaces.	Supratidal plains and emerged banks of tidal flats and lagoons.
Rhizolites (D08)	Massive dolosiltites with centimetre-long vertical, straight or downward-bifurcating root casts.	Supratidal areas and/or intertidal salt marshes.
Fenestral dolostones (= loferites; D09)	Micropeloidal dolostones containing abundant, laterally elongate and linked fenestrae; pores occluded by pendant and blocky cements.	Drying and wetting of a deposit in exposed areas.
Wavy- to planar-bedded dolostones (D10)	Unfossiliferous dolostones composed of alternating undulatory bands of grey dolosiltites and yellow peloidal dolomitic packstones; commonly mottled by bioturbation; rare small erosional channels.	Intertidal zones.
Cryptalgal laminites (D11)	Fine-grained dolostones composed of alternating laminae of microbial micrite and dolomitic silt; common truncation of lamination and reworking to clasts; sporadic fenestrae, sheet cracks, and mudcracks.	Intertidal zones.
Stromatolites (D12)	Hemispheroids, 30 cm high and 50 cm across, with simple to compound internal lamination consisting of dolomitic silt laminae impregnated by aphanitic microbial films; sporadic lilliputian sponges and spar-filled moulds after ?cyanobacterial filaments.	Low-energy subtidal areas within restricted lagoons.
Bioturbated dolosiltites (D13)	Unfossiliferous, fine-grained dolostones containing abundant burrows <i>Balanoglossites</i> and <i>Thalassinoides</i> infilled with dolomitic mud or fine-grained peloidal sand.	Ephemeral tidal ponds or low-energy subtidal areas within restricted lagoons.
Dolosiltites (D14)	Platy to medium-bedded, structureless, dolomitic mudstones composed of micrite or microspar (minor fine-grained peloidal wackestones); local accumulations of bioclasts.	Low-energy subtidal areas within restricted lagoons.
Intraformational dolomitic conglomerates (D15)	Dolosiltites (D14) containing flat pebbles of dololutites and dolosiltites; pebbles poorly sorted, commonly aligned parallel to bedding planes (rarely imbricated), and locally infested by the boring <i>Trypanites</i> .	Rapid deposition of mixed material in tidally-influenced lagoonal areas.
Peloidal dolostones (D16)	Peloidal grainstones and packstones (rarely wackestones), containing rare bioclasts, ooids, and oncoids; peloids poorly to well-rounded and poorly to moderately sorted; common symmetrical ripples and dunes; rare planar bedding and trough, tabular, and herringbone cross-bedding; locally extensive <i>Balanoglossites</i> burrow systems.	High-energy subtidal areas within restricted lagoons.
Green algal (Dasycladaceae) dolostones (D17)	Green algal grainstones-packstones and rudstones with some bioclasts; matrix comprises poorly sorted and moderately rounded peloids.	Subtidal, low-energy, mud-free areas of restricted lagoons.
Oncoidal dolostones (D18)	Oncoidal rudstones and floatstones with matrix consisting of peloids, bioclasts, and cortoids; oncoids are up to 4 cm in diameter, subspherical, poorly sorted, and randomly oriented; oncoidal cortices display concentric to partially overlapping lamination consisting of thicker microsparitic laminae impregnated by dark micritic film.	Temporarily turbulent settings within restricted lagoons.
Ooidal dolostones (D19)	Ooidal packstones containing frequent bioclasts and rare peloids, cortoids and lithoclasts of ooidal packstones; ooids are ~0.5 mm in diameter (rarely ~1.0 mm) and mainly composed of small peloid nuclei and thick radial-fibrous (minor tangential) cortices; common polyoids; grains enclosed in microspar; rare high-angle cross-bedding.	“Low-energy”, tidally dominated areas within restricted lagoons.

Table 2

Summary of principal characteristics of limestone lithofacies and their environmental interpretation

Lithofacies type	Lithological characteristics	Environment/process
Ferricretes (L01)	Thin micronodular, iron oxide crusts containing dispersed oncoids, peloids, marine bioclasts, and quartz grains.	Emerged shoal sands or lime muds.
Green algal (Dasycladaceae) limestones (L02)	Green algal grainstones-packstones and rudstones with some open-marine fauna; matrix composed of poorly sorted and moderately rounded peloids; grains surrounded by rims of early marine cements.	Tranquil, well-circulated, shallow subtidal areas.
Ooidal limestones (L03)	Grainstones composed of large (~1 mm across) ooids that either have small peloid nuclei and thick concentric cortices (normal ooids) or have large peloid/bioclast nuclei and thin radial-fibrous cortices (superficial ooids); rare peloids, bioclasts, cortoids, and polyoids.	Tidally dominated bars and deltas.
Oncoidal limestones (L04)	Floatstones and rudstones, locally packstones and grainstones comprising either: 1) <i>Girvanella</i> oncoids, 0.5–2 cm across; 2) large (0.5–4 cm across) microbial oncoids, cortices of which display concentric to partially overlapping lamination consisting of thicker microsparitic-sparitic and thinner micritic laminae; or 3) small (up to 5 mm across), microbial oncoids having regular concentric laminations. Abundant bioclasts, cortoids, superficial ooids, and lithoclasts of grey calcilutites; matrix composed of peloids; rare low-angle, tabular, trough, and herringbone cross-bedding as well as dunes.	Calm to turbulent, normal-marine shoals.
Cortoidal limestones (L05)	Rudstones and grainstones (minor floatstones and packstones) composed of disarticulated bioclasts with thin, non-laminated micritic rims; common symmetrical ripples and dunes.	Normal-marine, subtidal areas with longer periods of substrate stability.
Bioclastic limestones (L06)	Floatstones and rudstones (rarely wackestones-grainstones) consisting of: 1) bivalve and brachiopod shells aligned parallel to bedding planes; 2) articulated and/or disarticulated crinoid ossicles; or 3) gastropod conchs. Occur as coquinas 1–30 cm thick with scoured bases and normal grading or as thick amalgamated units; sporadic dunes and ripples.	Normal-marine, high-energy shoals or proximal tempestites deposited on lower shoreface.
Peloidal limestones (L07)	Grainstones and packstones (rarely wackestones) composed either of: 1) lobate-shaped peloids (micritized aggregate grains); 2) small ellipsoidal peloids (pellets); or 3) large (~1 mm in diameter) well-rounded peloids with vague ooid-type laminations (recrystallized ooids). Occur as hummocky cross-stratified layers with sharp bases or thick amalgamated packages with low-angle, tabular, trough, and herringbone cross-bedding, locally <i>Arenicolites</i> isp. and <i>Skolithos</i> isp.	Normal-marine, high-energy shoals or distal tempestites deposited on lower shoreface.
Sponge buildups (L08)	Biostromes: 3–10 cm thick and arranged in metre-thick, laterally continuous bodies. Bioherms: domes 6 m high and 25 m across; corals and reef dwellers locally present. Sponges preserved as etched siliceous skeletons, mummies or recrystallized cavernous limestones.	Biostromes: lower shoreface. Bioherms: upper shoreface.
Intraformational limestone conglomerates (L09)	Bioclastic limestones (L06) containing flat pebbles of peloidal packstones, bioclastic floatstones, and fine-grained limestones; pebbles poorly sorted, either randomly oriented, imbricated or aligned parallel to bedding planes; some clasts encrusted by the bivalve <i>Placunopsis</i> or bored with <i>Trypanites</i> .	Proximal tempestites deposited on lower shoreface.
Bedded calcisiltites and calcilutites (L10)	Mudstones and fine-grained peloidal wackestones with finely comminuted bioclasts; occur as beds 5–30 cm thick with parallel lamination or hummocky and low-angle cross-bedding.	Distal tempestites or suspension-settled deposits.
Platy-bedded limestones (L11)	Platy calcisiltites and calcilutites with sporadic dispersed bioclasts.	Calm, open-marine environments.
Wavy-bedded limestones (L12)	Thin, undulated to crumpled layers of calcisiltites and calcilutites draped locally by black limey claystones; common ball-and-pillow structures, load structures, slumps, and slides.	Collapse of unstable, layered, open-marine sediments.
Nodular limestones (L13)	Nodular calcisiltites and calcilutites with scattered fine bioclasts; nodules either amalgamated or separated by black limey claystone; locally abundant trace fossils, predominantly the burrow <i>Rhizocorallium</i> filled with elliptical coprolites or micrite.	Calm, open-marine environments.
Marls and limey claystones (L14)	Unfossiliferous, laminated, fine-grained deposits composed of silt-sized quartz grains and mica flakes dispersed in carbonate mud.	Increased terrigenous input to calm, open-marine environments.
Firmgrounds (L15)	Mudstones and fine-grained peloidal wackestones with abundant burrows <i>Balanoglossites</i> and <i>Thalassinoides</i> infilled with faecal pellets or detrital sediment; occur as layers 5–30 cm thick; locally even lamination preserved.	Sediment-starved, calm, open-marine settings.
Hardgrounds (L16)	Laterally discontinuous surfaces typified by encrustations of the bivalve <i>Placunopsis</i> or the boring <i>Trypanites</i> .	Sediment-starved, calm, open-marine settings.

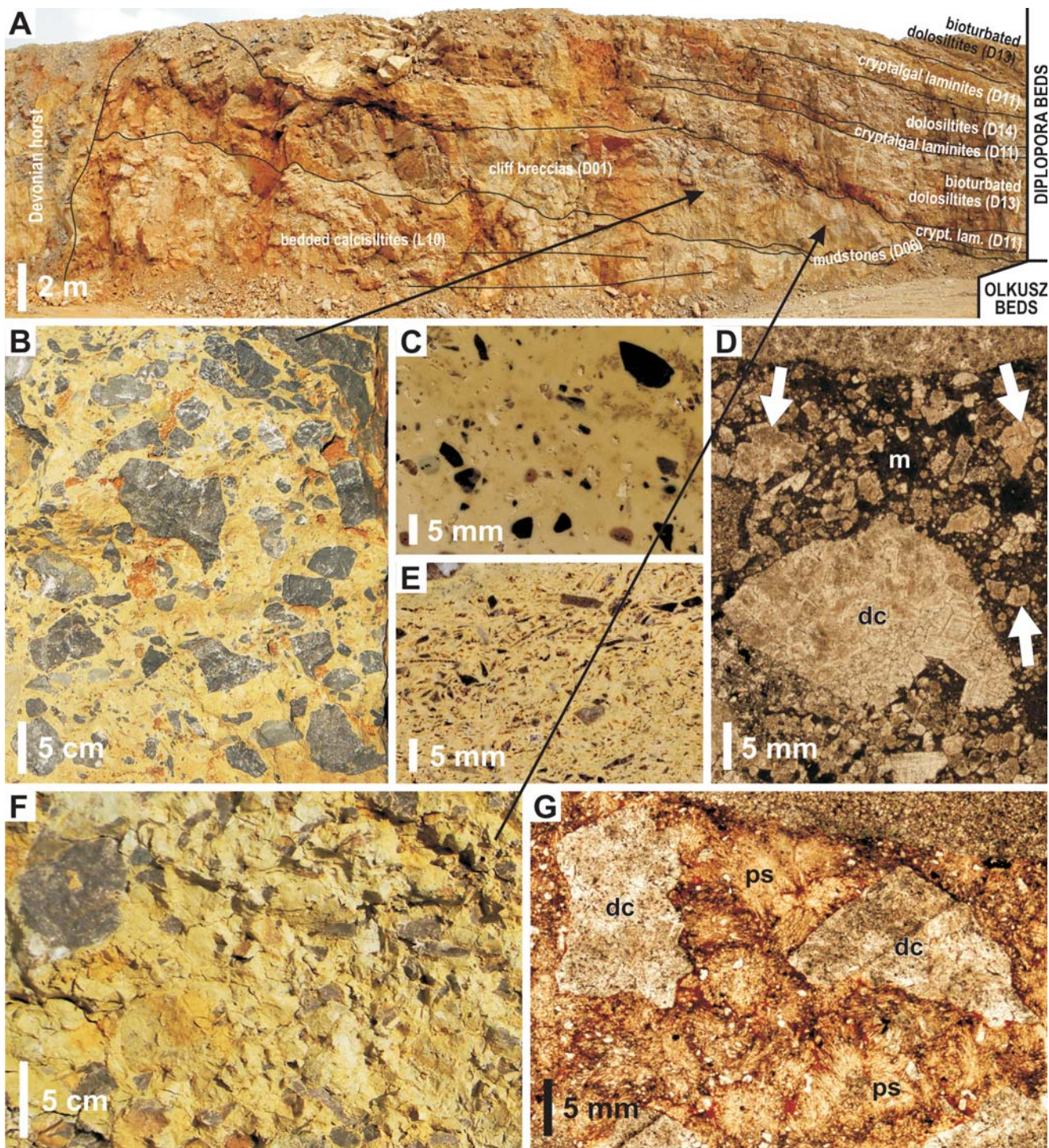


Fig. 7. Examples of cliff breccia. **A.** Lenticular breccia body attached to the cliff of a Devonian island and vertically juxtaposed with various carbonate lithofacies (the picture is resized horizontally to 65% of its original size). “GZD” Quarry in Nowa Wioska. **B.** Vertical outcrop view of very poorly sorted cliff breccia consisting of randomly oriented, angular lithoclasts of black Devonian dolostones surrounded by yellow dolosiltite. **C.** Detail of B. Small black lithoclasts floating in dolosiltite. **D.** Photomicrograph of C, showing a large lithoclast of Devonian dolostone (dc) surrounded by a number of sand-sized fragments (arrows) embedded in dark dolomitic mudstone (m). **E.** Vertically oriented slab of cliff breccia composed of small black lithoclasts floating in bioclastic (bivalve) dolomitic wackestone, indicating deposition in a marine environment. **F.** Vertical outcrop view of cliff breccia, the matrix of which is composed of green dolosiltite with lithoclasts and peloids of dense aphanitic and clotted-micropeloidal automicrite, indicating deposition in a continental setting. **G.** Photomicrograph, showing lithoclasts of Devonian dolostones (dc) enclosed by carbonate pseudomorphs after sulphates.

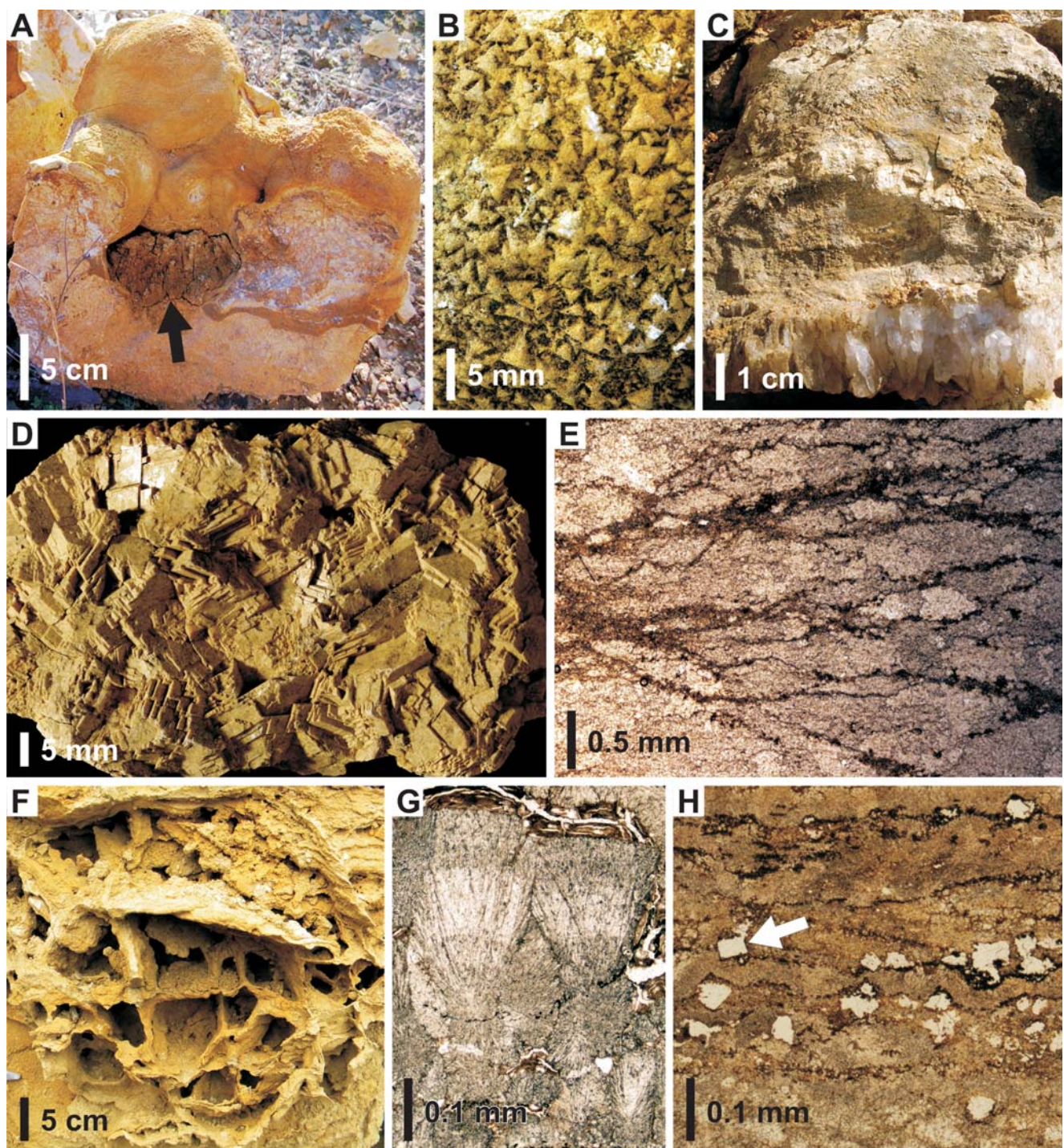


Fig. 8. Lithofacies essentially related to precipitation and evaporation processes. **A.** Outcrop view of red-tan residual clay (arrow) filling a cavity between bulbous speleothems. **B.** Close-up view of speleothem surface, displaying triangle terminations of calcite crystals. **C.** Vertical outcrop view of dripstone cement precipitated underneath a speleothem, in open cavity formed owing to subaerial dissolution of precursor carbonates and/or evaporites. **D.** Crystalline dolostone consisting of overgrown, euhedral dolomite crystals. **E.** Photomicrograph of crystalline dolostone composed of anhedral dolomite crystals. **F.** Cellular dolostone comprising cubic-shaped voids after dissolved halite crystals. **G.** Photomicrograph of F, showing calcite/dolomite pseudomorphs after sulphate. **H.** Photomicrograph of F, showing calcite/dolomite pseudomorphs after halite (arrow). Pictures: A–E – Tarnowice Beds, Opole region; F–H – Zellenkalk2 horizon of Gogolin Formation, Opole region.

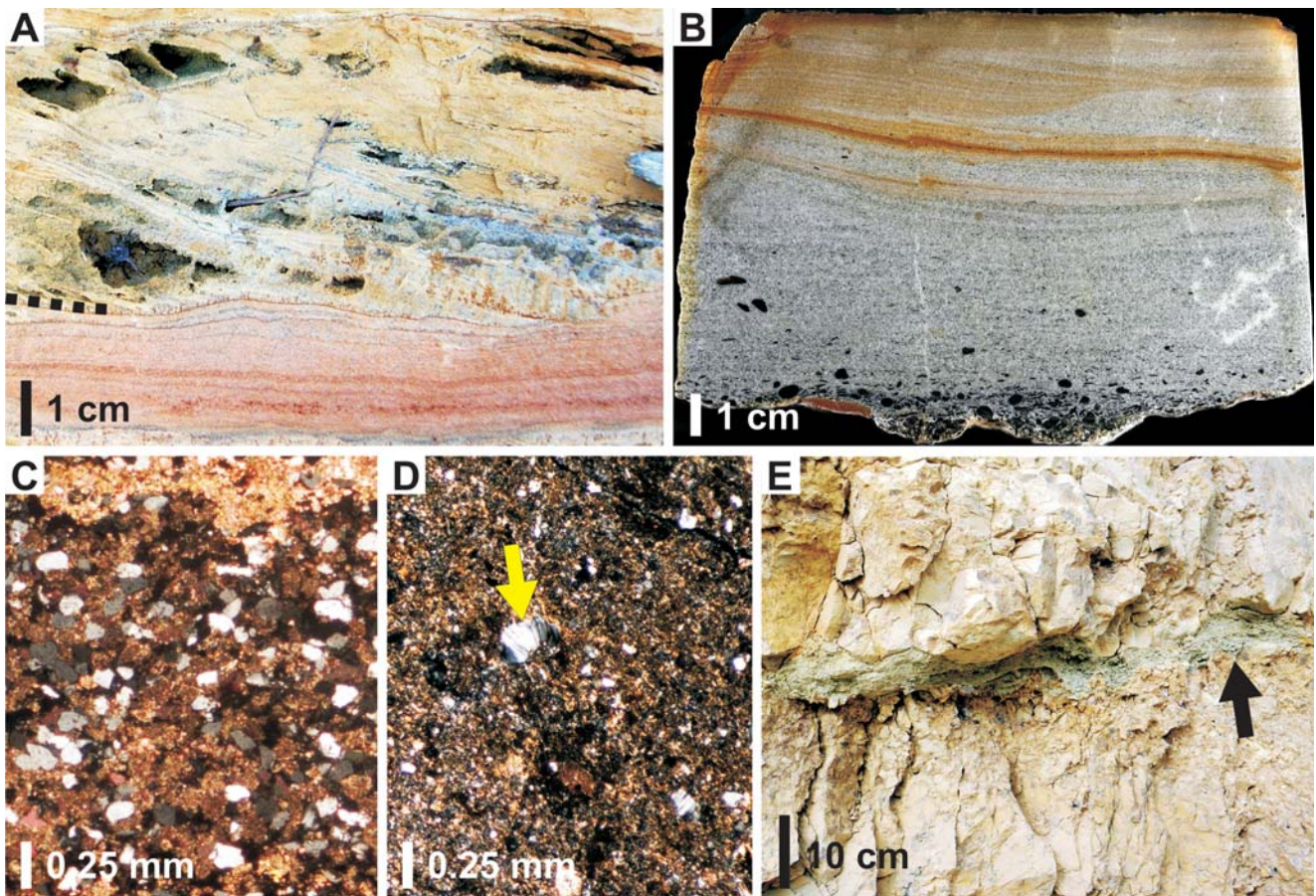


Fig. 9. Siliciclastic lithofacies. **A.** Vertical outcrop view of red, low-angle bedded sandstone overlain by yellow, cellular dolostone. **B.** Vertically oriented slab of sandstone displaying normal grading and ripple cross-bedding, and containing plant debris (black grains). **C.** Photomicrograph of fine-grained sandstone, illustrating poikilotopic calcite cementing subrounded, horizontally-oriented quartz grains. **D.** Photomicrograph of mudstone, showing silt-sized quartz grains (arrow points at one example) dispersed in dolomitic mud. **E.** Green mudstone capping irregular, subaerially-weathered surface (arrow) of brecciated dolocrete. Pictures: A, C – Tarnowice Beds, Opole region; B – Boruszowice Beds, Opole region; D, E – Diplopora Beds, Kraków-Silesia region.

the case of the modern coastal sabkhas at Abu Dhabi, ascending continental groundwaters (not marine waters) supply ions to the capillary zone (Wood *et al.*, 2002). Locally occurring selenite crystals confirm precipitation under conditions of submergence.

Sandstones (D05)

Characteristics

These yellow-orange-grey deposits are composed primarily of subrounded quartz grains that reach 0.01–0.20 mm across (Fig. 9). The grains may be widely or densely spaced, but do not touch one another. Aligned parallel to bedding planes or to cross-bedding, the quartz grains are embedded in micrite, microspar or poikilotopic calcite cement (Fig. 9C).

The sandstones of the Tarnowice Beds are typically rich in muscovite flakes and show planar bedding and low-angle cross-bedding (Fig. 9A). The sandstones of the Boruszowice Beds contain bone fragments and plant debris, and show normal grading and small-scale ripple cross-bedding (Fig. 9B).

Environment

The sandstones alone are difficult to interpret in terms of depositional environments, but the associated lithofacies permit some inferences to be drawn. In the Tarnowice Beds, the sandstones are interbedded with cellular dolostones (D04) of a probable sabkha environment and accordingly they are considered to have formed in the supratidal zone (Figs 3, 4A). In the Boruszowice Beds, in contrast, the sandstones are vertically juxtaposed with black mudstones (D06) containing cephalopods, and therefore they may be interpreted as shallow-marine deposits (Fig. 3).

Mudstones (D06)

Characteristics

These are laminated, fine-grained deposits, composed of horizontally oriented, silt-sized quartz grains and muscovite flakes, floating in a carbonate mud (Fig. 9D). The mudstones of the Diplopora and Tarnowice beds are green-grey-orange, unfossiliferous and occur as centimetre-thick layers, capping an irregular, subaerially weathered surface (Fig. 9E). In contrast, the mudstones of the Boruszowice Beds are black, form metre-thick units and contain cephalopods.

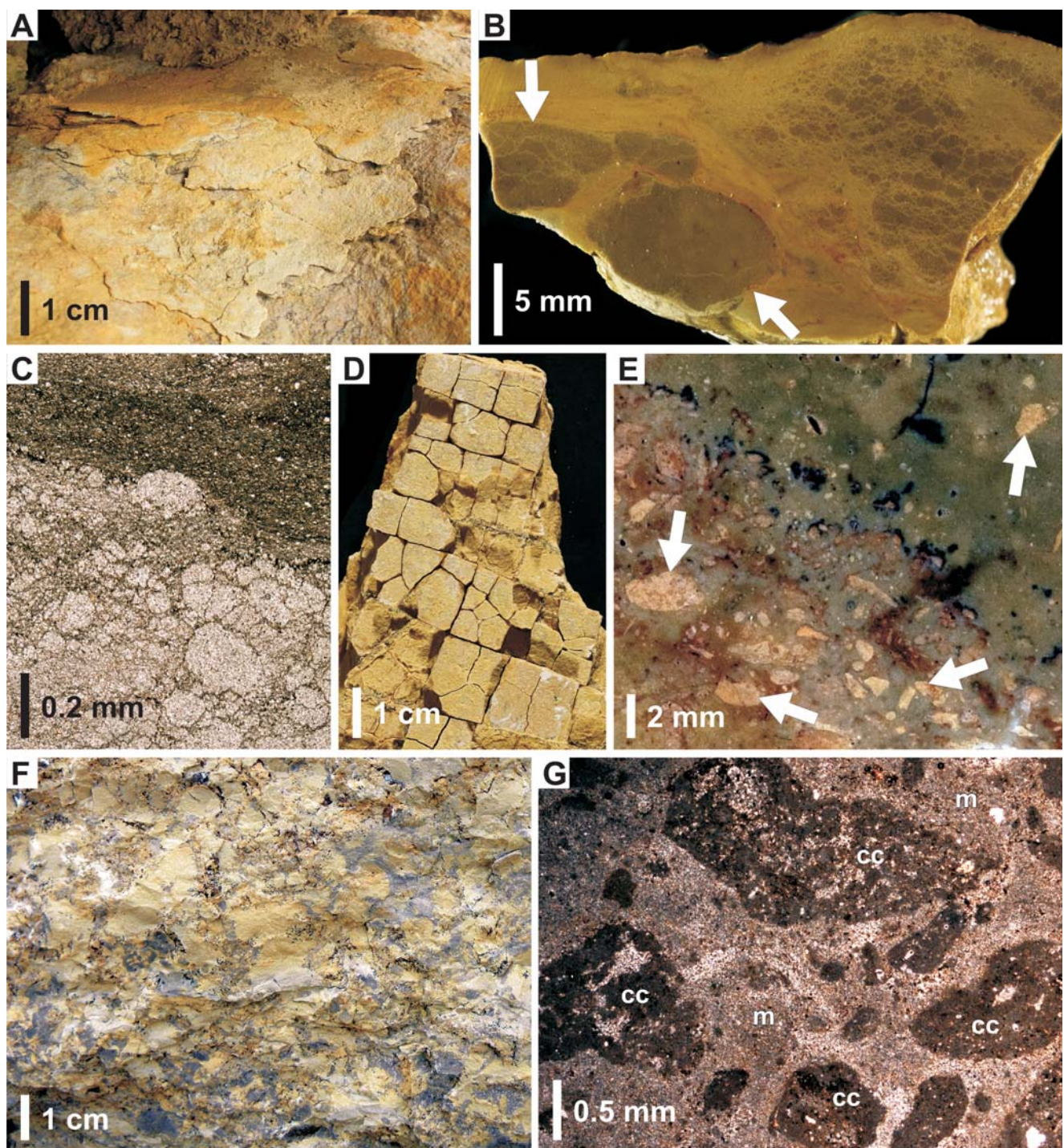


Fig. 10. Examples of dolocrete. **A.** Bedding plane view of dolocrete crust. **B.** Vertically oriented slab of dolocrete crust displaying micronodular fabric with remnants of a host rock (arrows). **C.** Microphotograph of B, showing micronodular lower part overlain by micritic upper part. **D.** Bedding plane view of desiccation cracks developed in the topmost part of a dolocrete. **E.** Vertically oriented slab of green massive dolocrete containing small lithoclasts and peloids formed of dense aphanitic or clotted-micropeloidal automicrite (arrows). **F.** Vertical outcrop view of massive dolocrete comprising yellow-green, large, lobate lithoclasts of dense aphanitic or clotted-micropeloidal automicrite surrounded by dark matrix. **G.** Photomicrograph of F, showing clotted-micropeloidal lithoclasts (cc) floating in microspar (m). Pictures: A–C, E–G – Diplopora Beds, Kraków–Silesia region; D – Zellenkalk2 of Gogolin Formation, Kraków–Silesia region.

Environment

The mudstones capping a subaerially weathered surface are interpreted as having been formed in the supratidal zone, on emerged banks and on the peripheral plains of tidal flats (Figs 3, 4A). The mudstones of the Boruszowice Beds represent a subtidal, nearshore setting, as indicated by the occurrence of cephalopods (Fig. 3).

Dolocretes (D07)

Characteristics

These are yellow-orange-green-grey dololutites and dolosiltites, usually resting on top of an irregularly undulating surface. Most dolocretes form centimetre- to decimetre-thick crusts and exhibit nodular fabrics, composed of allo-micrite or microspar (Fig. 10A–C). Some dolocretes are structureless (massive) and contain peloids and lobate lithoclasts of dense aphanitic or clotted-micropeloidal automicrite, embedded within allo-micrite or microspar (Fig. 10E–G). Both the lithoclasts and matrix contain sporadic forams and ostracods. Some dolocretes display mudcracks with polygons up to 10 cm in width (Fig. 10D).

The dolocretes occur commonly in the Diplopora Beds and sporadically in the Zellenkalk2 of the Gogolin Formation (Figs 2, 5). They also make up the lowermost part of the Olkusz Beds, overlapping the Devonian island at the “Stare Gliny” Quarry in Jaroszowiec (Fig. 6).

Environment

The dolocretes were formed in the supratidal zone, possibly on the peripheral plains and emerged banks of tidal flats and lagoons (Figs 3, 4A). Dolocretes are a widely accepted indicator of semi-arid and arid conditions (Esteban and Klappa, 1983; Wright and Tucker, 1991). The peloids and lithoclasts of dense aphanitic or clotted-micropeloidal automicrite were presumably formed within soils as a consequence of microbial activity.

Rhizolites (D08)

Characteristics

These are beige-yellow-green, massive (structureless) dolosiltites with centimetre-long vertical, straight or downward-bifurcating root casts (Fig. 11A, B). The concentration of root casts usually increases upward in a given rhizolite layer and consequently its topmost part contains a complex network of filiform voids. The rhizolites locally contain rare peloids and small lithoclasts, composed of dense aphanitic or clotted-micropeloidal automicrite. A centimetre-sized lens of sulphates was found within a rhizolite layer (Fig. 11C, D).

The rhizolites are quite common in the Diplopora Beds of the Kraków–Silesia region and very rare in the Zellenkalk2 of the Gogolin Formation (Figs 2, 5). Like the dolocretes (D07), they also form the lowermost part of the Olkusz Beds, overlapping the Devonian island exposed at the “Stare Gliny” Quarry in Jaroszowiec (Fig. 6).

Environment

The rhizolites most likely were formed on permanently emerged areas (Esteban and Klappa, 1983; Wright and Tu-

cker, 1991), but they may represent intertidal salt marshes, as well (e.g., Shinn *et al.*, 1969; Figs 3, 4A).

Fenestral dolostones (= loferites) (D09)

Characteristics

These are yellow, laminated dolosiltites, displaying a laminoid-fenestral fabric (Fig. 11E). Laminae are composed of micropeloids with sporadic ostracods (Fig. 11F) and are separated by fenestrae, which are elongate (rarely subspherical), arranged concordant with the stratification and often linked together laterally (Fig. 11E). The fenestrae are generally filled with pendant cement, followed by blocky cement (Fig. 11F). The fenestral dolostones are rare and occur exclusively in the Diplopora Beds of the Kraków–Silesia region.

Environment

A laminoid-fenestral fabric is generally regarded as originating from the wetting and drying of carbonate mud or a cyanobacterial mat in intertidal and supratidal settings (Fischer, 1964; Shinn, 1968; Figs 3, 4A). Rare subspherical fenestrae might have been produced by air and gas bubbles, trapped during the deposition of the host sediment or generated by the post-depositional decay of organic matter (Shinn, 1968).

Wavy- to planar-bedded dolostones (D10)

Characteristics

These unfossiliferous dolostones are composed of alternating layers of grey dolosiltites and yellow peloidal dolarenites, around 1 cm thick (mostly packstones; Fig. 11G, H). The layers are wavy to parallel in form. They are frequently disturbed by bioturbation and occasionally cut by erosional channels (about 1 m wide and 30 cm deep). The wavy- to planar-bedded dolostones occur in the lower part of the Olkusz Beds overlapping two Devonian islands, exposed at the “Promag” and “GZD” quarries in Nowa Wioska.

Environment

The wavy- to planar-bedded dolostones are very similar to the wavy-, flaser- and lenticular-bedded deposits, characteristic of modern siliciclastic tidal flats (e.g., Reineck and Singh, 1980) and many ancient examples (e.g., Demicco, 1983; Pratt and James, 1986). Therefore, they are also interpreted as intertidal deposits (Figs 3, 4A). This interpretation is further supported by the lack of skeletal fossils and the presence of abundant burrows that might have been created for shelter during the ebb tide.

Cryptalgal laminites (D11)

Characteristics

These yellow-grey dolostones are composed of alternating millimetre-thick laminae of microbial and detrital origins (Fig. 12A, B). The microbial laminae display dense aphanitic (minor clotted-micropeloidal) microfabrics, whereas the detrital laminae are composed of silt- to mudsized lime particles (Fig. 12B). The lamination is usually even (rarely undulatory) and parallel to the bedding planes (Fig.

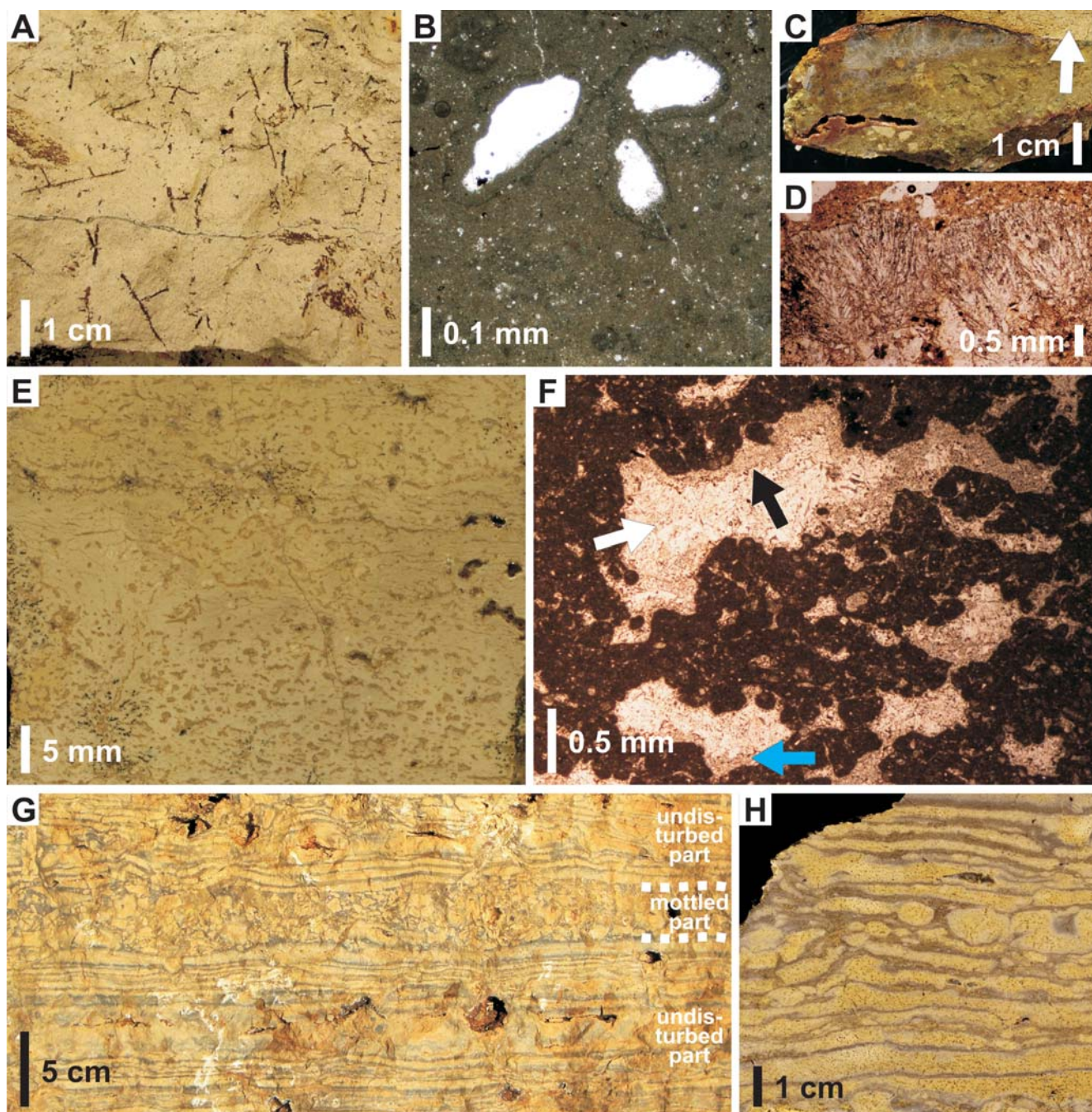


Fig. 11. Examples of inter- to supratidal lithofacies. **A.** Vertical outcrop view of rhizolite with small, straight root casts. **B.** Photomicrograph of rhizolite, showing three vugs after roots penetrating dolomitic mudstone, consisting of dispersed, dense, aphanitic peloids. Note the distinct rim around each vug, which might have been produced by microbial activity. **C.** Vertically oriented slab of evaporite lens occurring within a rhizolite (arrow). **D.** Photomicrograph of C, showing carbonate pseudomorphs after sulphates. **E.** Vertically oriented slab of fenestral dolostone (loferite) displaying laminoid-fenestral fabric with horizontally elongated and laterally linked fenestrae. **F.** Photomicrograph of E, showing amalgamated, clotted peloids with elongated cavities filled by pendant cement (black arrow) and later blocky cement (white arrow). Some fenestrae contain ?recrystallized internal sediment (blue arrow). **G.** Vertical outcrop view of wavy- to planar-bedded dolostone displaying alternation of bioturbated and undisturbed bedsets. **H.** Vertically oriented slab of G, showing thicker layers of yellow peloidal dolomitic packstone sandwiched by thinner layers of grey dolosiltite. Pictures: A – the lowermost part of the Olkusz Beds overlapping the Devonian island exposed at the “Stare Gliny” Quarry, in Jaroszowiec; B–F – Diplopora Beds, Kraków–Silesia region; G, H – the lower part of the Olkusz Beds overlapping the Devonian island exposed at the “Promag” Quarry, in Nowa Wioska.

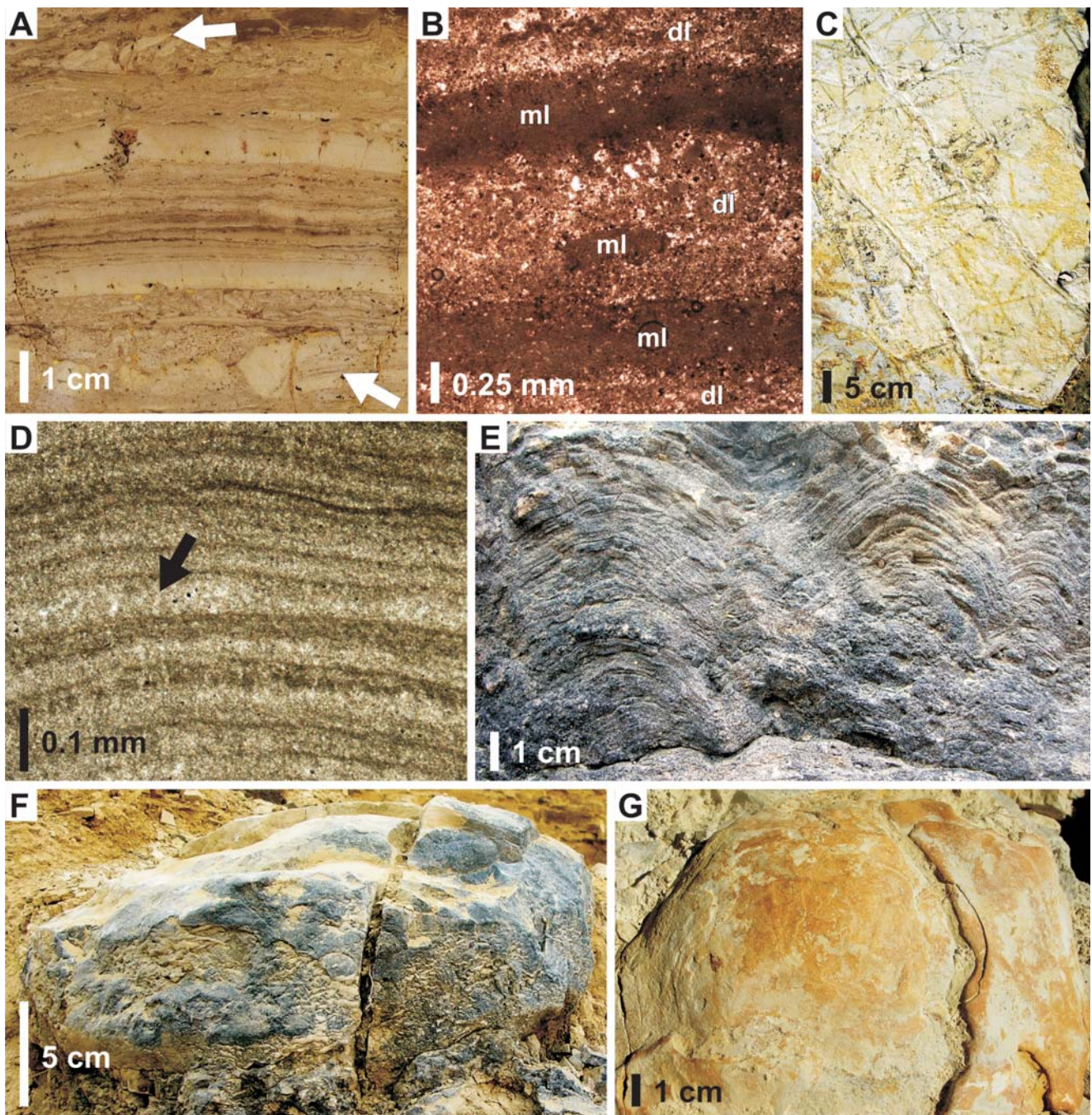


Fig. 12. Examples of organosedimentary lithofacies. **A.** Vertically oriented slab of cryptalgal laminitite. Note intraclasts of reworked laminites (arrows) incorporated into laminae. **B.** Photomicrograph of cryptalgal laminitite, illustrating darker microbial laminae (ml) alternated by more transparent detrital laminae (dl). **C.** Bedding plane view of desiccation cracks developed within a cryptalgal laminitite. **D.** Photomicrograph of domal stromatolite, showing thinner, dark microbial laminae and thicker, more transparent laminae composed of dolomititic mudstone and containing vertical spar-filled moulds of ?cyanobacterial filaments (arrow). **E.** Vertical outcrop view of three small, laterally linked stromatolitic domes. **F.** Vertical outcrop view of stromatolitic hemispheroid. **G.** Plane view of calichefied upper surface of stromatolite hemispheroid containing wind-blown mica flakes. All pictures illustrate Diplopora Beds of Kraków-Silesia region.

12A). The sets of laminae are often truncated and discordantly capped by another cryptalgal layer. Laminitic layers are commonly torn up into intraclasts, which may be incorporated into successive laminations or form conglomerates and breccias (Fig. 12A). Flat and rounded intraclasts are lo-

cally imbricated. The cryptalgal laminites generally exhibit non-porous fabrics (Fig. 12A), with occasional only fennestral pores, sheet cracks and mudcracks with polygons up to 50 cm across (Fig. 12C). Small gastropods can be found within the laminations.

The cryptalgal laminites are characteristic of the Diplopora Beds of the Kraków–Silesia region. They were also recognized in the Zellenkalk2 of the Gogolin Formation (Figs 2, 5).

Environment

The cryptalgal laminites were formed in the intertidal zone of tidal flats (Figs 3, 4A) owing to the trapping of mud by microbial mats (Ginsburg, 1960; Fischer, 1964; Kendall and Skipwith, 1968; Shinn *et al.*, 1969; Hardie, 1977; Kinsman and Park, 1976; Alsharhan and Kendall, 2003; Rankey and Berkeley, 2012). The lack of bioclasts and coarse sediments may reflect a relatively great distance to the subtidal zones on the one hand, and limited storm-generated transport on the other (e.g., Pratt and James, 1986). The truncation of laminitic layers and production of intraclasts most likely resulted from the activity of tidal currents. The depositional area must have been regularly flooded, as evidenced by the non-porous fabric of the cryptalgal laminites (e.g., Shinn, 1968). The gastropods, found within the laminations, are interpreted as *in situ* accumulations of mat-grazing organisms.

Stromatolites (D12)

Characteristics

These grey dolostones are made up of alternating detrital and microbial laminae. The microbial laminae occur as very thin, dark, aphanitic films between the thicker, light, detrital laminae composed of silt-sized lime particles (Fig. 12D). Some laminae additionally contain vertical spar-filled moulds of ?cyanobacterial filaments (Fig. 12D) and lilliputian sponges preserved *in situ* (Szulc, 1997, 2000). The laminae are wrinkled into a series of small (centimetre-sized) cones that are vertically stacked together to form hemispheroids, 30 cm high and 50 cm across (Fig. 12E, F). The hemispheroids are laterally contiguous, but not linked together. The upper surface of some hemispheroids is truncated and capped by reddish dolocrete crusts, containing muscovite flakes (Fig. 12G). Sporadic stromatolite hemispheroids have been found in the Tarnowice Beds of the Opole region (J. Szulc, pers. comm., 2014); however, the most prominent stromatolitic horizon marks the upper boundary of the Diplopora Beds in the Kraków–Silesia region (Myszkowska, 1992; Szulc, 2000; Matysik, 2012; Figs 2, 5).

Environment

Stromatolites of similar size and morphology are known to grow at present in the shallowest subtidal zone of the Hamelin Pool embayment, Australia (Burne and James, 1986; Reid *et al.*, 2003; Jahnert and Collins, 2011) and the Highborne Cay back-reef area, Bahamas (Andres and Reid, 2006). By analogy to these two well-documented examples, the stromatolites studied probably formed in the shallow subtidal zone (Figs 3, 4A). The overall fine-grained fabric, lacking macrofossils and constructional voids, indicates that stromatolite accretion took place in a tranquil setting, away from areas of grain production and protected from storms. The dolocrete crusts capping some hemispheroids are evidence of a longer sea-level drop that presumably terminated stromatolite growth.

Bioturbated dolosiltites (D13)

Characteristics

These are beige-yellow-orange-grey, unfossiliferous, fine-grained dolostones that are extensively bioturbated (*Balanoglossites* isp., *Thalassinoides* isp.; Fig. 13A, B). The burrows are passively infilled by dolomitic mud or fine-grained peloidal sand. The bioturbated dolosiltites commonly form units, 0.5–1.5 m thick, lacking internal erosional surfaces. In other cases, they occur as either centimetre-thick intercalations within other lithofacies, or decimetre-thick amalgamated packages. The bioturbated dolosiltites occur in the Diplopora Beds of the Kraków–Silesia region (Figs 2, 5).

Environment

The bioturbated dolostones are interpreted as the sediments of the shallow subtidal zone, deposited in areas, protected from the influence of vigorous tidal currents (Figs 3, 4A). Thinner units of bioturbated dolostones might have been formed in ephemeral tidal ponds (e.g., Shinn *et al.*, 1969; Rankey and Berkeley, 2012), whereas thicker ones rather were deposited in long-term coastal lagoons and embayments (e.g., Kendall and Skipwith, 1969; Purser and Evans, 1973; Alsharhan and Kendall, 2003). The absence of skeletal fossils points to restricted life conditions, probably related to increased salinity, but still feasible for pervasive bioturbation. *Thalassinoides* isp. and *Balanoglossites* isp. are characteristic of well-aerated substrates (e.g., Rhoads, 1975; Savrda and Bottjer, 1986; Savrda, 2007).

Dolosiltites (D14)

Characteristics

These are beige-yellow, structureless, platy or medium-bedded dolomitic mudstones (Fig. 13C, D), composed of micrite or microspar, and rarely fine-grained peloidal wackestones (Fig. 13E). The dolosiltites, occurring in the Diplopora Beds and in the Zellenkalk2 of the Gogolin Formation, sporadically contain biomoulds after the dissolved shells of bivalves and gastropods (Fig. 13D). The dolosiltites of the Tarnowice Beds are generally unfossiliferous, except for the occurrence of vertebrate bones.

Environment

The dolosiltites presumably were formed in the tranquil areas of restricted lagoons (Figs 3, 4A), as evidenced by the lack of sedimentary structures, the overall paucity of fossils and the dolomitic nature of the sediment.

Intraformational dolomitic conglomerates (D15)

Characteristics

This facies consists of dolosiltites (D14) as matrix with grey-beige pebbles of dololutite and dolosiltite (Fig. 13F), containing sporadic forams (Fig. 13G). The pebbles are flat to ellipsoidal (up to 30 cm long), moderately to well-rounded and poorly sorted. They are commonly aligned parallel to bedding planes and only rarely imbricated.

This lithofacies type is rare and it occurs chiefly in the Diplopora Beds of the Kraków–Silesia region (Fig. 5). One

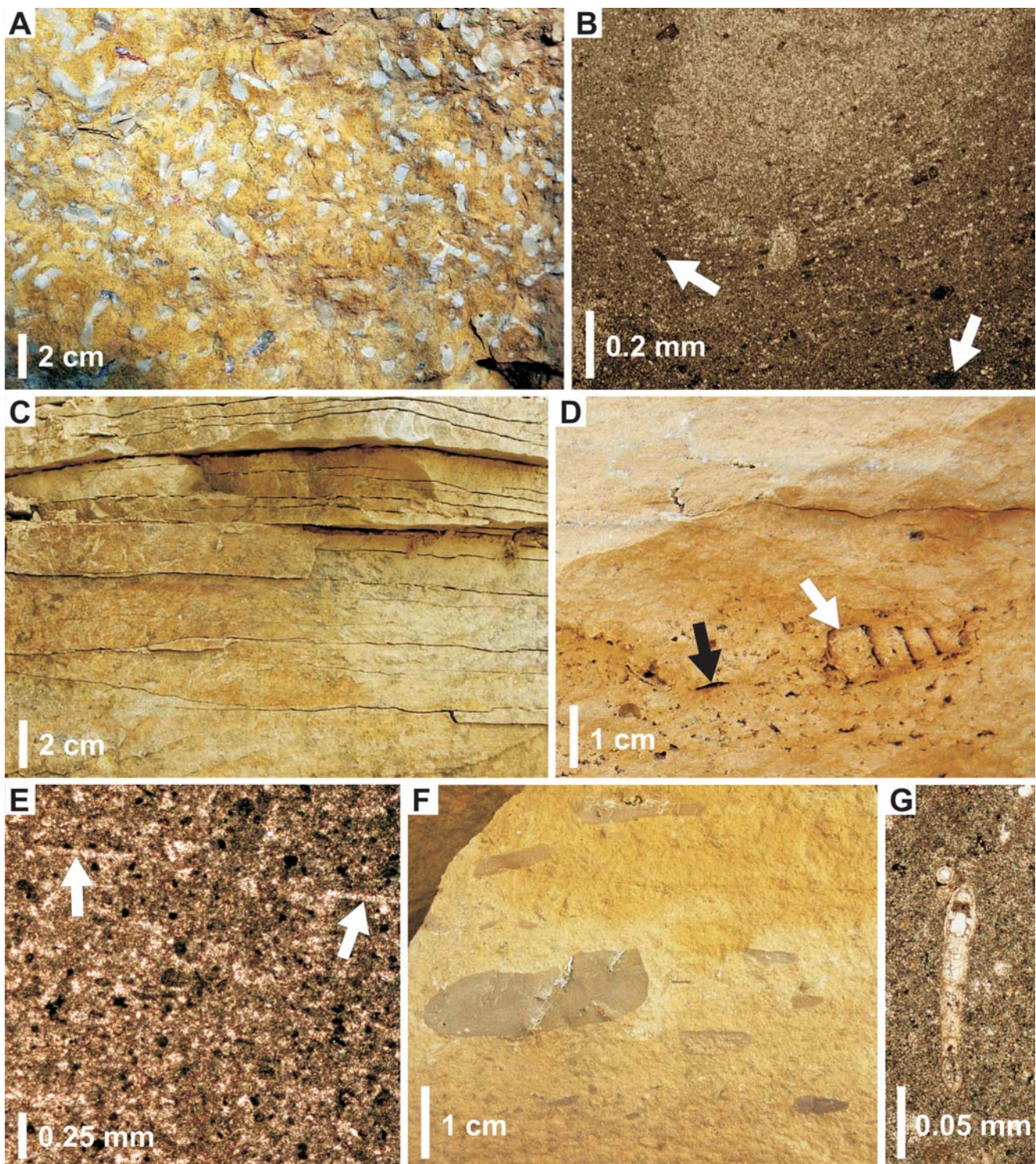


Fig. 13. Examples of shallow subtidal, dolomitic, mud-dominated lithofacies. **A.** Vertical outcrop view of bioturbated dolosiltite. **B.** Photomicrograph of A, showing the contact between burrow and surrounding microsparitic deposit containing sparse peloids (arrows). Note that the alignment of peloids follows the margins of the tubular feature, which indicates that it was produced by bioturbation. **C.** Vertical outcrop view of platy-bedded dolosiltite. **D.** Vertical outcrop view of medium-bedded dolosiltite containing vugs after dissolved bivalves (black arrow) and gastropods (white arrow). **E.** Photomicrograph of D, showing peloidal wackestone with sporadic bivalve shells (arrows). **F.** Vertical outcrop view of matrix-supported intraformational dolomititic conglomerate. Grey, horizontally oriented, flat pebbles of dolosiltite float in dolosiltite matrix. **G.** Photomicrograph of flat pebble, showing foram test enclosed by microspar. Pictures: A, B, D–G – Diplopora Beds, Kraków–Silesia region; C – Tarnowice Beds, Kraków–Silesia region.

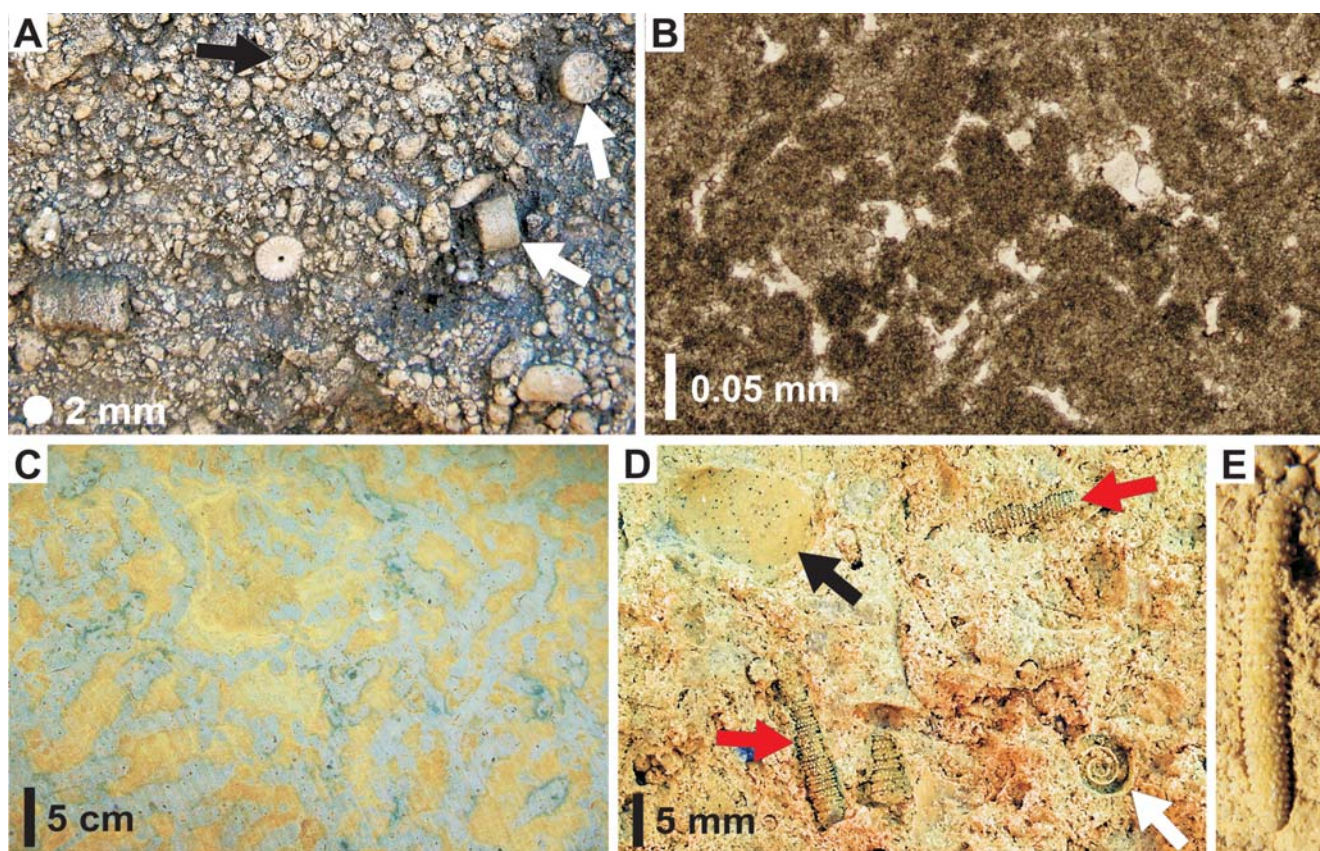


Fig. 14. Examples of shallow subtidal, dolomitic, sand-dominated lithofacies. **A.** Bedding plane view of coarse-grained, peloidal dolomitic packstone with sparse crinoid ossicles (white arrows) and gastropods (black arrow). **B.** Photomicrograph of A, showing well-rounded and poorly sorted peloids. **C.** Polished slab along bedding planes, illustrating dense network of the burrow *Balanoglossites*. **D.** Bedding plane view of fine-grained, peloidal dolomitic packstone containing frequent green algae (red arrows) and less common gastropods (white arrow) and bivalves (black arrow). **E.** 13-mm-long fragment of green alga. All pictures illustrate Diplopora Beds of Kraków–Silesia region.

horizon of intraformational conglomerate, found in the Tarnowice Beds, comprises lithoclasts containing the boring *Trypanites* (Fig. 5).

Environment

Like dolosiltites (D14), the intraformational dolomitic conglomerates represent shallow subtidal zones (Figs 3, 4A). The lithoclasts may represent eroded hardened crusts, occupying lagoon floors or inter- and supratidal flats. The dominant horizontal alignment of pebbles and concurrent lack of sedimentary structures within the surrounding sediment indicate rapid deposition of mixed material, transported in suspension by strong currents of inferred tidal or storm origin.

Peloidal dolostones (D16)

Characteristics

These are yellow-grey, peloidal grainstones and packstones (dolarenites), rarely wackestones (dolosiltites), containing rare bioclasts (green algae, crinoids, gastropods, bivalves), ooids and oncoids (Fig. 14A). The peloids are generally well-rounded and moderately sorted (Fig. 14B), but some layers are composed of poorly rounded and poorly

sorted ones. The peloidal dolostones form thick amalgamated packages. They hardly ever display planar bedding or cross-bedding (trough, tabular, or herringbone), but their tops may be shaped as symmetrical ripples (10–20 cm long) and dunes (0.5–1.5 m long). Locally, the peloidal dolostones contain well-developed networks of the burrow *Balanoglossites* infilled by dolomitic mud (Fig. 14C). The peloidal dolostones fill all of several recognized tidal channels (Matysik, 2012, 2014).

The peloidal dolostones are the most abundant lithofacies of the Diplopora Beds of the Kraków–Silesia region. They also occur as sparse intercalations within the Tarnowice and Boruszowice beds (Figs 2, 5).

Environment

The peloidal dolostones are interpreted as the deposits of shallow subtidal settings isolated from normal-marine conditions (Figs 3, 4A). Some of them might have been formed in a high-energy milieu, as indicated by occasional current cross-bedding and grainstone texture; however, most peloids must have accumulated in relatively tranquil areas. Frequent symmetrical ripples and dunes indicate that the area was subjected to wave activity, which also could have been responsible for removing the mud. Locally, sedimenta-

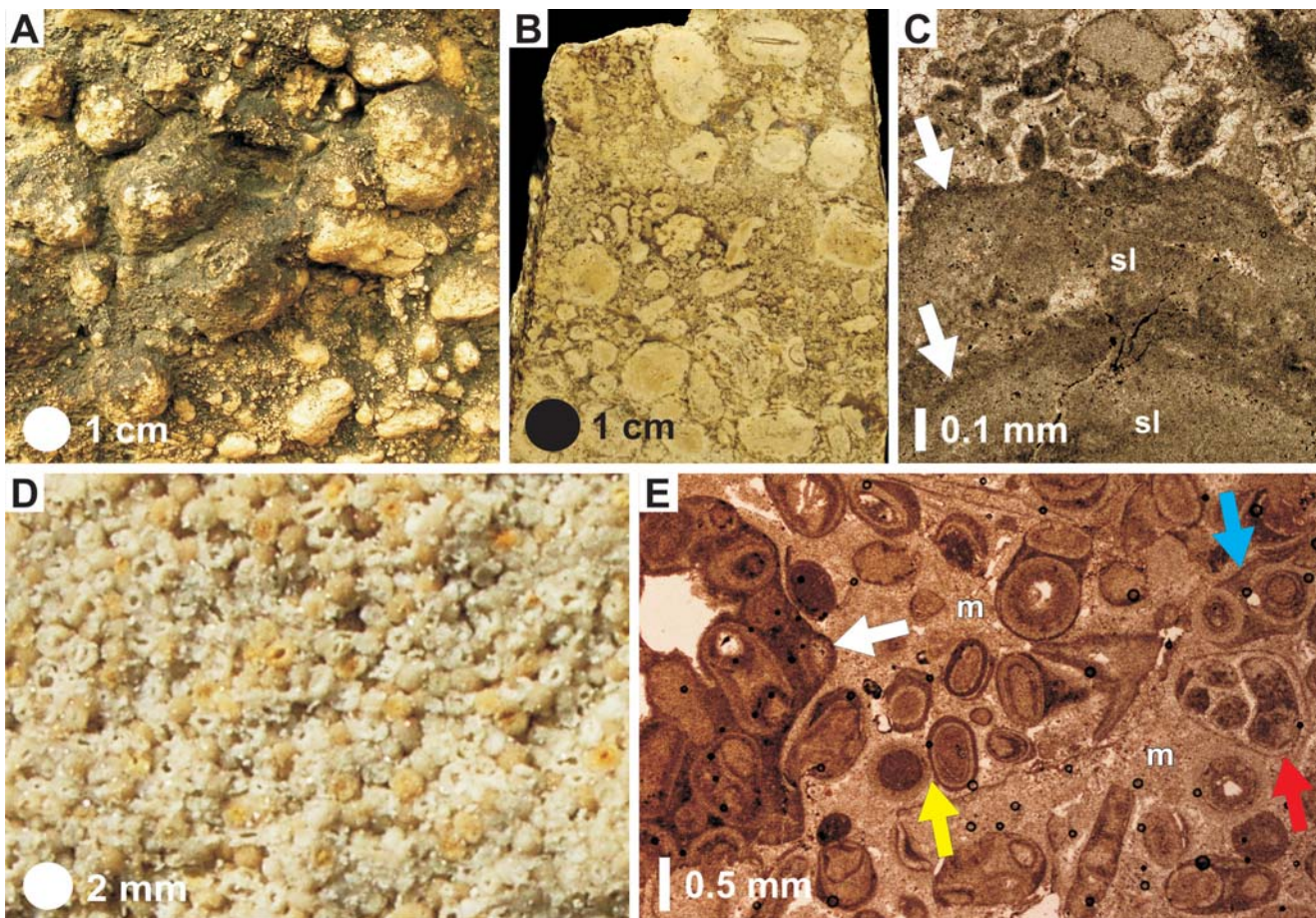


Fig. 15. Examples of shallow subtidal, dolomitic, coated grain lithofacies. **A.** Vertical outcrop view of structureless, poorly sorted, oncoidal dolomitic rudstone. **B.** Vertically oriented slab of A, showing randomly oriented, subspherical and flattened oncoids, floating in peloid-dominated matrix. **C.** Photomicrograph of B, showing oncoid cortex composed of two sets of dark, thinner micritic laminae (arrows) and light, thicker microsparitic-sparitic ones (sl). The oncoid is covered by peloidal grainstone. **D.** Vertical outcrop view of ooidal dolomitic packstone. **E.** Photomicrograph of D, showing microsparitic matrix (m) enclosing small (~0.5 mm across) ooids with radial-fibrous fabric, polyooids (blue arrow), gastropods (red arrow) and lithoclasts of ooidal packstone (white arrow). Note that contacts between ooids possess dissolved margins (yellow arrow). All pictures illustrate Diplopora Beds of Kraków–Silesia region.

tion ceased for a long time to enable the extensive colonization of the substrate by opportunistic infauna and the development of the trace fossil *Balanoglossites*.

have been at least semi-restricted to facilitate the early diagenetic dolomitization of the accumulated sediments (Figs 3, 4A). The lack of sedimentary structures suggests that the green algal debris was generally deposited *in situ*.

Green algal (*Dasycladaceae*) dolostones (D17)

Characteristics

These are yellow-orange-grey, green algal grainstones-packstones and rudstones, also containing frequent gastropods and bivalves (Fig. 14D, E). The matrix consists of poorly sorted and moderately rounded peloids and forams. Some peloids are an abrasional product of algae. The green algal dolostones show no sedimentary structures. This facies type occurs exclusively in the Diplopora Beds of both the Kraków–Silesia and Opole regions (Figs 2, 5).

Environment

Green algae typically form meadows in low-energy, mud-free, open lagoons and bays (Wray, 1977; Berger and Kaever, 1992). However, this particular environment must

Oncoidal dolostones (D18)

Characteristics

These are yellow, structureless, oncoidal rudstones and floatstones (Fig. 15A, B), with a matrix consisting of poorly rounded and sorted peloids, bioclasts (forams, green algae, bivalves, gastropods, crinoids) and cortoids. The oncoids are 0.5–4 cm in diameter, subspherical to ellipsoidal in shape and symmetrical in cross-section (sporadically asymmetrical), poorly sorted and display random orientation within a layer. The oncoids have thick cortices, composed of dark, thinner, micritic laminae and light, thicker, microsparitic-sparitic ones (Fig. 15C). The laminae have lobate shapes and are arranged in a concentric or partially overlapping manner. Some oncoids seem to contain no nucleus;

other oncoids developed around a disarticulated micritized bivalve shell or a peloidal-bioclastic deposit. Locally, the internal structure of oncoids is obliterated, owing to recrystallization.

The oncoidal dolostones exclusively form the middle part of the Diplopora Beds in the Kraków–Silesia region (Figs 2, 5), where they are regarded as a widespread correlation horizon (Alexandrowicz, 1971; Bilan and Golonka, 1972; Myszkowska, 1992). However, Matysik (2014) has recognized that in many sections the oncoidal dolostones are laterally replaced by green algal dolostones (D17) and peloidal dolostones (D16).

Environment

Large oncoids with lobate laminae, including the most external ones, are typically formed in “low-energy” settings (Flügel, 2010); nevertheless the prevailing subspherical shape and symmetrical cross-sections of the oncoids discussed indicate frequent overturning. Some oncoids accreted in a stationary position, as indicated by their asymmetrical growth patterns. The alternation of dark, thinner, micritic laminae and light, thicker, microsparitic-sparitic ones points to short-term changes in environmental conditions during oncoid growth. Random orientation and poor sorting of the oncoids indicate that transport before final deposition was short or even absent. The dolomitic nature of these deposits and overall paucity of fossils most likely reflect elevated salinity of this environment. In summary, the oncoidal dolostones are considered to represent a restricted and temporarily turbulent setting, probably a back-barrier area (Figs 3, 4A).

Ooidal dolostones (D19)

Characteristics

These are yellow, ooidal packstones (Fig. 15D), containing frequent bioclasts (gastropods and bivalves) and rare peloids, cortoids and lithoclasts of ooidal packstones (Fig. 15E). The ooids are small (abundantly ~0.5 mm, occasionally ~1.0 mm in diameter), rounded and moderately to well-sorted. Most ooids have small peloid nuclei and thick cortices, displaying a well-preserved radial-fibrous fabric (Fig. 15E); ooids with a thin cortex around a large peloid nucleus, or ooids with a concentrical (tangential) fabric are rare. The margin of some ooids was dissolved at the contact with other ooids. Two or more ooids are commonly bound together to form the nuclei for a new larger composite ooid (polyooid). All grains are embedded within microspar. The ooidal dolostones rarely display high-angle cross-bedding.

The ooidal dolostones occur as sparse intercalations within the Tarnowice Beds. They also make up a horizon 50 cm thick that directly underlies the hemispheroidal stromatolites (D12) of the Diplopora Beds in the Kraków–Silesia region (Figs 2, 5).

Environment

Marine ooids are formed in turbulent, tidally influenced settings, where the supply of potential nuclei is considerable and the waters are oversaturated with respect to carbonates. A radial-fibrous fabric is typical of ooids precipitating in “low-energy” conditions, as proved by laboratory experi-

ments (e.g., Davies *et al.*, 1978; Deelman, 1978; Ferguson *et al.*, 1978) and investigations of modern depositional settings (e.g., Loreau and Purser, 1973; Davies and Martin, 1976; Land *et al.*, 1979). The overall small size of the ooids discussed confirms that the site of ooid precipitation was characterized by “weak” agitation. The microsparitic matrix and rare cross-bedding indicate that the ooids also accumulated in calm areas. Taking these considerations into account, the ooidal dolostones are interpreted as representing a “low-energy”, tidally dominated environment, namely restricted embayments and their tidal inlets (Figs 3, 4A).

Ferricretes (L01)

Characteristics

These are orange-red, centimetre-thick crusts, resting on an irregular, subaerially weathered or bioturbated and bored surface (Fig. 16A, B). The ferricretes exhibit a micro-nodular texture, accentuated by iron oxides. They contain dispersed oncoids, peloids, bioclasts (mostly crinoids and rare bivalves, gastropods and forams) and silt-sized quartz grains (Fig. 16C). The ferricretes mark the upper boundary of the Górażdże Formation (Figs 2, 6).

Environment

The ferricretes formed on emerged peloidal-oncoidal shoal sands or lime muds (Fig. 3). The carbonate and quartz grains might have been blown onto the ferricrete surface by the wind.

Green algal (*Dasycladaceae*) limestones (L02)

Characteristics

These yellow-orange-grey green algal grainstones-packstones and rudstones (Fig. 16D, E) are locally rich in gastropods, bivalves, crinoids and corals. The matrix consists of poorly sorted, angular peloids and forams. Some peloids are an abrasional product of the algae. The grains are in many cases surrounded by thick rims of early marine cements (Fig. 16E). The green algal limestones do not display any sedimentary structures. They occur locally in the Diplopora Beds of the Opole region (Figs 2, 6).

Environment

The green algal limestones probably represent tranquil, clear, well-circulated, shallow subtidal areas within embayments or lagoons (Wray, 1977; Berger and Kaever, 1992) or behind high-energy bars (Figs 3, 4B). The precipitation of early marine cements is generally enhanced by decreased sedimentation rates and the intense pumping of sea water through the sediment.

Ooidal limestones (L03)

Characteristics

These are white-yellow, ooidal grainstones, consisting of large (~1 mm in diameter) ooids (Fig. 16F) with some contribution of peloids, cortoids, polyooids and bioclasts (gastropods, bivalves, brachiopods and crinoids). Some ooid margins show evidence of solution at the contact with

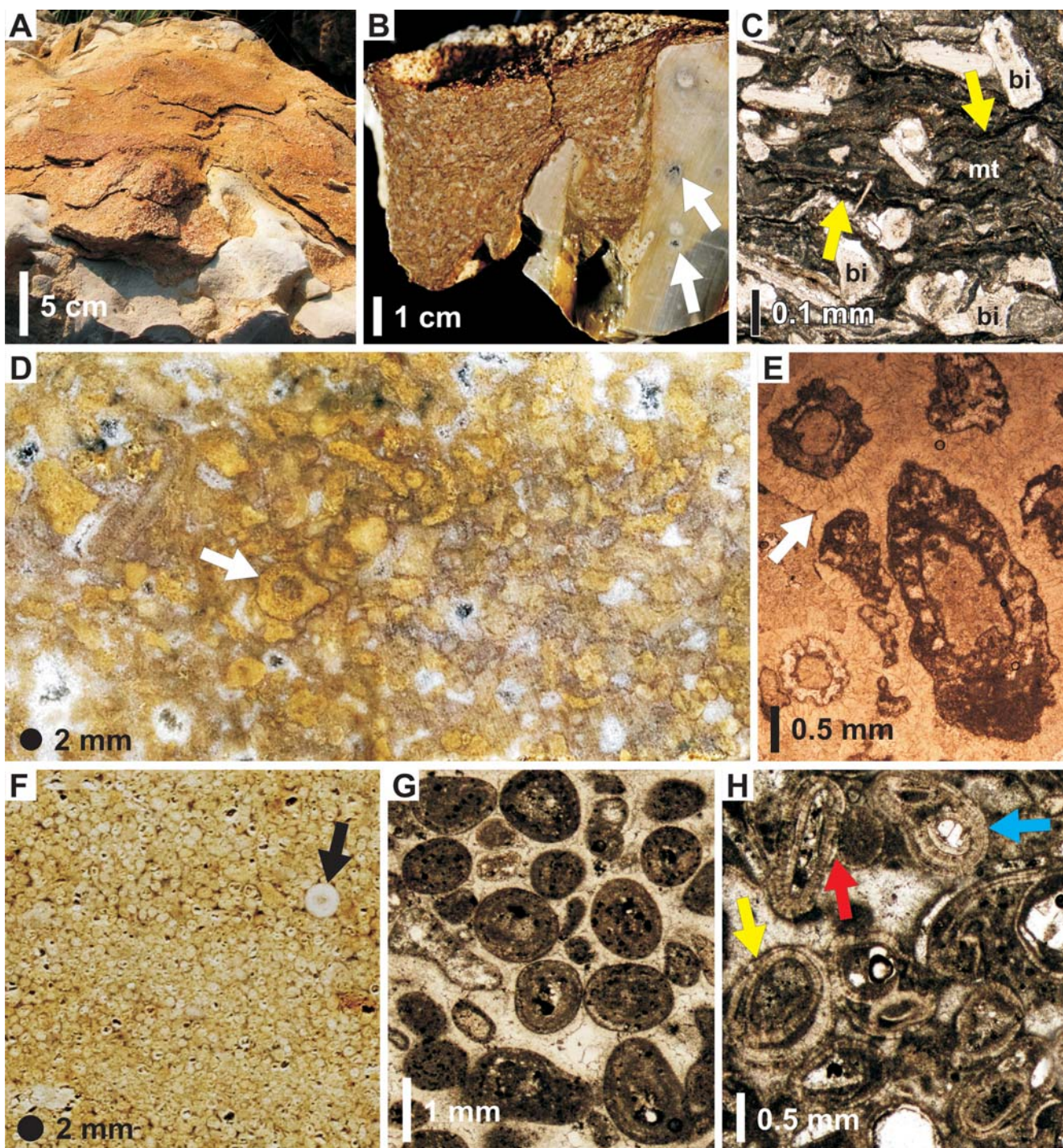


Fig. 16. Examples of supratidal and shallow subtidal, limestone lithofacies. **A.** Vertical outcrop view of ferricrete crust developed on firmground. **B.** Vertically oriented slab of ferricrete crust capping irregular, subaerially weathered hardground with the boring *Trypanites* (arrows). **C.** Detail of B, showing micronodular texture (mt) accentuated by iron oxides (arrows). The bioclasts (bi) might have been blown onto ferricrete surface by wind. **D.** Vertically oriented slab of green algal grainstone-rudstone. All the yellowish elements are fragments of green algae in different sections (arrow points at transverse section). **E.** Photomicrograph of D, showing several ring-like fragments of green algae enclosed by thick rims of early-marine cements (arrow). **F.** Vertically oriented slab of ooidal grainstone containing sparse crinoid elements (arrow). **G.** Photomicrograph of F, showing large (~1 mm across) normal ooids with poorly preserved concentrical lamination enclosed by sparry cement. **H.** Photomicrograph of ooidal packstone-grainstone consisting of large (~1 mm across) superficial ooids with radial-fibrous cortices. Note that many ooids are regenerated (yellow arrow), coated together to form polyooids (blue arrow), and possess dissolved margins at contacts with other ooids (red arrow). Pictures: A–C – topmost part of Górażdże Formation, Opole region; D–G – Diplopora Beds, Opole region, H – the lowermost part of Gogolin Formation, Kraków–Silesia region.

other ooids. On the basis of ooid internal structure, two subdivisions can be recognized:

A) These ooids have small peloid nuclei and thick cortices (= normal ooids), displaying poorly-preserved concentric laminations (Fig. 16H). The ooids are moderately to well-sorted and well-rounded. This subtype is characteristic of the lowermost part of the Diplopora Beds (Figs 2, 6) which overlies the sponge bioherms (L08) in the Opole region (Fig. 4B).

B) These ooids have large peloid or bioclast nuclei and thin cortices (= superficial ooids) that display well-preserved radial-fibrous fabric (Fig. 16G). The ooids are poorly to moderately sorted and moderately to well-rounded (depending on the shape of the nucleus). Some ooids are broken and regenerated. This subtype is common in the lowermost part of the Gogolin Formation (Figs 2, 5).

Environment

Marine ooids generally represent turbulent, tidally influenced settings. The overall large size of the ooids discussed and the total lack of micrite between the grains indicate that both the sites of ooid precipitation and deposition were characterized by strong agitation. However, the superficial ooids of subtype B were formed in “lower-energy” conditions than the normal ooids of subtype A, as evidenced by the differences in arrangement of the crystals within their cortices (e.g., Loreau and Purser, 1973; Davies and Martin, 1976; Davies *et al.*, 1978; Deelman, 1978; Ferguson *et al.*, 1978; Land *et al.*, 1979). Today, the latter ooids occur on the crests of bars and tidal deltas over the Bahama platforms (e.g., Newell *et al.*, 1960; Bathurst, 1975) and along the Trucial Coast (e.g., Loreau and Purser, 1973).

Oncoidal limestones (L04)

Characteristics

Their matrix consists of poorly to moderately sorted and rounded peloids, rare to frequent bioclasts (brachiopods, bivalves, gastropods, green algae, forams, crinoids) and cortoids, sporadic superficial ooids and angular to subrounded lithoclasts of grey calcilutites. The oncoids developed around disarticulated and micritized bioclasts, peloidal-bioclastic deposits or without any specific nucleus, which determined the oncoid shape. On the basis of oncoid size and cortex composition, three subdivisions can be recognized:

A) White-beige, oncoidal floatstones and rudstones (Fig. 17A). The oncoids are 0.5–2 cm across and generally symmetrical in cross-section. Most of them have thick cortices with well-preserved *Girvanella* tubes (Fig. 17B), which form either a continuous coat around the central part (laminar growth form) or several contiguous columns (lobate growth form). This subtype occurs in the lowermost part of the Gogolin Formation and just above the sponge-coralline bioherms of the Karchowice Formation (Figs 2, 4B, 6).

B) White-yellow, oncoidal floatstones and rudstones (Fig. 17C). The oncoids are 0.5–4 cm in diameter and symmetrical to highly asymmetrical. They have thick cortices, composed of alternating dark thinner micritic and light thicker microsparitic-sparitic laminae, which have irregular

lobate shapes and have a concentric to partially overlapping arrangement (Fig. 17D, E). The cortices contain sparry fenestrae and serpulid encrustations. The oncoids of reefal settings may contain coral fragments as nuclei (Fig. 17E). This subtype is characteristic of the middle part of the Górażdże Formation and the lowermost part of the Diplopora Beds, capping directly the sponge biostromes and filling the pockets between the sponge-coralline bioherms of the Karchowice Formation (Figs 2, 4B, 6).

C) White-beige-grey, oncoidal grainstones and rudstones (Fig. 17F), rarely wackestones-packstones and floatstones. The oncoids are characterized by small dimensions (usually 1–3 mm across, rarely 4–5 mm), regular shapes and dense micritic cortices, exhibiting vague, concentric laminations (Fig. 17G). Forams (*Pillamina* sp.) are commonly incorporated into the cortices. This subtype occurs exclusively in the Górażdże Formation (particularly in its lower and upper parts), and in the Hauptcrinoidenbank of the Dziewkowice Formation (Figs 2, 6).

Regardless of the subtype, the oncoids are aligned with their long axes parallel to the bedding or cross-bedding planes. The oncoidal limestones usually form amalgamated packages 0.3–1.5 m thick that only rarely display cross-bedding (low-angle, tabular, trough and herringbone). The tops of many oncrites are shaped as straight or sinusoidal, bifurcating, symmetrical dunes 0.5–1.5 m long (occasionally up to 10 m long; Fig. 17H).

Environment

The three subtypes of oncoidal limestones distinguished differ from one another in many respects, especially in oncoid composition, size, shape and growth pattern, which reflect different environmental conditions. The *Girvanella* oncoids of subtype A were unequivocally formed in clear waters, whereas the microbial oncoids of subtype B and C did not require access to the light (Flügel, 2010). Regarding the water energy, the oncoids of subtype C apparently grew in a high-energy, permanently turbulent setting, evidenced by their small size, concentric symmetrical growth patterns and common subspherical shape (Flügel, 2010). They were also deposited in a similar regime of higher energy, responsible for creating grain-supported textures. In contrast, the oncoids of subtype A and B generally display features, regarded as typical of quiet-water oncoids, such as the large size or lobate shape of laminae (Flügel, 2010). On the basis of these considerations, the oncoidal limestones of subtype C are interpreted as representing high-energy banks and bars (Fig. 3), whereas the oncoidal limestones of subtypes A and B were formed in generally calm, normal-marine setting, in back-barrier areas and between organic buildups (Fig. 4B).

Cortoidal limestones (L05)

Characteristics

These are beige, cortoidal rudstones and grainstones (Fig. 18A), rarely floatstones and packstones. The facies is composed predominantly of bioclasts (mostly bivalves, brachiopods and crinoids, subordinately gastropods), exhibiting thin, non-laminated micritic rims that originated both from constructive and destructive micritization (Fig. 18B, C).

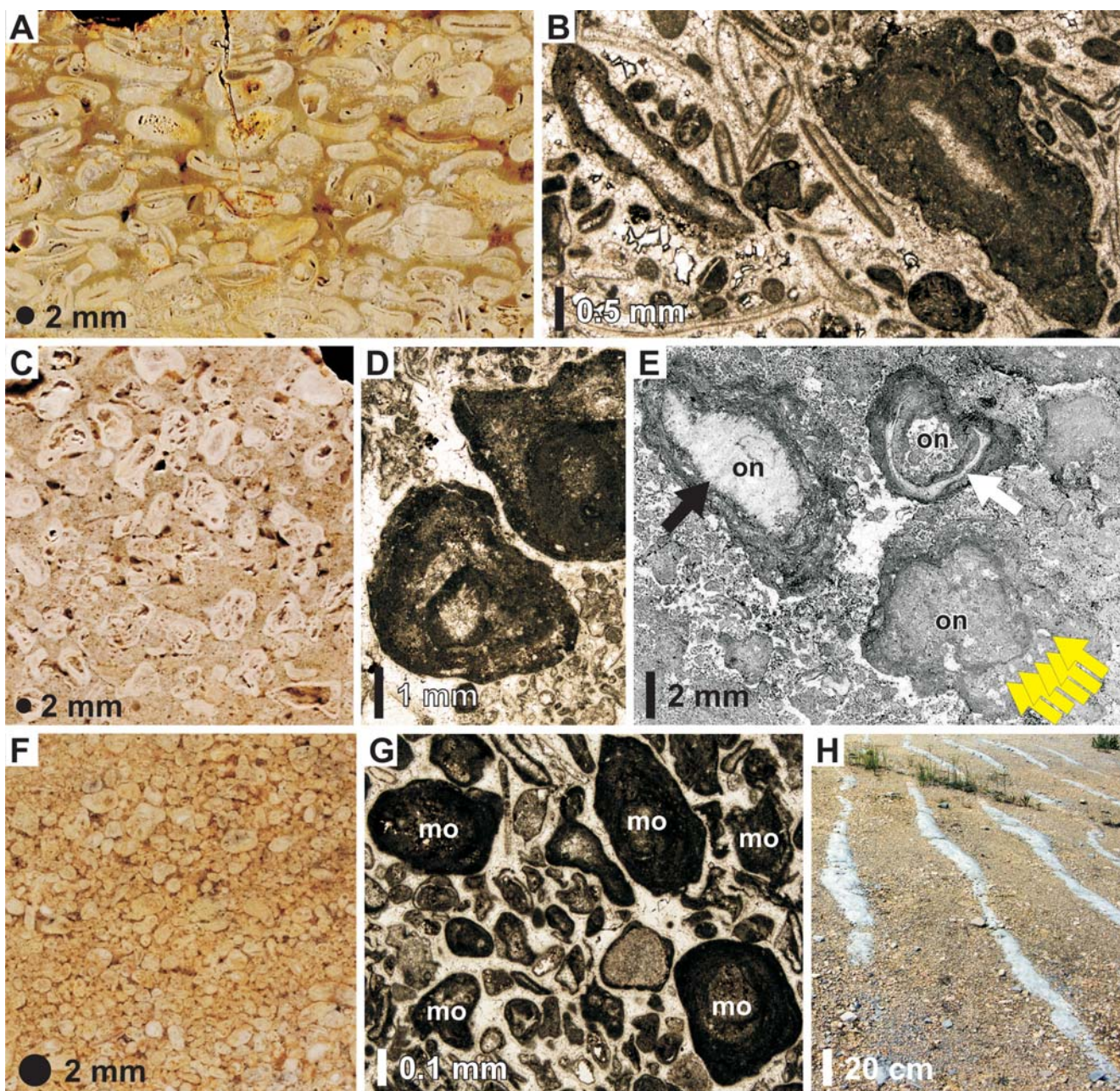


Fig. 17. Examples of oncoidal limestones. **A.** Vertically oriented slab of oncoidal floatstone composed of mixed symmetrical to highly asymmetrical, large (~1 cm across), ellipsoidal to flattened *Girvanella* oncoids. **B.** Photomicrograph of oncoidal rudstone consisting of *Girvanella* oncoids surrounded by peloidal-bioclastic matrix and spar cement. *Girvanella* tubes form continuous coat around the bioclastic nuclei. **C.** Vertically oriented slab of oncoidal rudstone consisting of large (~1 cm across), irregularly shaped, microbial oncoids. **D.** Photomicrograph of C, illustrating two microbial oncoids composed of several sets of dark thinner micritic laminae and light thicker microsparitic-sparitic ones. **E.** Photomicrograph of oncoidal floatstone with peloidal-micrite matrix. The oncoids (on) developed around brachiopod shells (white arrow) and coral fragments (black arrow). The oncoid cortices are composed of alternating thinner micritic and thicker microsparitic laminae. The latter include spar-infilled serpulid encrustations (yellow arrows). **F.** Vertically oriented slab of oncoidal grainstone composed of small (up to 2 mm across) regular microbial oncoids. **G.** Photomicrograph of F, showing small, ellipsoidal, microbial oncoids with vague concentric laminations (mo), enclosed by peloidal matrix and sparite. **H.** Outcrop view of top surface of oncoidal limestone shaped as 1-m-long sinusoidal, symmetrical dunes. Pictures: A – Gogolin Formation, Kraków–Silesia region; B – Karchowice Formation, Opole region; C–G – Górażdże Formation, Opole region.

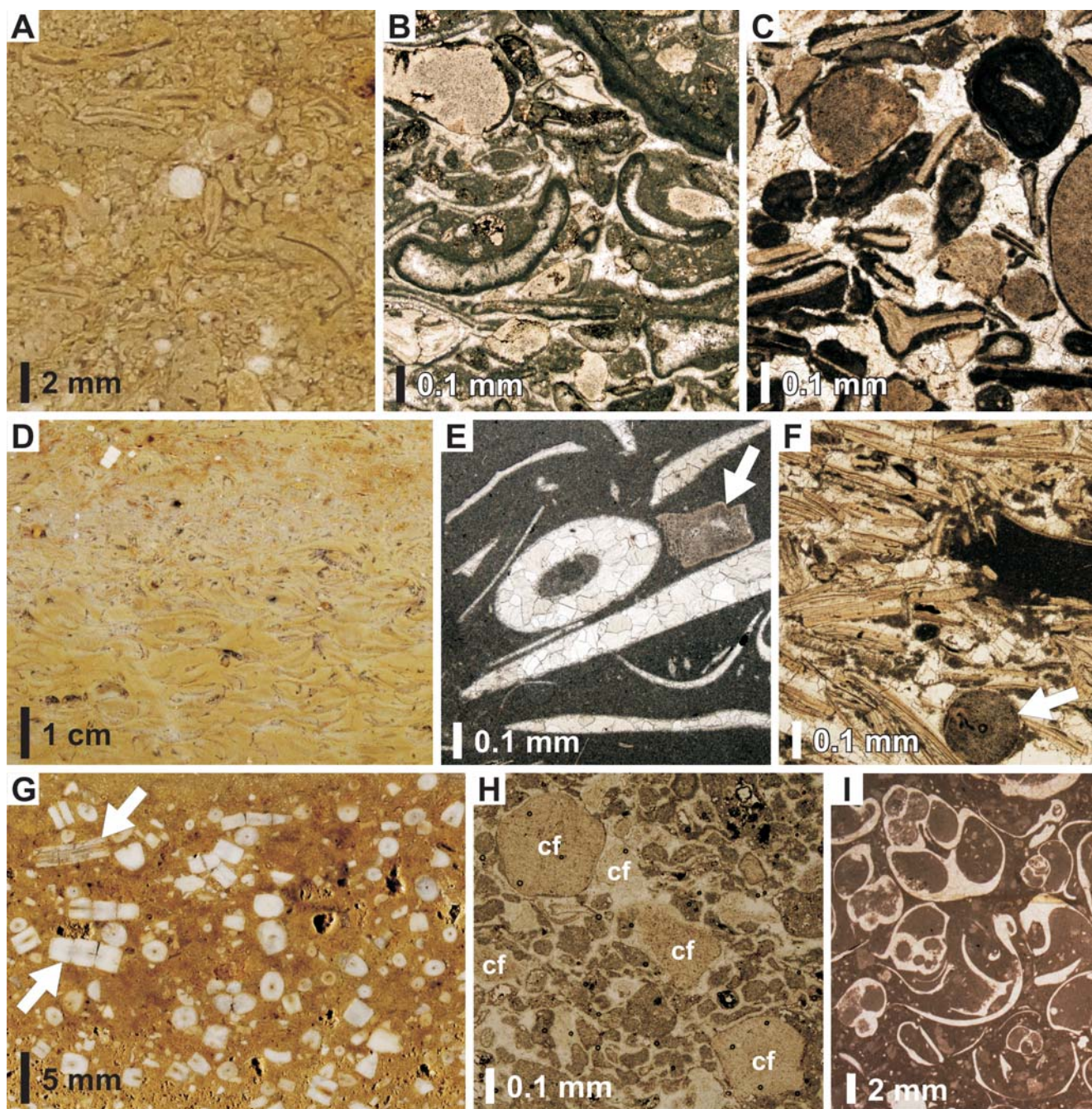


Fig. 18. Examples of bioclast-dominated limestone lithofacies. **A.** Vertically oriented slab of cortoidal rudstone. **B, C.** Photomicrographs of cortoidal floatstone and rudstone composed of bioclasts, mostly possessing thin non-laminated micritic rims. **D.** Vertically oriented slab of brachiopod floatstone grading upwards into bivalve wackestone. Note horizontal alignment of shells. **E, F.** Photomicrographs of brachiopod floatstone and bivalve rudstone, both containing sporadic crinoid ossicles (arrows). **G.** Vertically oriented slab of crinoid floatstone. Note that some crinoid ossicles are articulated (arrows), indicating rapid burial. **H.** Photomicrograph of G, showing disarticulated crinoid fragments (cf) enclosed by peloidal matrix and spar cement. **I.** Photomicrograph of gastropod floatstone. Pictures: A, B, G, H – Karchowice Formation, Opole region; C, I – Dziewkowice Formation, Opole region; D–F – Gogolin Formation, Kraków–Silesia region.

Interiors of some bioclast reveal the microborings of microbes and fungi; however, in many cases they have been destroyed almost completely by microborer activity. Non-coated bioclasts, peloids, superficial ooids and micritic oncoids are accessory constituents. The cortoidal limestones commonly form straight or sinusoidal, bifurcating, symmet-

rical ripples (0.2–0.4 m long) and dunes (0.5–2.0 m long), which are amalgamated in packages, several metres thick. The cortoidal limestones occur in the lowermost part of the Gogolin Formation, in the Hauptcrinoidenbank of the Dziewkowice Formation and in the Karchowice Formation (Figs 2, 4B, 6).

Environment

The cortoidal limestones represent sedimentation in the shallow, subtidal zone, above the fair-weather wave base (Fig. 3). The formation of micrite envelopes required longer periods of substrate stability and bioclast exposure on the sea floor, enabling the colonization of grain surfaces by microborers (Bathurst, 1966; Swinchant, 1969).

Bioclastic limestones (L06)

Characteristics

These are grey-beige-white, bioclastic floatstones and rudstones, rarely wackestones-grainstones with a matrix, composed of poorly rounded and poorly sorted peloids. Depending on the dominant type of bioclasts, three subdivisions can be recognized:

A) The main constituents are bivalve and brachiopod shells, which may be articulated, disarticulated and/or broken (Fig. 18D–F). The shells are commonly aligned parallel to bedding planes and oriented convex-up or concave-up, depending on the mechanism of deposition. This subtype is abundant in the Gogolin and Dziewkowice formations, and sporadic in the Olkusz Beds and the Karchowice Formation (Figs 2, 5, 6).

B) The main constituents are crinoid ossicles, which may be articulated and/or disarticulated (Fig. 18G, H). This subtype typically occurs on the flanks of sponge-coral bioherms of the Karchowice Formation (Figs 2, 4B, 6, see also Fig. 20A). It is rare in the Gogolin and Dziewkowice formations and the Olkusz Beds.

C) The main constituents are gastropod shells (Fig. 18I). This subtype is uncommon; it appears rarely in the Gogolin and Dziewkowice formations.

The bioclastic limestones commonly occur as coquinas, 1–30 cm thick, displaying sharp scoured bases, normal grading and rare small-scale cross-bedding. The coquinas occur as intercalations in the fine-grained limestones listed below (lithofacies L11–L16). The bioclastic limestones of subtype B also form thick, amalgamated packages. Some layer tops are shaped as straight or sinusoidal, bifurcating, symmetrical dunes, 0.5–2.0 m long, or as oscillatory ripples, 20–40 cm long. The bioclastic limestones of the Gogolin Formation are locally rich in glauconite.

Environment

The bioclastic coquinas display typical tempestite features, such as sharp scoured bases and normal grading (Harms *et al.*, 1975; Kreisa, 1981; Walker, 1982; Aigner, 1985; Duke, 1985; Myrow and Southard, 1996; Einsele, 2000). In addition, the bivalve and brachiopod elements are abundantly oriented convex-down, as a consequence of material settling from suspension during a weakening storm (e.g., Clifton, 1971). Also articulated crinoid ossicles are an indicator of rapid burial, which prevented the post-mortem disarticulation of crinoid skeletons (Meyer, 1971; Liddel, 1975; Brower and Veinus, 1978). Therefore, the bioclastic coquinas of the type discussed are regarded as proximal tempestites by many authors (Dżułyński and Kubicz, 1975; Chudzikiewicz, 1982; Bodzioch, 1985; Szulc, 2000; Matyśkik, 2010). They apparently were deposited on the lower

shoreface, the zone between the storm and fair-weather wave base, since they occur as intercalations in the fine-grained limestones (Fig. 3).

The thick, amalgamated packages of bioclastic limestones of subtype B indicate in turn sedimentation in a high-energy, mud-free zone, probably on the upper shoreface (Fig. 3). The rapid burial, exemplified by common articulated crinoid ossicles (Meyer, 1971; Liddel, 1975; Brower and Veinus, 1978), may in this case be related to high carbonate production in a circum-reefal environment.

Peloidal limestones (L07)

Characteristics

These are white-beige-grey, peloidal grainstones and packstones (Fig. 19A), rarely wackestones, containing sporadic to abundant bioclasts (bivalves, brachiopods, gastropods, crinoids, forams and green algae), cortoids, oncoids and lithoclasts of grey calcilutites. On the basis of peloid size, shape, internal structure and degree of sorting, several subdivisions of this facies can be recognized:

A) The peloids are poorly rounded and poorly sorted and many exhibit a lobate outline (Fig. 19B). This subtype is the most ubiquitous in the limestone domain and widespread throughout all the formations (Figs 2, 4B, 5, 6, 20A).

B) The peloids are small (commonly <0.5 mm in diameter), well-sorted, and have ellipsoidal shapes (Fig. 19C). This subtype occurs in the lower part of the Olkusz Beds (Figs 2, 5).

C) The peloids are large (~1 mm in diameter), well-rounded and well-sorted (Fig. 19D). Their internal structure is commonly recrystallized, but some of them display very poorly preserved ooid-type concentric laminations. This kind of peloid is characteristic for the upper part of the Olkusz Beds (Figs 2, 5).

Many peloidal limestones are structureless, although some display either sharp bases, normal grading and hummocky cross-stratification (features indicative of storm environments; Fig. 19E), or have top surfaces with the shape of straight or sinusoidal, bifurcating, symmetrical dunes, 0.5–10 m long (a feature common in wave-dominated settings). Other limestones form amalgamated packages, exhibiting low-angle, tabular, trough and herringbone cross-bedding as well as laterally accreted bedsets (features diagnostic of current deposition; Fig. 19F). The amalgamated packages locally contain *Arenicolites* isp. and *Skolithos* isp.

Environment

As evidenced by sedimentary structures, the peloidal limestones represent various mechanisms of deposition and various depositional settings (Fig. 3). Hummocky cross-stratification, sharp bases and normal grading are diagnostic of storm deposition (Harms *et al.*, 1975; Kreisa, 1981; Walker, 1982; Aigner, 1985; Duke, 1985; Myrow and Southard, 1996; Einsele 2000). Trough and tabular cross-bedding are formed by unidirectional, strong currents on the upper shoreface. Herringbone cross-bedding indicates deposition from reversing tidal currents. Low-angle cross-bedding is typical of upper plane-bed conditions, which characterize the foreshore (e.g., Reading, 1978).

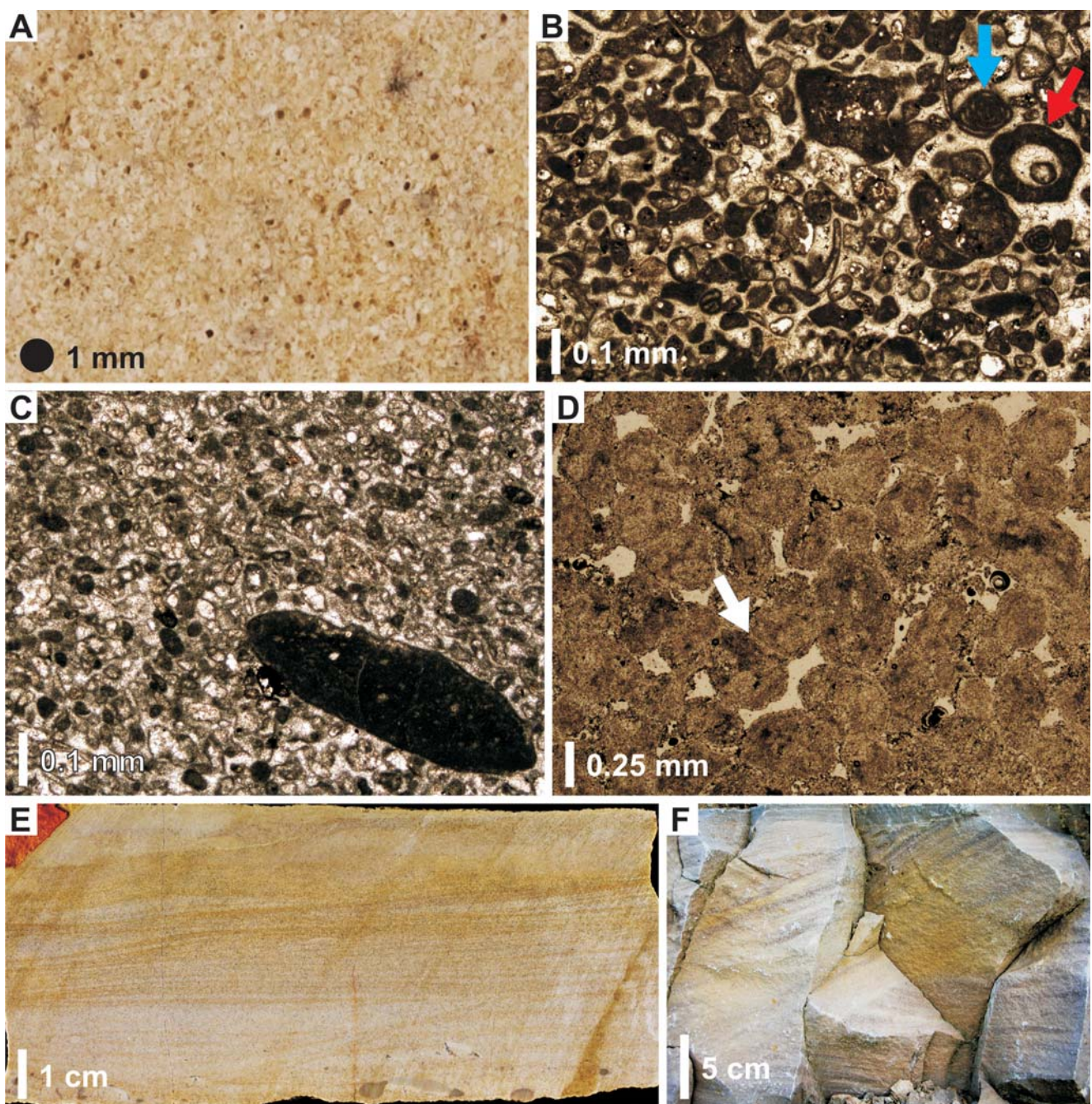


Fig. 19. Examples of peloidal limestones. **A.** Vertical outcrop view of peloidal grainstone. **B.** Photomicrograph of peloidal grainstone consisting of lobate peloids (micritized ?aggregate grains), and sporadic forams (blue arrow) and green algae (red arrow). **C.** Photomicrograph of peloidal grainstone consisting of ellipsoidal peloids (?faecal pellets) and rare micritic lithoclasts. **D.** Photomicrograph of peloidal grainstone consisting of subrounded recrystallized peloids, which occasionally display ooid-type concentric lamination and possess dissolved margins at contacts with other peloids (arrow). **E.** Vertically oriented slab of hummocky cross-stratified fine-grained peloidal packstone. **F.** Vertical outcrop view of planar-bedded medium-grained peloidal packstone (the right side of the picture), truncated by a high-angle cross-bedded one (the left side of the picture). Pictures: A, B, F – Górażdże Formation, Opole region; C, D – Olkusz Beds, Kraków–Silesia region, E – Gogolin Formation, Kraków–Silesia region.

The peloids themselves are also of various modes of origin. The large, spherical peloids of subtype C that occasionally display crude, concentrical lamination are most likely ooids, the internal structure of which was obliterated owing to recrystallization. The facies therefore might have originated in high-energy, tidally influenced settings. The ellipsoidal peloids of subtype B may be faecal pellets. The

best known, modern examples of massive accumulation of coprolites are low-energy areas with reduced sedimentation rates, occupying the interior of the Bahama platform and the inner South Florida shelf (e.g., Kornicker and Purdy, 1957; Enos and Perkins, 1977; Land and Moore, 1980; Wanless *et al.*, 1981). The lobate-shaped peloids of subtype A are presumably aggregate grains, which underwent complete mi-

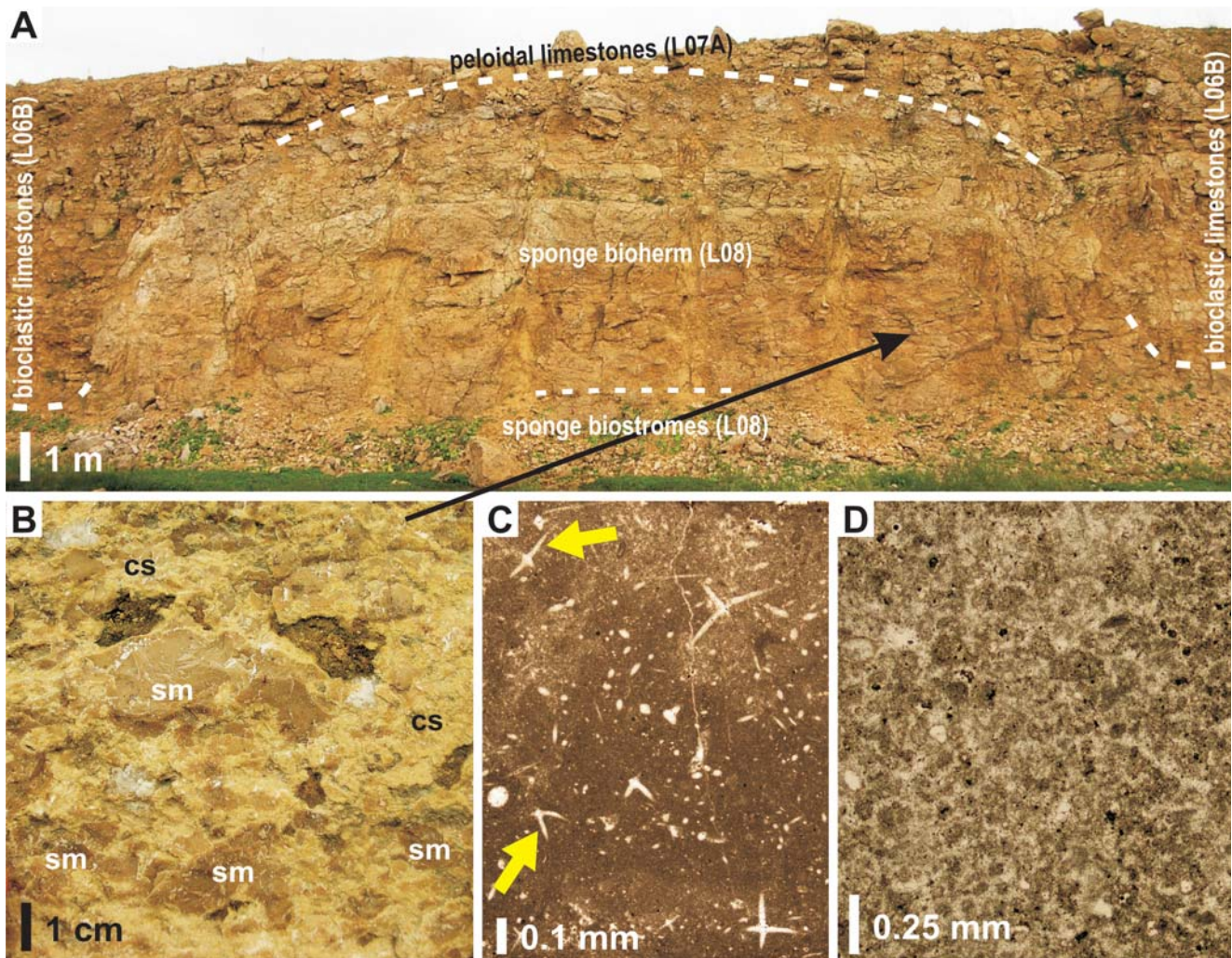


Fig. 20. Sponge buildups. **A.** Outcrop view of sponge bioherm enclosed by bioclastic limestones and capped by peloidal limestone. Tarnów Opolski. **B.** Vertical outcrop view of internal composition of a bioherm, showing mesoclotls of sponge automicrite (sm) surrounded by yellow calcisiltite (cs). **C.** Photomicrograph of sponge fragments composed of micrite with calcified spicules (arrows). **D.** Photomicrograph, showing clotted-peloidal microfabric of poorly recrystallized cavernous limestone that makes up some of the sponge bioherms. All pictures show Karchowice Formation of Opole region.

critization. The formation of aggregate grains requires periods of sediment stabilization and cementation (Illing, 1954; Purdy, 1963; Taylor and Illing, 1969; Winland and Matthews, 1974; Wanless *et al.*, 1981). Cementation is triggered by cyanobacteria, algae and fungi that live in the interstices between grains (e.g., Fabricius, 1977).

Sponge buildups (L08)

Characteristics

The sponge buildups include biostromes and bioherms. The individual biostromes are 3–10 cm thick, but they are amalgamated in laterally extensive units, several metres thick (Bodzioch, 1989; Matysik, 2010). The bioherms have hemispherical cross-sections and reach 6 m in height and 25 m in diameter (very rarely ~0.5–2 m high and 0.5–1 m across; Bodzioch, 1989; Szulc, 2000; Matysik, 2010; Fig. 20A). The framework of both biostromes and bioherms is predominantly formed by hexactinellid sponges (Pisera and Bodzioch, 1991; Bodzioch, 1993) that may be preserved as:

1) etched, siliceous, endosomal skeletons; 2) mummies and mesoclotls, composed of sponge automicrite with calcified spicules (Fig. 20B, C); or 3) recrystallized, cavernous limestones. In the latter case, the caverns are regarded as incompletely filled sponge paragasters and cavities between sponge bodies (Bodzioch, 1989; Szulc, 2000; Matysik, 2010) and where recrystallization was not advanced, the clotted-peloidal microfabric is discernible (Fig. 20D). In addition to sponges, some bioherms are also constructed by scleractinian corals and crinoids (Morycowa, 1988; Szulc, 2000; Morycowa and Szulc, 2010), and contain rich assemblages of dwellers and encrusters, including bivalves, brachiopods, gastropods, polychaetes, bryozoans, echinoderms, ostracods and green algae (Morycowa and Szulc, 2010).

The sponge buildups are characteristic of the Karchowice Formation, where they are concentrated in two stratigraphic horizons (Figs 2, 4B, 6). Each horizon, about 10 m thick, commences with a biostrome unit overlain by isolated sponge bioherms, enclosed in and separated by cortoidal limestones (L05), Bioclastic limestones (L06B) and peloi-

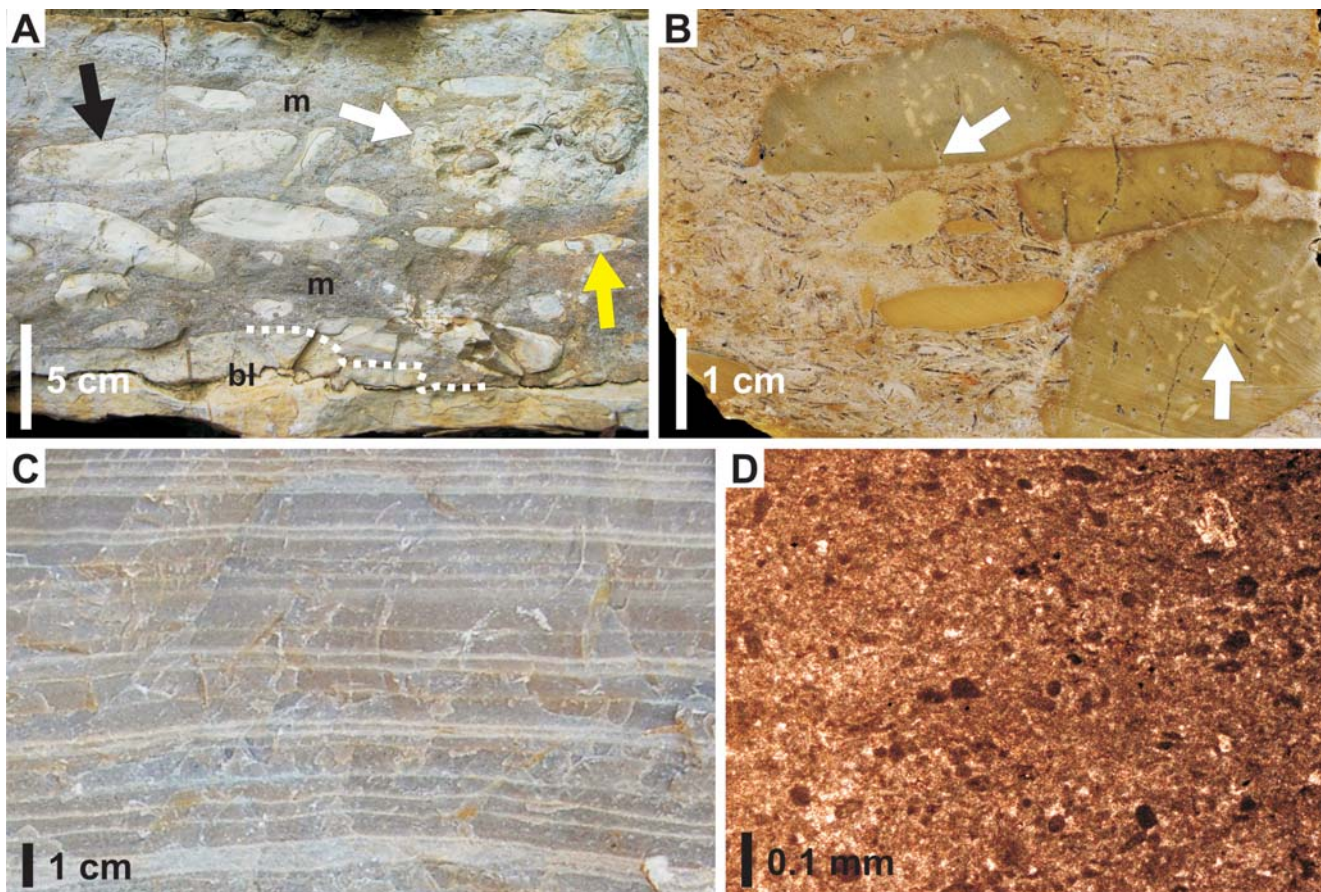


Fig. 21. Examples of intraformational limestone conglomerates and bedded fine-grained limestones. **A.** Vertical outcrop view of matrix-supported conglomerate layer composed of mixed horizontally-oriented flat pebbles of bioclastic limestone (white arrow), micritic limestone (yellow arrow), and micritic limestone with the boring *Trypanites* (black arrow), floating in peloidal-bioclastic groundmass (m). Note that the basal layer of the micritic limestone (bl) is partially reworked and presumably supplied some intraclasts to the conglomeratic layer. **B.** Vertically oriented slab of matrix-supported conglomerate comprising flat and surrounded pebbles of micritic limestone, embedded in bioclastic-peloidal matrix. Note that some pebbles are extensively bored (arrows). **C.** Vertical outcrop view of bedded calcisiltites exhibiting parallel lamination. **D.** Photomicrograph of C, showing sparse, horizontally-oriented peloids in micrite. Pictures: A, B – Gogolin Formation, Kraków–Silesia region; C, D – Górażdże Formation, Opole region.

dal limestones (L07A). The bioherms occur in a NE–SW-trending belt, which is interpreted as a slightly elevated (?tectonic) element of the sea-floor that was the first one to have risen up above the fair-weather wave base during the progressive filling of the area (Matysik, 2010). Smaller bioherms have also been found within the lowermost part of the Diplopora Beds in the Opole region (Fig. 2). These bioherms are laterally juxtaposed to composite buildups, surrounded by oncoidal limestones (L04B) and peloidal limestones (L07A).

Environment

The environmental controls on the development of sponge buildups have been discussed in detail by Bodzioch (1989, 1997a), Szulc (2000), Matysik (2010), and Morycowa and Szulc (2010). The sponge bioherms probably formed in the zone between storm and fair-weather wave base, in conditions of reduced sedimentation rate, while the sponge bioherms grew in a high-energy belt, under high input of calcareous detritus (Figs 2, 3, 4B, 6). Thus, the re-

placement of sponge biostromes by bioherms in the succession reflects the progressive shallowing of the area with a concomitant increase in energy.

Intraformational limestone conglomerates (L09)

Characteristics

These are bioclastic limestones (L06A), containing flat lithoclasts (Fig. 21A, B). The pebbles are commonly aligned parallel to bedding planes (rarely imbricated or randomly oriented) and distributed rather uniformly throughout the layer (Kubicz, 1971; Chudzikiewicz, 1975, 1982). The pebbles are composed of peloidal packstone, bioclastic floatstone and wackestone, calcisiltite or calcilutite. Some calcilutite pebbles contain the boring *Trypanites* or encrustations of the oyster-like bivalve *Placunopsis ostracina* (Schlotheim). One layer of intraformational conglomerate may comprise all lithological types of lithoclasts (Fig. 21A). The intraformational limestone conglomerates form laterally discontinuous kilometre-sized lenses that generally oc-

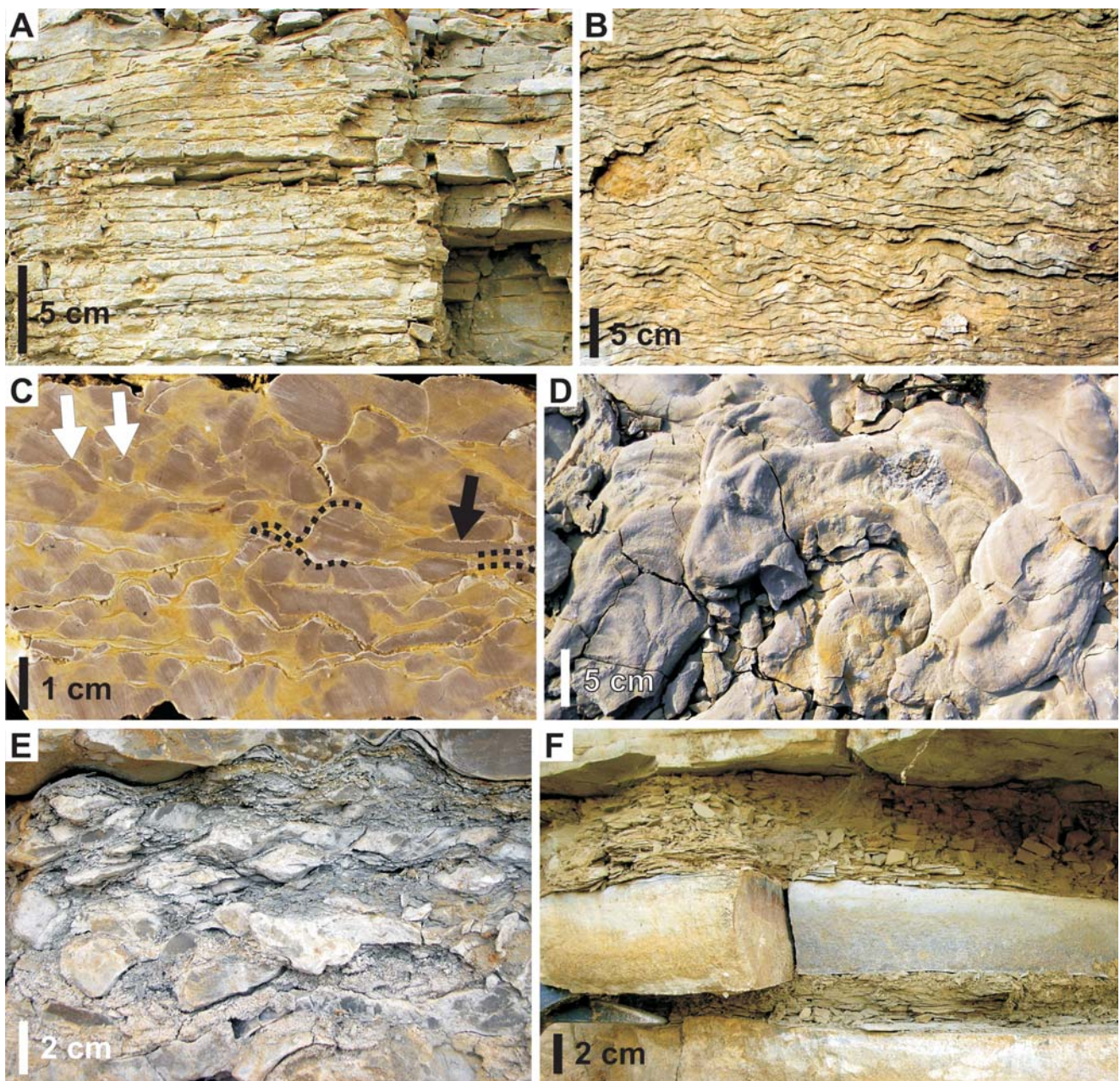


Fig. 22. Examples of open-marine, fine-grained limestone lithofacies. **A.** Vertical outcrop view of platy-bedded calcisiltite. **B.** Vertical outcrop view of clay-free wavy-bedded calcisiltite formed owing to syndepositional deformation of platy-bedded, precursor deposit. **C.** Vertically oriented slab of clay-free, nodular calcilutite with amalgamated nodules (dotted line) and numerous burrow *Rhizocorallium* in cross-section (white arrows) and oblique section (black arrow). **D.** Bedding plane view of nodular calcisiltite, showing horizontal, U-shaped, spreite burrow *Rhizocorallium* isp. completely filled with faecal pellets. **E.** Vertical outcrop view of nodular calcilutite. The nodules are enclosed by black claystone. **F.** Vertical outcrop view of two layers of limey claystone capping a basal intraformational conglomerate and sandwiching bedded calcisiltites (middle and top layer). A–D, F – Gogolin Formation, Kraków–Silesia region; E – Dziewkowice Formation, Opole region.

cur as intercalations in the fine-grained limestones listed below (lithofacies L11–L16).

The intraformational limestone conglomerates occur abundantly in the Wilkowice Beds and in the upper part of the Gogolin Formation (Figs 2, 5, 6). Rare conglomeratic intercalations were also found in the Dziewkowice Formation and in the lower part of the Gogolin Formation.

Environment

Like the bioclastic limestones (L06A), the intraformational limestone conglomerates are interpreted to represent proximal tempestites, deposited on the lower shoreface (Fig. 3). The occurrence of multi-generational rounded pebbles within one tempestite suggests multiple reworking and deep erosion of consolidated, lithologically differentiated

substrate (Sepkoski, 1982; Osleger and Read, 1991). The dominant horizontal alignment of pebbles and lack of an internal hiatus within the conglomerate layers seem to indicate the rapid deposition of both pebbles and matrix, transported in the mass of a dense flow (Chudzikiewicz, 1975).

Bedded calcisiltites and calcilutites (L10)

Characteristics

These are grey-beige lime mudstones and fine-grained, peloidal wackestones (Fig. 21C, D), containing rare forams and broken bivalves. The facies forms distinct beds, 5–30 cm thick and intercalated with the thin-bedded limestones listed below (lithofacies L11–L16). Parallel lamination, normal grading, hummocky cross-stratification or low-angle cross-bedding are occasionally present and transected by unidentifiable bioturbation structures. The bedded calcisiltites and calcilutites occur sporadically in the Gogolin, Góraždże, Olkusz, Dziewkowice and Wilkowice formations (Figs 2, 5, 6).

Environment

The hummocky cross-stratified deposits may be interpreted unequivocally as distal tempestites. In contrast, the parallel lamination, preserved in some beds, indicates the deposition of carbonate silt and mud from suspension (Fig. 3).

Platy-bedded limestones (L11)

Characteristics

These are grey-yellow lime mudstones (calcsiltites and calcilutites) that form layers, 1–2 cm thick and characterized by parallel bedding planes and considerable horizontal continuity (Fig. 22A). The platy-bedded limestones occur as decimetre-thick packages in the Gogolin and Dziewkowice formations.

Environment

The fine-grained nature of this deposit and overall lack of fossils indicate deposition in a calm, poorly oxygenated setting, probably in the offshore or on the shoreface (Fig. 3). Mud accretion must have been episodic, but frequent, as evidenced by the thin-bedded character of the sediment. It is enigmatic that the platy-bedded limestones are completely devoid of trace fossils. The most acceptable explanation is provided by a deficiency of organic matter within the deposit, due to the augmented oxygenation, but the cause of oxygen level fluctuations still remains unclear.

Wavy-bedded limestones (L12)

Characteristics

These are grey lime mudstones (calcsiltites and calcilutites) that form undulated to crumpled layers, 1–2 cm thick and exhibiting in most cases considerable horizontal continuity (Fig. 22B). Some layers are sandwiched between millimetre-thick layers of black, limey claystone. The wavy-bedded limestones occur as decimetre-thick packages, which show internal folding and faulting and contain ball-and-pillow structures (Dżułyński and Kubicz, 1975).

The packages of wavy-bedded limestones are common in the Gogolin and Dziewkowice formations and minor in

the Góraždże Formation (Figs 5, 6). They are regarded as local key horizons (Bogacz *et al.*, 1968).

Environment

Like the platy-bedded limestones (L11), the wavy-bedded limestones also represent offshore and shoreface deposits (Fig. 3). The formation of wavy-crumpled fabric, as shown by the experiments of Bogacz *et al.* (1968), resulted from the collapse of an unstable water-laden sequence of alternating limey and marly sediments. The collapse was locally accompanied by sliding and contortion of the entire package, as well as by sinking of the overlying bedded sediment (Dżułyński and Kubicz, 1975). Potential triggers for such sediment mobilization include storms, seismic shocks, gravitation and overloading by water or sediment. Earthquake events appear to have been the most reliable trigger mechanism, because the Upper Silesian threshold was a part of the tectonically active Silesian-Moravian Gate and was attached to an archipelago of fault-bounded islands (Szulc, 1989, 1993).

Nodular limestones (L13)

Characteristics

These are grey lime mudstones (calcsiltites and calcilutites) that form nodules, 1–5 cm thick, displaying irregularity in shape and limited horizontal continuity (Fig. 22C, E). The nodular limestones form either distinct decimetre-thick packages or centimetre-thick intercalations within other carbonate lithofacies. The nodular limestones of the Gogolin and Dziewkowice formations contain numerous trace fossils, predominantly coprolite-filled *Rhizocorallium communae* (Fig. 22C, D). In addition, individual nodules commonly are enclosed in and separated from other nodules by millimetre-thick layers of black limey claystone (Fig. 22E). In contrast, the nodular limestones of the Góraždże Formation and Olkusz Beds exhibit unidentifiable trace fossils (rare *Rhizocorallium isp.*), and the nodules are amalgamated.

Environment

Like the platy-bedded limestones (L11), the nodular limestones represent background sedimentation in an open-marine environment (Fig. 3). During certain time intervals, carbonate accumulation was interrupted additionally by increased siliciclastic influx, recorded as millimetre-thick claystone between the nodules. The abundance of trace fossils implies that the nodular fabric resulted from the extensive burrowing of originally layered deposits, rather than from late pressure solution and compaction or early submarine lithification under weak bottom currents (Mullins *et al.*, 1980). *Rhizocorallium isp.* is regarded as an indicator of oxygen-depleted deposits (Martin, 2004; Knaust, 2013).

Marls and limey claystones (L14)

Characteristics

These are yellow-orange-grey-green, unfossiliferous fine-grained deposits, displaying parallel or flaser lamination (Fig. 22F). In thin sections, one can observe silt-sized, rounded quartz grains and mica flakes, scattered in a car-

bionate mud. The marls and limey claystones usually form 1– to 10-cm-thick layers occurring interbedded in other carbonate lithofacies within the Gogolin and Dziewkowice formations (Figs 5, 6).

Environment

The marls and limey claystones are considered to represent periods of increased supply of terrigenous material and/or reduced production and transport of carbonates. Such conditions appear often below the zone of storm-wave reworking (Fig. 3).

Firmgrounds (L15)

Characteristics

These are grey lime mudstones (calcsiltites and calcilutites) and fine-grained, peloidal wackestones, containing rare forams, broken bivalves and crinoid ossicles (Fig. 23A). They form layers, 5–30 cm thick, that include chiefly the burrows *Balanoglossites* and *Thalassinoides* (Fig. 23B, C). The burrows are filled either with faecal pellets (active fill) or a yellow, peloidal-bioclastic-micritic sediment (passive fill). In most cases, the bioturbation obliterated the original parallel lamination of the deposits. The burrows are commonly surrounded by a black diagenetic halo that fades gradually into the grey mudstone background.

The firmgrounds form much of the sedimentary succession of the Olkuszu Beds and Karchowice Formation. They occur subordinately in the Gogolin and Dziewkowice formations (Figs 2, 5, 6).

Environment

The homogenously laminated structure of firmgrounds, lacking internal erosional surfaces, implies that the carbonate mud was deposited from suspension as a single event, presumably after storms (Matysik, 2010). Subsequent development of a firmground omission surface required a prolonged time span of ceased sedimentation (Bodzionek, 1989; Szulc, 2000; Matysik, 2010). The diagenetic haloes around the burrows *Balanoglossites* and *Thalassinoides* represent a zone impregnated with mucus, introduced by the ichnofauna to prevent the collapse of the burrows (e.g., Myrow, 1995; Bertling, 1999). The firmgrounds are interpreted as having been formed in a sediment-starved, open-marine, low-energy setting, below fair-weather wave base (Fig. 3).

Hardgrounds (L16)

Characteristics

These subtle surfaces are marked by: 1) encrusting bivalve *Placunopsis ostracina* that grew on each other like oysters to form centimetre-thick buildups (Fig. 23D, E); or 2) the boring *Trypanites* that usually developed in elevated elements of the sea bottom, such as domes or lenses (Fig. 23F, G). The hardgrounds are laterally discontinuous, both on regional and local scales, and many were reworked and the clasts incorporated into intraformational limestone conglomerates (L09).

The hardgrounds are relatively common in the upper part of the Gogolin Formation and in the Wilkowice Beds.

One hardground horizon was recognized in the topmost part of the Górażdże Formation and one at the base of the Karchowice Formation (Figs 5, 6).

Environment

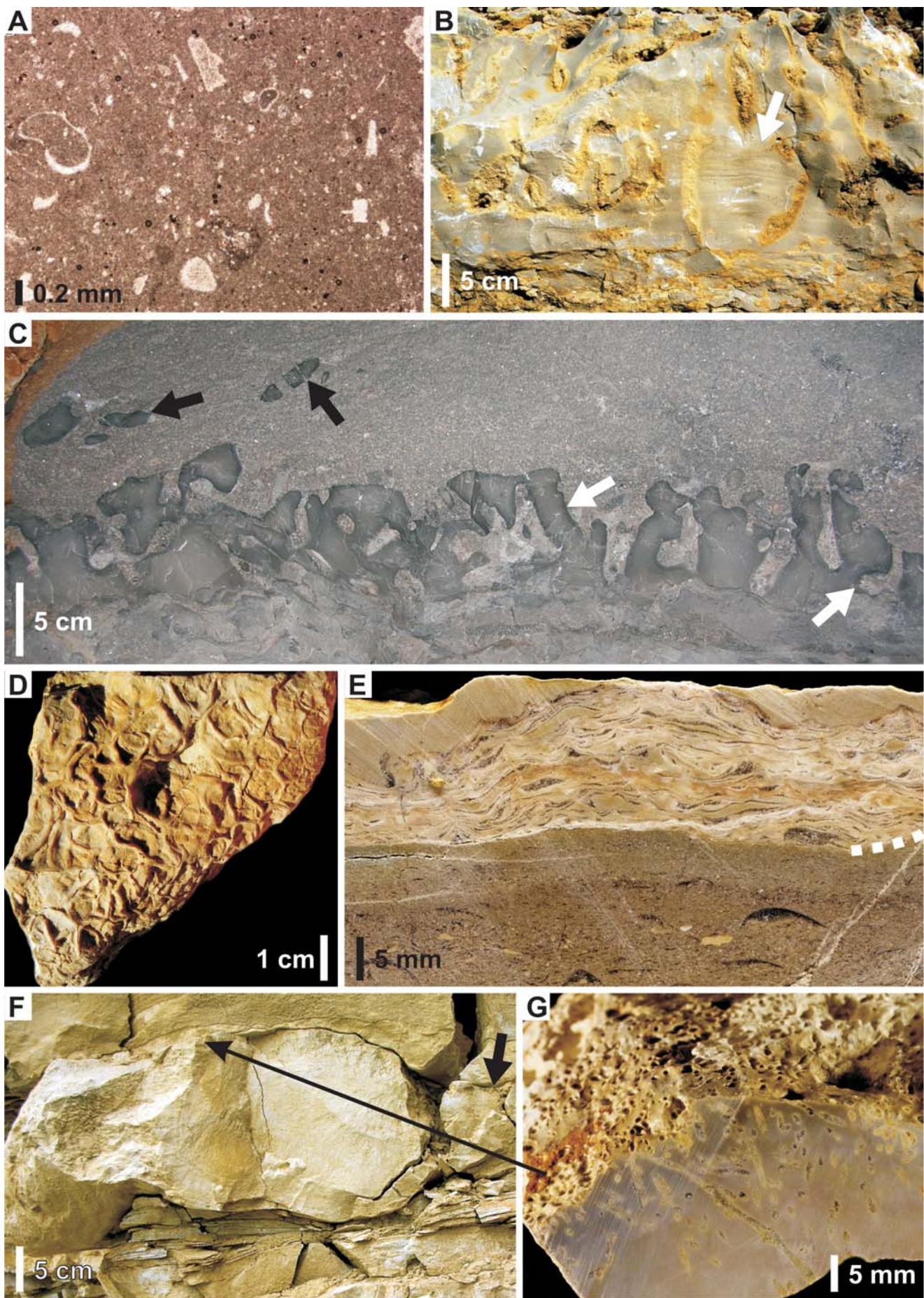
Like firmgrounds (L15), the hardgrounds indicate breaks in sediment input, which typically occur in low-energy areas, below fair-weather wave base (Fig. 3). The limited horizontal persistence of these surfaces suggests that sedimentation hiatus were of local importance only.

DISTRIBUTION OF LITHOFACIES WITHIN AND BETWEEN DEPOSITIONAL SEQUENCES

The Upper Silesian Muschelkalk comprises four depositional sequences, representing major transgressive pulses from the Tethys Ocean via the Silesian-Moravian Gate (Szulc, 2000; Matysik, 2012, 2014). The vertical and horizontal organization of the lithofacies delineated within the sequences is generally complex, but the degree of complexity varies between particular sequences and systems tracts (Figs 2, 5, 6).

The first depositional sequence, equated with the lower Gogolin Formation, begins with a high-energy shoal package, which reaches a thickness of 1–3 m and is largely composed of peloidal limestones (L07A; Figs 2, 5, 6). This facies is locally accompanied by bioclastic limestones (L06) and in some sections of the Kraków-Silesia region also by “low-energy” ooidal limestones (L03B), oncoidal limestones (L04A) or cortoidal limestones (L05). The occurrence of the coated grain lithofacies in the Kraków-Silesia region indicates that this area was generally shallower than the Opole region. Common centimetre- (occasionally decimetre-) thick intercalations of platy-bedded limestones (L11), wavy-bedded limestones (L12), nodular limestones (L13), and marls and limey claystones (L14) were deposited during fair-weather periods or in protected topographic lows (e.g., between dunes or bars).

This basal package is succeeded by a 3–6 m thick set of alternating fine-grained limestones and tempestites (Figs 2, 5, 6), representing sedimentation on the lower shoreface. The frequently occurring nodular limestones (L13) and wavy-bedded limestones (L12) typically contain millimetre-thick, black, limey claystones, enclosing single nodules and interbedded with wavy-shaped layers. Marls and limey claystones (L14) are also widespread. The presence of siliciclastics may be explained as a consequence of an intense supply of terrigenous material during the progressive flooding of adjacent land areas, namely the Małopolska and Bohemian Massifs. On the other hand, the tempestites are predominantly represented by bioclastic limestones (L06A) and less frequent peloidal limestones (L07A, B) and bedded calcsiltites and calcilutites (L10; Figs 2, 5, 6). The thickness, abundance and composition of storm layers as well as their tendency to amalgamation vary between sections, reflecting proximality-distality trends (Myrow and Southard, 1996; Einsele, 2000); thick (up to 30 cm in thickness) bioclastic coquinas that are commonly amalgamated and sand-



wiched mostly between centimetre-thick fine-grained limestones predominate in northeastern proximal areas (toward the archipelago of Devonian islands), whereas scarce, thinner (up to 15 cm thick), peloidal interbeds tend to predominate towards the southeastern margin of the Upper Silesian platform (towards the Tethys Ocean).

The following interval of maximum flooding is recorded by monotonous, clay-rich, nodular limestones (L13) and wavy-bedded limestones (L12; Figs 2, 5, 6), locally accompanied by platy-bedded limestones (L11) and marls and limey claystones (L14). These offshore facies are sharply overlain, without apparent Highstand Systems Tract (HST) deposits, by the so-called Zellenkalk2 (Assmann, 1944), a horizon 0.5–2 m thick that marks the sequence boundary (Szulc, 2000). It is chiefly composed of cellular dolostones (D04) and dolosiltites (D14) with a subordinate contribution by dolocretes (D07), rhizolites (D08) and cryptalgal laminites (D11).

Like the first depositional sequence, the second sequence commences with (i) the high-energy shoal package grading upward into (ii) the tempestite set (upper Gogolin Formation), both characterized by a minor, lateral lithofacies variability. The former package, 1–2 m thick, is composed of peloidal limestones (L07A) and bioclastic limestones (L06A), which in some sections of the Kraków–Silesia region are accompanied by intraformational limestone conglomerates (L09) and “low-energy” ooidal limestones (L03B), reflecting shallower marine conditions. The tempestite set, 10–20 m thick, consists of clay-rich nodular limestones (L13), wavy-bedded limestones (L12), platy-bedded limestones (L11), marls and limey claystones (L14) and hardgrounds (L15) interspersed with storm-deposited bioclastic limestones (L06A), peloidal limestones (L07A, B), intraformational limestone conglomerates (L09) and bedded calcisiltites and calcilutites (L10; Figs 2, 5, 6). In contrast to the first depositional sequence, the tempestites of the second sequence display no spatial distribution trend, indicating that no evident proximal and distal zone existed in the time period discussed. This presumably resulted from the flattening and smoothing of the pre-Muschelkalk seafloor relief, when the Upper Silesian Sub-basin was gradually infilled by sediments. The presence of hardgrounds (L15) and intraformational limestone conglomerates (L09) indicates the highly episodic nature of sediment accumulation during this interval. The subsequent maximum flooding zone deposits are laterally uniform and dominated by clay-rich, nodular limestones (L13) and wavy-bedded limestones (L12) with minor contribution of other fine-grained limestones.

The HST2 exhibits marked vertical and horizontal lithofacies variability. The HST of the Kraków–Silesia region (Olkusz Beds) is 35 m thick. Its lower part, representing the lower shoreface, consists of alternating firmgrounds (L15) and peloidal limestones (L07A, B), chiefly of storm origin (Figs 2, 5). The thickness and abundance of tempestitic intercalations increase upwards in the interval discussed, reflecting gradual shallowing (Matysik, 2014). The succeeding high-energy shoal complex, deposited on the upper shoreface and foreshore, is built mostly of metre-thick units of peloidal limestones (L07B, C) sandwiched between much thinner firmgrounds (L15). In the Opole region, on the other hand, the laterally equivalent Górażdże Formation reaches 20 m in thickness and is tripartite. Its middle part is dominated by “low-energy” oncoidal limestones (L04B), while the lower and upper parts are composed of nodular limestones (L13) alternating with metre-thick, laterally continuous units of “high-energy” oncoidal limestones (L04C) and peloidal limestones (L07A; Figs 2, 6). The latter alternation reflects cyclic sedimentation on the lower and upper shoreface, respectively, caused by high-frequency sea-level fluctuations (Matysik, 2012). The described differences in HST composition between the Opole and Kraków–Silesia regions are unequivocally due to differentiated bathymetries: the eastern shallower part first experienced muddy and storm sedimentation and then high-energy shallow-water sedimentation, whereas the western deeper part was alternately covered by extensive oncoidal-peloidal sand bodies and mud units. The character of background (mud) sedimentation also differed between the two regions: highly episodic and rapid mud accretion caused the development of firmground omission surfaces in the eastern area, whereas punctuated mud accumulation and subsequent bioturbation led to the formation of nodular fabrics in the western area. The reason for this regional differentiation remains unclear, but it might reflect the lateral variation in carbonate production rates of unknown origin. It is noteworthy that all lithofacies types of the HST2, including deep-water nodular limestones (L13) and firmgrounds (L15), are devoid of siliciclastic material, which seems to reflect a dilution effect, related to extensive carbonate production and/or reduced subaerial denudation of the neighbouring land areas, due to the widespread flooding.

The capping sequence boundary is marked in the Opole region by a horizon with ferricretes (L01; Szulc, 2000), and in the Kraków–Silesia region by an erosional unconformity (Matysik, 2014). The following third depositional sequence was deposited during a maximum opening of the Silesian-

Fig. 23. Examples of starved basin lithofacies. **A.** Photomicrograph of firmground, showing sparse bioclasts in micrite. **B.** Vertical outcrop view of firmground omission surface with the burrow *Balanoglossites* filled with yellow peloid-bioclastic sediment. Note parallel lamination preserved in some places (arrow). **C.** Vertical outcrop view of firmground omission surface with *Balanoglossites* isp. overlain by crinoid-peloidal packstone. Note lithoclasts derived from the underlying firmground (black arrows) and characteristic dark haloes around burrows (white arrows). **D.** Bedding plane view of a *Placunopsis ostracina* “colony”. **E.** Vertically oriented slab of a *Placunopsis ostracina* encrustation developed on peloidal-bioclastic packstone. **F.** Vertical outcrop view of a small dome of calcilitute, upper surface of which contains the subvertical boring *Trypanites*. The surrounding sediment (arrow) was not infested by the endolithic biota. **G.** Close-up view of F, showing densely bored surface in cross-section and plane view (top of picture). Pictures: A, C – Karchowice Formation, Opole region; B – Olkusz Beds, Kraków–Silesia region, D–G – Gogolin Formation, Kraków–Silesia region.

Moravian Gate (Szulc, 2000). The sequence displays a substantial regional and local variability in lithofacies, which is evident for the HST and for the first time also for the Transgressive Systems Tract (TST). The TST3 in the Kraków–Silesia region (lower Diplopora Beds) is 10 m thick and comprises peritidal dolomitic facies (Figs 2, 5), including mudstones (D06), dolocretes (D07), rhizolites (D08), cryptalgal laminites (D11), bioturbated dolosiltites (D13), dolosiltites (D14), intraformational dolomitic conglomerates (D15) and peloidal dolostones (D16). Most of these rocks, especially the supra- and intertidal lithofacies, are characterized by a very low degree of lateral persistence, which in some cases does not exceed several tens of metres. The limited lateral extent of lithofacies implies that the depositional area was geomorphologically varied, with co-existing supratidal plains and banks, cyanobacterial mat flats, salt marshes, ephemeral tidal ponds, and protected lagoons and embayments with mud- and peloid-dominated areas (Matysik, 2012, 2014; Fig. 4A). The distribution of subenvironments partially followed the local antecedent topography, specifically the distribution of low-relief (1–2 m high and up to hundreds of metres across) elevations and depressions, interpreted as surface karstic topographies, which formed during the third-order emersion (Matysik, 2014). Nevertheless, much of this mosaic pattern was produced because the subenvironments migrated laterally and encroached upon each other as a response to changes in accommodation space which in turn was the result of regional eustasy and local subsidence, erosion and accumulation (Matysik, 2012). In contrast to the TST of the Kraków–Silesia region, the TST in the Opole region (Dziewkowice Formation) is laterally uniform and consists of open-marine facies (Figs 2, 6). It begins with a 2.5-m-thick unit of wavy-bedded limestones (L12), followed by a high-energy shoal package, 1.5 m thick, called Haupterinoidenbank (Assmann, 1944). This package is composed of “high-energy” oncoidal limestones (L04C), cortoidal limestones (L05), peloidal limestones (L07A) and bioclastic limestones (L06A). The overlying tempestite set, 8 m thick, comprises deeper-water, clay-rich nodular limestones (L13), wavy-bedded limestones (L12) and minor platy-bedded limestones (L11) intercalated with storm-deposited bioclastic limestones (L06A) and less frequent peloidal limestones (L07A, B; Figs 2, 6). The significant difference in the composition of the TST3 between the Opole and Kraków–Silesia regions indicates an even bigger differentiation of the westward-dipping Upper Silesian seafloor by comparison with the TST1 and TST2. Szulc (1993, 2000) suggested that the ultimate opening of the Silesian–Moravian Gate caused the tectonic drop of the Opole region, as he recognized a laterally continuous package of syndepositionally deformed, thin-bedded calcilutites there resting directly on the sequence boundary. One cannot exclude the possibility that the mentioned karstification of the subaerially exposed platform top produced not only local topographic structures, but also modified the entire platform relief.

The pronounced basin segmentation continued during the maximum flooding interval of the third sequence and is recorded as open-marine facies in the western deeper part and dolomitic facies in the eastern shallower part (Figs 2, 5,

6). The open-marine facies are laterally uniform and include clay-rich nodular limestones (L13), wavy-bedded limestones (L12) and locally platy-bedded limestones (L11). The dolomitic facies are represented by oncoidal dolostones (D18), green algal dolostones (D16) and peloidal dolostones (D15), which pass laterally into each other, mirroring local environmental conditions (Myszkowska, 1992; Matysik, 2012).

The subsequent HST3 is 30–40 m thick and exhibits the greatest lithofacies heterogeneity among all the Upper Silesian systems tracts (Fig. 2). The HST in the Kraków–Silesia region (upper Diplopora Beds) contains peritidal dolomitic facies, predominantly mudstones (D06), dolocretes (D07), rhizolites (D08), fenestral dolostones (D09), cryptalgal laminites (D11), bioturbated dolosiltites (D13), dolosiltites (D14), intraformational dolomitic conglomerates (D15) and peloidal dolostones (D16), and in the topmost part stromatolites (D12) and ooidal dolostones (D19; Figs 2, 5). Like in the TST3, most of these lithofacies pinch out laterally over less than a few kilometres as a consequence of the mosaic distribution of depositional settings and sedimentary processes within the tidal flat-lagoon system (Matysik, 2012; Fig. 4A). In contrast, the laterally equivalent HST of the Opole region generally represents a circum-reefal environment (Figs 2, 4B, 6). The Karchowice Formation commences with a complex of firmgrounds (L15) and storm-deposited bioclastic limestones (L06A; Figs 2, 6). The overlying reefal complex comprises from bottom to top (Figs 2, 4B, 6): 1) sponge biostromes (L08); 2) sponge-coral bioherms (L08) with laterally adjacent proximal cortoidal limestones (L05) and bioclastic limestones (L06B) and distal firmgrounds (L15); 3) “low-energy” oncoidal limestones (L04A) and peloidal limestones (L07A); 4) sponge biostromes (L08); and 5) sponge-coral bioherms (L08) enclosed by “low-energy” oncoidal limestones (L04B) and peloidal limestones (L07A). The final stage of the HST3 in the Opole region is represented by a back-reef depositional setting, consisting of “high-energy” ooidal limestones (L03A), peloidal limestones (L07A), bedded calcisiltites (L10) and green algal limestones (L02) of the Diplopora Beds, which prograded onto the reefal complex. All mentioned lithofacies types contain no siliciclastics, because the production and influx of terrigenous material strongly depended on sea-level position (transgression vs. highstand). The development of sponge(-coral) patch reefs was a key event in the depositional history of the Opole region during the HST3, because it modified the energy regime across a transect 30 km long, producing a characteristic horizontal gradient of lithofacies (Matysik, 2010): from firmgrounds (L15) and storm-deposited bioclastic limestones (L06A, B) of the distal fore-reef zone, through cortoidal limestones (L05), bioclastic limestones (L06B) and peloidal limestones (L07A) of the proximal and inter-reef areas, to “low-energy” oncoidal limestones (L04A, B), “high-energy” ooidal limestones (L03A), peloidal limestones (L07A) and green algal limestones (L02) of the back-reef zone (Figs 2, 4B).

The lithofacies diversity of the fourth depositional sequence cannot be analyzed in detail because of its poor exposures. Nevertheless, on the basis of a few available outcrops and previous papers (Assmann, 1913, 1926, 1929,

1944; Siedlecki, 1948, 1952; Kubicz, 1971; Szulc, 1991), it is possible to reconstruct the general facies evolution of the Upper Silesian platform during this transgressive pulse. The sequence begins with the Tarnowice Beds (Assmann, 1944), which are interpreted as a lowstand systems tract (LST4; Szulc, 2000). Over the entire Upper Silesia, this formation is built of dolosiltites (D14) with sparse interbeddings of sandstones (D05), mudstones (D06), intraformational dolomitic conglomerates (D15), peloidal dolostones (D16) and ooidal dolostones (D19; Figs 2, 5) deposited in a restricted, periodically emerged lagoon (Szulc, 2000). However, where the sponge(-coral) patch reefs of the Karchowice Formation occur beneath, the Tarnowice Beds consist of speleothems and residual clays (D02), crystalline dolostones (D03), cellular dolostones (D04), sandstones (D05), stromatolites (D12) and ooidal dolostones (D19; Figs 2, 6). This lithofacies assemblage generally represents a sabkha that was alternately replaced by a restricted lagoon and then abandoned for a long time, contributing to the dissolution of evaporites and the formation of caves and caverns (Matysik, 2012; Worobiec and Szulc, 2012). Although the reef belt had already been buried under an ooidal-peloidal-green algal sand body of the Diplopora Beds (Figs 2, 4B, 6), it still formed a morphological elevation at the beginning of the fourth transgression, changing the overall facies pattern within the Upper Silesian basin and determining the location of sabkha environments.

The lowstand deposits are succeeded by the transgressive Wilkowice Beds (Szulc, 2000). This TST4 is composed of open-marine nodular limestones (L13) and wavy-bedded limestones (L12), interbedded with storm-deposited bioclastic limestones (L06A), peloidal limestones (L07A, B) and intraformational limestone conglomerates (L09). The overlying HST4 (Boruszowice Beds) is 15 m thick and comprises subtidal mudstones (D06), sandstones (D05) and minor peloidal dolostones (D16), deposited in a lagoon or embayment. An increased supply of siliciclastic material reflected the ultimate closing of the Silesian-Moravian Gate at the end of Ladinian time (Szulc, 2000).

SPATIAL AND TEMPORAL CONTROLS ON LITHOFACIES – A SYNTHESIS

Large-scale controls on lithofacies distribution

Despite the abundance of diverse lithofacies and their complex organization within the Upper Silesian Muschelkalk (as discussed above), some predictable large-scale patterns in the vertical and horizontal facies arrangement are evident. Analysis of these trends allows conclusions to be drawn about the effect of extrinsic factors on the development and distribution of the lithofacies. These factors, already recognized by previous authors, include platform morphology, third-order eustasy, and long-term tectonic evolution of the Silesian-Moravian Gate (Wyczółkowski, 1971, 1982; Szulc, 2000). While the interplay of third-order eustasy and the long-term tectonic evolution of the area controlled the temporal lithofacies changes, the platform morphology dictated the facies pattern in the time interval investigated.

It is important to note that all four Transgressive Systems Tracts of the open-marine domain are characterized by a similar lithofacies composition and vertical succession, from a basal high-energy shoal package, through a tempestite set, to a maximum flooding interval (Fig. 2). The repetitive lithofacies assemblages and vertical succession of each TST implies that the overall environmental parameters were generally similar during each transgressive phase. This uniformity implies in turn that the environmental conditions during transgressions were influenced only to a minor degree by the long-term tectonic evolution of the Silesian-Moravian Gate and the individual character of each transgressive pulse (e.g., the rate and duration of sea-level rise, or the landward position of shoreline). In strong contrast to the TSTs, each HST comprises an individual (unique) lithofacies assemblage, which indicates that the environmental conditions differed markedly between particular highstands. This differing behaviour during transgressions and highstands appears to reflect the opening-closing trend of the Silesian-Moravian Gate and the relative magnitude of third-order eustatic pulses. The first transgression left no apparent HST deposits, because it took place when the Silesian-Moravian Gate was barely open. The progressive gate opening during the second transgression contributed to the development of a 20- to 30-m-thick highstand suite, representing a system of extensive peloidal-oncoidal-ooidal sand shoals. The third transgression, a peak one in Upper Silesia, coincided with the maximum opening of the Silesian-Moravian Gate (Szulc, 2000). This synchronism provided optimal conditions for the appearance of sponge (-coral) patch reefs that together with the circum-reefal facies build the 40-m-thick HST in the region. The fourth (last) transgressive pulse was accompanied by the gradual closing of the neighbouring gate, which resulted in a vast supply of terrigenous material and marked shallowing of the area. Consequently, the highstand deposits are dominated by shallow-subtidal mudstones and sandstones that barely reach a total thickness of 15 m.

The second regularity is that the TSTs typically contain siliciclastic intercalations, while the HSTs are completely devoid of siliciclastic material. This pattern illustrates that a vast supply of terrigenous material occurred during the sea-level rises and it disappeared once the shoreline reached its approximate maximum landward position. The only exception to this is the last HST, which is dominated by mudstones and sandstones, because it developed simultaneously with the progressive closing of the Silesian-Moravian Gate.

Another observation concerns the distribution of the coated-grain lithofacies. The “high-energy” coated-grain lithofacies (i.e., oolites with normal, concentric ooids, or oncolites with small regular microbial oncoids) are characteristic of the HSTs, while the “low-energy” coated-grain lithofacies (i.e., oolites with superficial, radial-fibrous ooids, oncolites with *Girvanella* oncoids or large irregular microbial oncoids, or cortoidal deposits) appear both in the HSTs and in the basal high-energy shoal package of the TSTs (Fig. 2). This pattern implies that the energy regime during initial transgression phases was overall lower than during the highstands, despite the fact that the water depth and general depositional environment were similar.

A. Gogolin Fm (TST1, TST2)

0	0	0	2	0	0	0	1	0	0	0	0	0	0	0	0	0	0	0	0
0	×	0	1	0	0	0	0	0	0	0	0	0	0	0	0	0	0	0	0
0	1	×	0	0	0	0	0	0	0	0	0	0	0	0	0	0	0	0	0
1	0	1	×	0	0	0	1	1	1	1	0	0	0	0	0	0	0	0	0
0	0	0	0	0	0	0	0	2	2	2	0	0	0	0	0	0	0	0	0
0	0	0	0	0	0	0	1	3	1	0	1	0	0	1	0	0	0	0	0
0	0	0	0	0	1	0	1	2	1	0	0	0	0	1	0	0	0	0	0
0	0	0	0	0	1	3	0	4	6	0	7	1	2	100	60	0	0	0	0
0	0	0	0	4	5	45	1	0	3	18	1	3	89	125	0	0	0	0	0
0	0	0	0	0	0	0	0	0	3	0	0	0	0	12	8	0	0	0	0
0	0	0	0	1	1	1	9	18	0	0	1	0	10	2	3	0	0	0	0
0	0	0	0	0	0	0	2	1	1	1	0	3	2	1	0	0	0	0	0
0	0	0	0	0	0	0	1	1	3	0	2	0	32	1	1	0	0	0	0
0	0	0	6	0	0	1	89	96	9	11	1	34	0	10	1	0	0	0	0
0	0	0	1	0	0	0	58	53	6	4	0	1	5	0	0	0	0	0	0
0	0	0	0	0	0	0	0	0	0	0	0	0	5	0	0	0	0	0	0
OVERLYING LITHOFACIES																			
cellular dolostones (D04)	dolocretes (D07)	cryptalgal laminites (D11)	dolostilites (D14)	ooloidal limestones (L03B)	oncoidal limestones (L04A)	coritoidal limestones (L05)	bioclastic limestones (L06)	peloidal limestones (L07)	intraform. l. conglom.	bedded cs. and cl.	platy-bedded limestones (L11)	wavy-bedded limestones (L12)	nodular limestones (L13)	marls and limy claystones (L14)	hardgrounds (L16)				

UNDERLYING LITHOFACIES	
cellular dolostones (D04)	w
dolocretes (D07)	
cryptalgal laminites (D11)	
dolosiltites (D14)	
ooloidal limestones (L03B)	
oncoidal limestones (L04A)	
cortoidal limestones (L05)	
bioclastic limestones (L06)	marl
peloidal limestones (L07)	
intraform. I. conglom. (L09)	
bedded calcisiltites and calcilutites (L10)	
platy-bedded limestones (L11)	
wavy-bedded limestones (L12)	
nodular limestones (L13)	
marls and limey claystones (L14)	
hardgrounds (L16)	
	des (L04B)

C. Olkusz Beds (HST2)

nd conglomerates (D01)
06)
07)
i)
ar-bedded dolostones (D1
loslites (D13)
tones (D16)
tones (L07)
d cl. (L10)
ones (L11)
.15)

B. Góraždże Fm (HST2)

L10)	oncoidal limestones (L04B) cortoidal limestones (L05) bioclastic limestones (L06) peloidal limestones (L07) bedded cs. and cl. (L10) platy-bedded limestones (L11) wavy-bedded limestones (L12) nodular limestones (L13)	firme grounds (L15)
OVERLYING LITHOFACIES		
	ferricretes (L01) oncoidal limestones (L04B) oncoidal limestones (L04C) peloidal limestones (L07B) bedded cs. and cl. (L10)	OVERLYING LITHOFACIES
	wavy-bedded limestones (L12) nodular limestones (L13) marls and limey claystones (L14)	LITHOFACIES
	firmgrounds (L15) hardgrounds (L16)	

	3	1	0	0	0	1	1	oncoidal limestones (L04B)
1	×	2	0	0	0	5	0	cortoidal limestones (L05)
0	1	×	0	0	4	22	0	bioclastic limestones (L06)
0	0	2	×	0	0	0	2	peloidal limestones (L07)
0	0	0	0	×	0	0	1	bedded cs. and cl. (L10)
0	0	0	0	0	3	0	0	platy-bedded limestones (L11)
1	1	2	0	0	1	×	5	wavy-bedded limestones (L12)
1	4	21	4	1	0	4	×	nodular limestones (L13)
4	0	0	0	0	0	0	0	firmgrounds (L15)

D. Dziewkowice Fm (TST3)

OVERLYING LITHOFACIES

cliff brec. and congl. (D01)

	UNDERLYING LITHOFACIES															
	0	0	2	2	0	25	0	6	1	0	1	0	0	0	0	0
mudstones (D06)	0	2	X	2	0	44	0	17	19	0	8	1	1	0	0	0
dolocretes (D07)	0	0	1	X	0	5	0	2	0	0	0	0	0	0	0	0
rhizolites (D08)	0	0	0	0	X	2	0	0	0	0	0	0	0	0	0	0
fenestral dolostones (D09)	0	19	39	7	2	X	0	15	56	2	26	2	1	2	0	0
cryptalgal laminites (D11)	0	0	1	0	0	0	X	0	0	0	0	0	0	0	0	0
stromatolites (D12)	0	9	15	3	0	22	0	X	4	0	46	0	0	0	0	0
bioturbated dolosiltites (D13)	1	7	13	0	0	43	0	4	X	0	15	0	2	0	0	0
dolosiltites (D14)	0	0	0	1	0	1	0	1	0	X	2	0	0	0	0	0
intriform, d. conglomer. (D15)	0	0	6	0	0	8	0	42	22	4	X	1	26	0	0	0
peloidal dolostones (D16)	0	0	0	0	4	0	0	0	0	1	X	0	0	0	0	0
green algal dolostones (D17)	0	0	1	0	0	0	0	3	0	12	0	X	0	0	0	0
oncoidal dolostones (D18)	0	0	0	0	0	1	1	0	0	0	0	0	0	0	0	0
ooidal dolostones (D19)	0	0	0	0	0	0	1	1	0	0	0	0	X	0	0	0
ooidal limestones (L03A)	0	0	0	0	0	0	0	0	0	0	0	0	0	X	0	1
oncoidal limestones (L04C)	0	0	0	0	0	0	0	0	0	0	0	0	1	X	0	1
peloidal limestones (L07)	0	0	0	0	0	0	0	0	0	0	0	0	0	0	X	1
green algal limestones (L02)	0	0	0	0	0	0	0	0	0	0	0	0	0	0	2	0
sponge buildups (L08)	0	0	0	0	0	0	0	0	0	0	0	0	0	1	X	0
bedded cs. and cl. (L10)	0	0	0	0	0	0	0	0	0	0	0	0	0	1	0	0
firmgrounds (L15)	0	0	0	0	0	0	0	0	0	0	0	0	1	0	0	2

E. Karchowice Fm (HST3)

F. Diplopora Beds (TST3, HST3)

The final point is the impact of sea-floor morphology on the local and regional facies distribution. All of the four depositional sequences display horizontal lithofacies variability, but its degree differs between depositional sequences: 1) it is much higher for the HSTs than for the TSTs; and 2) it increases from the first sequence to the third sequence, and drops again thereafter (Figs 2, 5, 6). The TST1 and TST2 are characterized by a subordinate lateral variation in lithofacies composition only, which depends primarily on the occurrence of shallower lithofacies in the Kraków–Silesia region, namely coated-grain lithofacies in the basal high-energy shoal packages and proximal tempestites in the tempestite sets. The first clearly observable highstand (HST2) exhibits a substantial horizontal variability; alternating nodular and peloidal-oncoidal limestones in the Opole region correspond to the firmgrounds and peloidal-oooidal limestones of the Kraków–Silesia region. The third depositional sequence developed completely differently in both regions which may be a result of tectonic segmentation of the basin due to the ultimate opening of the Silesian-Moravian Gate (Szulc, 2000). The eastern part represents a tidal flat-lagoon domain and accordingly is composed of various peritidal lithofacies. These have a limited horizontal continuity, both within the TST3 and the HST3, showing a mosaic distribution of peritidal subenvironments over an irregular antecedent topography on the one hand and a frequent geomorphologic reorganization of the tidal landscape on the other (Matysik, 2012, 2014). In contrast, the TST3 in the Opole region is laterally uniform, in contrast to the succeeding HST3, which shows a great lithofacies variability. Characteristic is the transition from fore- to back-reef facies, generated by the sponge (-coral) patch reefs, which developed on a NE–SW-trending elevated fragment of the sea-floor (Matysik, 2010). The distribution of circum-reef facies also had an impact on the facies pattern within the LST4, determining the location of a sabkha environment on the top of the underlying reef belt.

Controls on specific lithofacies assemblages

Inspection of numerous lithostratigraphic logs measured and matrices showing the number of over- and underlying contacts between each lithofacies (Fig. 24) revealed that some lithofacies types within the same domain are never or hardly ever juxtaposed vertically, whereas other lithofacies types appear strictly connected with one or two particular lithofacies. These specific connections warrant further discussion in terms of possible controlling factors.

Amongst the seven supratidal lithofacies of the tidal

flat-lagoon domain, dolocretes (D07) are the most common and they were found to be overlying almost all other lithofacies of dolostone domain, including biolaminites as well as the dolomitic sand and mud facies (Figs 5, 24A, F). Mudstones (D06) and rhizolites (D08), the second and third most frequent supratidal lithofacies, were not seen to cap the dolomitic sand facies (Figs 5, 24C, F). The reason why dolcretes (D07) were formed twice as often as mudstones (D06) and five times more often than rhizolites (D08) may be attributed to the semi-arid climate, which presumably hindered the intense production of siliciclastic material and massive expansion of plants. It favoured in contrast recurring dissolution and reprecipitation of carbonates, responsible for the development of dolocrete crusts (Esteban and Klappa, 1983; Wright and Tucker, 1991). On the other hand, the fact that mudstones (D06) and rhizolites (D08) did not develop on emerged dolomitic sand bodies may be explained in two ways: 1) the dolomitic sands were deposited in more distal (seaward) parts of lagoons and embayments than dolomitic muds and biolaminites, and despite emersion those areas might have been inaccessible to plants and significantly separated from a terrigenous supply; and 2) perhaps more likely, the emerged dolomitic sands were more susceptible to wind or storm redeposition than cohesive dolomitic muds and microbial bindstones and the instability of the substrate precluded the encroachment of plants and the accumulation of fine siliciclastics as distinct caps. In short, it seems that the development of rhizolites and supratidal mudstones occurred more rapidly in easily accessible areas and was enhanced by substrate stability, whereas the dolcretes were less dependent on local conditions, substrate types and topography.

The microbialites occur as two distinct morphological forms: planar cryptalgal laminites (D11) and domal stromatolites (D12). The planar structures recur frequently in the Diplopora Beds and may be vertically juxtaposed with all subtidal lithofacies of the tidal flat-lagoon domain, though the most common is an association with bioturbated dolosiltites (D13), dolosiltites (D14) and peloidal dolostones (D16; Figs 5, 24A, F). Conversely, the domal structures appear only in the topmost part of the Diplopora Beds and in the Tarnowice Beds, where they are strictly associated with ooidal dolostones (D19; Figs 2, 5). These connections between particular lithofacies types emphasize a clear correlation between morphology of microbial buildups and water energy. During the extended time interval when the Diplopora Beds were deposited, the dolomitic muds and peloidal sands accumulated in lagoons and embayments, whereas planar biolaminites largely occupied the adjacent intertidal

Fig. 24. Matrices showing the numbers of contacts between lithofacies in the six well-exposed formations of the Upper Silesian Muschelkalk. Lithofacies arranged horizontally are the overlying lithofacies and those arranged vertically are the underlying lithofacies. For example, in the Gogolin Formation bioclastic limestones (L06) are overlain by peloidal limestones (L07) 46 times, by nodular limestones (L13) a hundred times, by platy-bedded limestones (L11) once, and so on. The data set was derived from the author's unpublished Ph.D. dissertation (see Matysik, 2012) and is based on more than a hundred lithostratigraphic logs measured in 83 outcrops, giving a total stratigraphic thickness of approximately 2.3 km. Abbreviations: TST – Transgressive Systems Tract; HST – Highstand Systems Tract; cliff brec. and congl. – cliff breccias and conglomerates; intraform. d. conglom. – intraformational dolomitic conglomerates; intraform. l. conglom. – intraformational limestone conglomerates; bedded cs. and cl. – bedded calcisiltites and calcilutites; lst. – limestones.

areas. Once the energetic regime within the lagoons became permanently turbulent at the beginning of the Tarnowice Beds, allowing precipitation of ooidal coatings around peloids, the microbial mats began to form domal structures.

The sponges of the Karchowice Formation also adapted the shape of their bioconstructions to the ambient conditions (Bodzioch, 1989; Szulc, 2000; Matysik, 2010). The sponge biostromes developed in the zone between storm and fair-weather wave base (lower shoreface), in conditions of reduced sedimentation rate, as indicated by their association with firmgrounds (L15) and bioclastic limestones (L06A) of storm origin (Figs 2, 6). In contrast, the sponge bioherms that overlie the sponge biostromes in the succession are enveloped in and separated laterally by packages of bioclastic limestones (L06B), peloidal limestones (L07A), and minor cortoidal limestones (L05; Fig. 2, 4B, 6), each several metres thick. This assemblage indicates in turn that the high-relief sponge buildups grew in a mud-free setting, most likely in the zone above fair-weather wave base (upper shoreface), under high input of calcareous sands.

Hardgrounds (L16) and intraformational limestone conglomerates (L09) occur almost exclusively in the upper Gogolin Formation and the Wilkowice Beds, while the lithologically similar Dziewkowice Formation and lower Gogolin Formation generally lack these two lithofacies (Figs 5, 6, 24A, D). Moreover, many hardgrounds were reworked to form intraformational conglomerates, as evidenced by the pebbles with the boring *Trypanites* and/or *Placunopsis* encrustations. This lithofacies relationship indicates that the major control on the development of deep-water intraformational conglomerates was the occurrence of long breaks in sedimentation, not the severity of storms, as assumed by Sepkoski (1982) and Osleger and Read (1991). Presumably, even weak storms might have produced numerous intraclasts, if the substrate was fully consolidated.

CONCLUSIONS

The 150-m-thick Muschelkalk (Anisian–Ladinian) succession of Upper Silesia in southern Poland was deposited on a small independent carbonate platform, during four major marine-transgressive pulses from the Tethys Ocean through the Silesian–Moravian Gate. Facies development was strongly controlled by extrinsic factors: platform morphology, third-order eustasy and the long-term tectonic evolution of the area. The interplay between the three processes on the one hand resulted in a mosaic distribution of depositional environments in the basin, as shown by the wide variety of lithofacies types (Tables 1 and 2) and their overall complex organization within the succession (Figs 2, 5, 6), but on the other hand produced some repetitive patterns in the arrangement of facies:

1) The Transgressive Systems Tracts generally display a similar lithofacies composition and vertical succession, while the Highstand Systems Tracts comprise individual (unique) lithofacies assemblages. This pattern indicates that the transgressive facies were much less sensitive than the highstand facies to large-scale changes in the region.

2) The TSTs typically contain siliciclastic intercalations,

while the HSTs do not. This regularity indicates a profound effect of sea-level position on the production and input of terrigenous material. The one exception to this rule is the last HST, dominated by mudstones and sandstones, which developed together with a progressive closing of the Silesian–Moravian Gate.

3) The thickness of the HSTs reflected changes in accommodation space, matching the opening-closing trend of the adjacent Silesian–Moravian Gate and changing from zero (when the gate was barely open) to 40 m (as the gate reached maximum opening).

4) The degree of horizontal variability in lithofacies composition is generally much higher for the HSTs than for the TSTs and increases from the first to the third depositional sequence, whereas subsequently it drops again. These trends imply that the complexity of facies patterns within the Upper Silesian basin was not simply a function of antecedent topography, but also depended on sea-level position (transgression vs. highstand) and the opening-closing trend of the Silesian–Moravian Gate.

Acknowledgements

I would like to thank Joachim Szulc (Jagiellonian University, Poland) for ongoing encouragement, constant help and stimulating discussions on different aspects of sedimentology. Alfred Uchman and Stanisław Leszczyński (Jagiellonian University, Poland) are acknowledged for consultations about trace fossils and sedimentary structures, respectively. Ioan Bucur (Babeş-Bolyai University, Romania), Hans Hagdorn (Muschelkalkmuseum, Germany) and Elżbieta Morycowa (Jagiellonian University, Poland) determined the green algae, crinoid and coral taxa, respectively. Radosław Makula assisted in climbing during the exploration of some quarry walls. I appreciate the kind hospitality of Andrzej Gwózdek and of all the staff of ‘‘Cementownia Strzelce Opolskie’’ during several periods of field activity. For granting permission for the field study, I am grateful to the management of ‘‘Cemex’’ Polska Sp. z o.o., ‘‘GiGa’’ Sp. z o.o., ‘‘Góraždze Cement’’ S.A., ‘‘GZD’’ S.A., KiPD ‘‘Żelatowa’’ S.A., PPH ‘‘Dolomit’’ Sp. z o.o., ‘‘PPKMiL’’ Sp. z o.o., PPUH ‘‘Dolomit’’ S.A., PW ‘‘Promag’’ Sp. z o.o., ‘‘Tribag’’ Sp. z o.o., ZGH ‘‘Bolesław’’ S.A. and ZW ‘‘Lhoist’’ S.A. Reviewers Thilo Bechstädt and Tadeusz Peryt and Editor Michał Gradziński provided helpful comments on the manuscript. This research was a part of the author’s Ph.D. dissertation at the Jagiellonian University, Kraków, and was funded by Research Grant No. N307 119938 from the National Science Centre, Poland.

REFERENCES

- Aigner, T., 1985. *Storm Depositional Systems: Dynamic Stratigraphy in Modern and Ancient Shallow-Marine Sequence. Lecture Notes in Earth Sciences Series*, 3. Springer-Verlag, Berlin-Heidelberg-New York-Tokyo, 174 pp.
- Aigner, T. & Bachmann, G. H., 1992. Sequence stratigraphic framework of the German Triassic. *Sedimentary Geology*, 80: 1–21.
- Alexandrowicz, S. W., 1971. Relationship between Triassic Formations and the Palaeozoic basement between Klucze and Bydlin. *Rudy i Metale Nieżelazne*, 16: 468–470. [In Polish, with English summary.]
- Alsharhan, A. S. & Kendall, C. G. St. C., 2003. Holocene coastal carbonates and evaporites of the southern Arabian Gulf and

- their ancient analogue. *Earth-Science Reviews*, 61: 191–243.
- Andres, M. S. & Reid, R. P., 2006. Growth morphologies of modern marine stromatolites: a case study from Highborne Cay, Bahamas. *Sedimentary Geology*, 185: 319–328.
- Assmann, P., 1913. Beitrag zur Kenntnis der Stratigraphie des oberschlesischen Muschelkalks. *Jahrbuch der Königlich Preussischen Geologischen Landesanstalt*, 34: 268–340.
- Assmann, P., 1926. Die Tiefbohrung "Oppeln". *Jahrbuch der Preussischen Geologischen Landesanstalt*, 46: 373–395.
- Assmann, P., 1929. Die Tiefbohrung Leschna und ihre Bedeutung für die Stratigraphie der oberschlesischen Trias. *Jahrbuch der Preussischen Geologischen Landesanstalt*, 44: 153–185.
- Assmann, P., 1944. Die Stratigraphie der oberschlesischen Trias. Teil II – Der Muschelkalk. *Abhandlungen des Reichsamts für Bodenforschung*, 208: 1–124.
- Bathurst, R. G., 1966. Boring algae, micritic envelopes and lithification of molluscan biosparites. *Geological Journal*, 5: 15–32.
- Bathurst, R. G. C., 1975. *Carbonate Sediments and their Diagenesis*. Elsevier, Amsterdam, 658 pp.
- Berger, S. & Kaever, M. J., 1992. *Dasycladales. An Illustrated Monograph of a Fascinating Algal Order*. Thieme, Stuttgart–New York, 247 pp.
- Bertling, M., 1999. Taphonomy of trace fossils at omission surfaces (Middle Triassic, East Germany). *Palaeogeography, Palaeoclimatology, Palaeoecology*, 149: 27–40.
- Bilan, W. & Golonka, J., 1972. Poziom onkolitowy w środkowym wapieniu muszlowym wschodniego obrzeżenia Zagłębia Górnospłaskiego. *Kwartalnik Geologiczny*, 16: 491–493. [In Polish.]
- Bodzionek, A., 1985. Palaeoecology and sedimentary environment of the Terebratula Beds (Lower Muschelkalk) from Upper Silesia (South Poland). *Rocznik Polskiego Towarzystwa Geologicznego*, 55: 127–140.
- Bodzionek, A., 1989. Biostratinomy and sedimentary environment of the echinoderm-sponge biostromes in the Karchowice beds, Middle Triassic of Upper Silesia. *Rocznik Polskiego Towarzystwa Geologicznego*, 59: 331–350.
- Bodzionek, A., 1993. Sponges from the Epicontinental Triassic of Europe. In: Haggdorn, H. & Seilacher, A. (eds), *Muschelkalk. Schöntaler Symposium 1991*. Goldschnecke, Stuttgart, pp. 235–244.
- Bodzionek, A., 1997a. Sponge/crinoidal/coral bioherms from the Muschelkalk of Upper Silesia (Middle Triassic, Poland). *Boletín de la Real Sociedad Española de Historia Natural (Sección Geológica)*, 92: 49–59.
- Bodzionek, A., 1997b. The Karchowice Formation: definition and stratigraphy. *Geologos*, 2: 165–199. [In Polish, with English summary.]
- Bodzionek, A. & Kwiatkowski, S. 1992. Sedimentation and early diagenesis of Cavernous Limestone (Roet) of Gogolin, Silesian–Kraków Region. *Annales Societatis Geologorum Poloniae*, 62: 223–254.
- Bogacz, K., Dżułyński, S., Gradziński, R. & Kostecka, A., 1968. Origin of crumpled limestone in the Middle Triassic of Poland. *Rocznik Polskiego Towarzystwa Geologicznego*, 38: 385–398.
- Brower, J. C. & Veinus, J., 1978. Middle Ordovician crinoids from Middle Ordovician crinoids from the Twin Cities area of Minnesota. *Bulletins of American Paleontology*, 74: 369–506.
- Burne, R. V. & James, N., 1986. Subtidal origin of club-shaped stromatolites, Shark Bay (abstract). In: *Proceedings of 12th International Sedimentological Congress, Canberra*, p. 49.
- Chilingar, G. V. & Terry, R. D., 1964. Relationship between porosity and chemical composition of carbonate rocks. *Petroleum Engineer*, B54: 341–342.
- Chudzikiewicz, L., 1975. Intraformational conglomerates in the Gogolin Beds (Middle Triassic, Southern Poland). *Rocznik Polskiego Towarzystwa Geologicznego*, 45: 3–20.
- Chudzikiewicz, L., 1982. Sedimentation of the Gogolin Beds in the eastern margin of the Upper Silesian Coal Basin (Southern Poland). *Studia Geologica Polonica*, 75: 7–83. [In Polish, with English summary.]
- Clifton, H. E., 1971. Orientation of empty pelecypod shells and shell fragments in quiet water. *Journal of Sedimentary Petrology*, 41: 671–682.
- Davies, P., Bubela, B. & Ferguson, J., 1978. The formation of ooids. *Sedimentology*, 25: 703–730.
- Davies, P. J. & Martin, K., 1976. Radial aragonite ooids, Lizard Island, Great Barrier Reef. *Geology*, 4: 120–122.
- Deelman, J. C., 1978. Experimental ooids and grapestones: carbonate aggregates and their origin. *Journal of Sedimentary Petrology*, 49: 1269–1278.
- Demicco, R. V., 1983. Wavy and lenticular-bedded carbonate ribbon rocks of the Upper Cambrian Conococheague Limestone, central Appalachians. *Journal of Sedimentary Petrology*, 53: 1121–1132.
- Duke, W. L., 1985. Hummocky cross-stratification, tropical hurricanes, and intense winter storms. *Sedimentology*, 32: 167–194.
- Dunham, R. J., 1962. Classification of carbonate rocks according to depositional texture. *American Association of Petroleum Geologists Memoir*, 1: 108–121.
- Dżułyński, S. & Kubicz, A., 1975. Storm accumulations of brachiopod shells and sedimentary environment of the Terebratula Beds in the Muschelkalk of Upper Silesia (Southern Poland). *Rocznik Polskiego Towarzystwa Geologicznego*, 45: 157–169.
- Eck, H., 1865. *Über die Formationen des bunten Sandsteins und des Muschelkalks in Oberschlesien und ihre Versteinerungen*. Friedländer und Sohn, Berlin, 148 pp.
- Einsele, G., 2000. *Sedimentary Basins: Evolution, Facies, and Sediment Budget*. Springer-Verlag, Berlin-Heidelberg-New York, 792 pp.
- Embry, A. F. & Klovan, J. E., 1971. A late Devonian reef tract on northeastern Banks Island NWT. *Bulletin of Canadian Petroleum Geology*, 19: 730–781.
- Enos, P. & Perkins, R. D., 1977. Holocene sediment accumulations on the south Florida shelf margin. In: Enos, P. & Perkins, R. D. (eds), *Quaternary sedimentation in South Florida*. Geological Society of America Memoir, 147: 1–130.
- Esteban, M. & Klappa, C. F., 1983. Subaerial exposure environment. In: Scholle, P. A., Bebout, D. G. & Moore, C. H. (eds), *Carbonate Depositional Environments*. American Association of Petroleum Geologists Memoir, 33: 1–54.
- Evamy, B. D., 1967. Dedolomitization and the development of rhombohedral pores in limestones. *Journal of Sedimentary Petrology*, 37: 1204–1215.
- Fabricius, F. H., 1977. Origin of marine ooids and grapestones. *Contributions to Sedimentology*, 7: 113 pp.
- Ferguson, J., Bubela, B. & Davies, P. J., 1978. Synthesis and possible mechanisms of formation of radial carbonate ooids. *Chemical Geology*, 22: 285–308.
- Fischer, A. G., 1964. The Lofer cyclothsems of the Alpine Triassic. *Kansas Geological Survey Bulletin*, 169: 107–149.
- Flügel, E., 2010. *Microfacies of Carbonate Rocks: Analysis, Interpretation and Application*. Springer, Berlin, 1007 pp.
- Ginsburg, R. N., 1960. Ancient analogues of Recent stromatolites. In: *International Geological Congress, Proceedings, 21st Session, Copenhagen, Section 22*. Copenhagen, pp. 26–35.
- Götz, A. E., 2004. Zyklen und Sequenzen im Unteren Muschelkalk des Germanischen Beckens. *Hallesches Jahrbuch für*

- Geowissenschaften, Reihe B*, 18: 91–98.
- Götz, A. E. & Lenhardt, N., 2011. The Anisian carbonate ramp system of Central Europe (Peri-Tethys Basin): sequences and reservoir characteristics. *Acta Geologica Polonica*, 61: 59–70.
- Grey, K., 1989. Handbook for the study of stromatolites and associated structures. *Stromatolite Newsletter*, 14: 82–171.
- Hagdorn, H. & Głuchowski, E., 1993. Palaeobiogeography and stratigraphy of Muschelkalk Echinoderms (Crinoidea, Echinoidea) in Upper Silesia. In: Hagdorn, H. & Seilacher, A. (eds), *Muschelkalk. Schöntaler Symposium 1991*. Stuttgart, Korb, pp. 165–176.
- Hardie, L. A., 1977. Introduction. In: Hardie, L. A. (ed.), *Sedimentation on the Modern Carbonate Tidal Flats of Northwest Andros Island, Bahamas. John Hopkins Studies in Geology*, 22. Johns Hopkins University Press, Baltimore, pp. 1–3.
- Harms, J. C., Spearing, D. R., Southard, J. B. & Walker, R. G., 1975. Depositional environments as interpreted from primary sedimentary structures and stratification sequences. *Society of Economic Paleontologists and Mineralogists, Short Course Notes*, 2. Dallas, 161 pp.
- Illing, L. S., 1954. Bahaman calcareous sands. *American Association of Petroleum Geologists Bulletin*, 38: 1–95.
- Jahnert, R. J. & Collins, L. B., 2011. Significance of subtidal microbial deposits in Shark Bay, Australia. *Marine Geology*, 286: 106–111.
- Kaim, A. & Niedzwiedzki, R., 1999. Middle Triassic ammonoids from Silesia, Poland. *Acta Palaeontologica Polonica*, 44: 93–115.
- Kendall, C. G. St. C. & Skipwith, P. A. d'E., 1968. Recent algal mats of a Persian Gulf lagoon. *Journal of Sedimentary Petrology*, 38: 1040–1058.
- Kendall, C. G. St. C. & Skipwith, P. A. d'E., 1969. Geomorphology of a Recent shallow-water carbonate province: Khor al Bazam, Trucial Coast, southwest Persian Gulf. *Geological Society of America Bulletin*, 80: 865–891.
- Kinsman, D. J. J. & Park, R. K., 1976. Algal belt and coastal sabkha evolution, Trucial Coast, Persian Gulf. In: Walter, E. M. (ed.), *Stromatolites*. Elsevier, Amsterdam, pp. 421–433.
- Knaust, D. 1997. Die Karbonatrampe am SE-Rand des Persischen Golfes (Vereinigte Arabische Emirate) – rezentes Analogon für den Unteren Muschelkalk der Germanischen Trias? *Greifswalder Geowissenschaftliche Beiträge*, 5: 101–123.
- Knaust, D., 2013. The ichnogenus *Rhizocorallium*: Classification, trace makers, palaeoenvironments and evolution. *Earth-Science Reviews*, 126: 1–47.
- Kornicker, L. S. & Purdy, E. G., 1957. A Bahamian faecal pellet sediment. *Journal of Sedimentary Petrology*, 27: 126–128.
- Kotański, Z., 1994. Middle Triassic Dasycladacea of the Upper Silesian-Cracov Region and their stratigraphical and palaeoecological significance. In: Kotański, Z. (ed.), *Proceedings of Third International Meeting of Peri-Tethyan Epicratonic Basins, Kraków*. Państwowy Instytut Geologiczny, Warszawa, pp. 59–66.
- Kotański, Z., 2013. *Anisian Dasycladales from Upper Silesia and adjacent regions*. Carnets de Géologie, Book 2, Paleopolis, 205 pp.
- Kowal-Linka, M., 2008. Formalization of the lithostratigraphy of the Gogolin Formation (Middle Triassic) in the Opole (Silesia) region. *Geologos*, 14:125–161. [In Polish, English abstract.]
- Kowal-Linka, M., 2009. The new lithostratigraphic units in rank of bed in the Gogolin Formation (Middle Triassic) in the Opole Silesia region. *Geologia*, 35: 153–174. [In Polish, with English abstract and summary.]
- Kreisa, R. D., 1981. Storm-generated sedimentary structures in subtidal marine facies with examples from the Middle and Upper Ordovician of southwestern Virginia. *Journal of Sedimentary Petrology*, 51: 823–848.
- Kubicz, A., 1971. Charakterystyka ławic konglomeratowych warstw wilkowickich na Śląsku Opolskim. *Sprawozdania z Posiedzeń Komisji Naukowej Polskiej Akademii Nauk*, 14: 633–635. [In Polish.]
- Land, L. S., Behrens, E. W. & Frishman, S. A., 1979. The ooids of Baffin Bay, Texas. *Journal of Sedimentary Petrology*, 49: 1269–1278.
- Land, L. S. & Moore, C. H., 1980. Lithification, micritization and syndepositional diagenesis of biolithites on the Jamaican island slope. *Journal of Sedimentary Petrology*, 50: 357–370.
- Liddell, W. D., 1975. Recent crinoid biostratinomy. *Geological Society of America Abstracts with Programs*, 7: 1169.
- Loreau, J. P. & Purser, B. H., 1973. Distribution and ultrastructure of Holocene ooids in the Persian Gulf. In: Purser, B. H. (ed.), *The Persian Gulf*. Springer-Verlag, Berlin, pp. 279–328.
- Martin, K. D., 2004. A re-evaluation of the relationship between trace fossils and dysoxia. In: McIlroy, D. (ed.), *The Application of Ichnology to Palaeoenvironmental and Stratigraphic Analysis*. Geological Society of London, Special Publications, 228, pp. 141–156.
- Matysik, M., 2010. Reefal environments and sedimentary processes of the Anisian Karchowice Beds in Upper Silesia, southern Poland. *Annales Societatis Geologorum Poloniae*, 80: 123–145.
- Matysik, M., 2012. *Origin of High-frequency Depositional Cycles in Muschelkalk of Southern Poland*. Unpublished Ph.D. Thesis, Jagiellonian University, 305 pp. [In Polish, with English abstract.]
- Matysik, M., 2014. Sedimentology of the “ore-bearing dolomite” of the Kraków-Silesia region (Middle Triassic, southern Poland). *Annales Societatis Geologorum Poloniae*, 84: 81–112.
- Meyer, D. L., 1971. Post mortem disarticulation of Recent crinoids and ophiuroids under natural conditions. *Geological Society of America Abstracts with Programs*, 3: 45–46.
- Morycowa, E., 1988. Middle Triassic Scleractinia from the Cracow-Silesia region, Poland. *Acta Palaeontologica Polonica*, 33: 91–121.
- Morycowa, E. & Szulc, J., 2010. Environmental controls on growth of early scleractinian patch reefs (Middle Triassic; Silesia; Poland). *Palaeoworld*, 19: 382–388.
- Mullins, H. T., Neumann, A. C., Wilber, R. J. & Boardman, M. R., 1980. Nodular carbonate sediment on Bahamian slopes: possible precursors to nodular limestones. *Journal of Sedimentary Research*, 50: 117–131.
- Myrow, P. M., 1995. *Thalassinoides* and the enigma of Early Palaeozoic open-framework burrow systems. *Palaios*, 10: 58–74.
- Myrow, P. M. & Southard, J. B., 1996. Tempestite deposition. *Journal of Sedimentary Research*, 66: 875–887.
- Myszkowska, J., 1992. Lithofacies and sedimentation of Diplopoda Dolomite (Middle Muschelkalk) in the east part of the Cracovian-Silesian region. *Annales Societatis Geologorum Poloniae*, 62: 19–62. [In Polish, with English summary.]
- Narkiewicz, K. & Szulc, J., 2004. Controls on migration of conodont fauna in peripheral oceanic areas. An example from the Middle Triassic of the Northern Peri-Tethys. *Geobios*, 37: 425–436.
- Nawrocki, J. & Szulc, J., 2000. The Middle Triassic magneto-stratigraphy from the Peri-Tethys Basin in Poland. *Earth and Planetary Science Letters*, 182: 77–92.
- Newell, N. D., Purdy, E. G. & Imbrie, J., 1960. Bahamian oolite sand. *Journal of Geology*, 68: 481–497.
- Niedzwiedzki, R., 2000. Lithostratigraphy of the Górażdże and the Dziewkowice Formations in Opole Silesia. *Prace Geolo-*

- gicznno-Mineralogiczne Uniwersytetu Wrocławskiego*, 71: 1–72. [In Polish, with English summary.]
- Osleger, D. A. & Read, J. F., 1991. Relation of eustasy to stacking patterns of meter-scale carbonate cycles, Late Cambrian, U.S.A. *Journal of Sedimentary Petrology*, 61: 1225–1252.
- Pawlowska, J., 1979. Criteria of lithostratigraphic subdivision of Triassic dolomite lithofacies of the Cracow-Silesian area. *Kwartalnik Geologiczny*, 23: 601–615. [In Polish, with English summary.]
- Pawlowska, J., 1982. Influence of a sedimentary environment and diagenetic processes on a formation of ore-bearing dolomites and lead-zinc deposits in the Silesian-Cracow region. *Biuletyn Instytutu Geologicznego*, 342: 5–34. [In Polish, with English summary.]
- Pawlowska, J., 1985. Facies development of the Triassic marine formation in the Silesia–Cracow area. *Biuletyn Instytutu Geologicznego*, 349: 41–88. [In Polish, with English summary.]
- Pawlowska, J. & Szwarzyński, M., 1979. Sedimentary and diagenetic processes in the Zn-Pb host rocks of Trzebionka. *Prace Instytutu Geologicznego*, 95: 13–58.
- Pisera, A. & Bodzioch, A., 1991. Middle Triassic lyssacinosan sponges from Upper Silesia (southern Poland), and the history of hexactinosan and lynchiscosan sponges. *Acta Geologica Polonica*, 41: 193–207.
- Pratt, B. R. & James, N. P., 1986. The St George Group (Lower Ordovician) of western Newfoundland: tidal flat island model for carbonate sedimentation in shallow epeiric seas. *Sedimentology*, 33: 313–343.
- Purdy, E. G., 1963. Recent calcium carbonate facies of the Great Bahama Bank. 2. Sedimentary facies. *Journal of Geology*, 71: 472–497.
- Purser, B. H. & Evans, G., 1973. Regional sedimentation along the Trucial Coast, SE Persian Gulf. In: Purser, B. H. (ed.), *The Persian Gulf, Holocene Carbonate Sedimentation in a Shallow Epeiric Continental Sea*. Springer, New York, pp. 211–232.
- Rankey, E. C. & Berkeley, A., 2012. Holocene Carbonate Tidal Flats. In: Davis, R. A., Jr. & Dalrymple, R. W. (eds), *Principles of Tidal Sedimentology*. Springer Science + Business Media B. V., Dordrecht-Heidelberg-London-New York, pp. 507–535.
- Reading, H. G., 1978. *Sedimentary Environments and Facies*. Blackwell, Oxford, 557 pp.
- Reid, P. R., James, N. P., Macintyre, I. G., Dupraz, C. P. & Burne, R. V., 2003. Shark Bay stromatolites: microfabrics and reinterpretation of origins. *Facies*, 49: 45–53.
- Reineck, E. & Singh, I. B., 1980. *Depositional Sedimentary Environments*. Springer-Verlag, Berlin, 549 pp.
- Rhoads, D. C., 1975. The paleoecological and environmental significance of trace fossils. In: Frey, R. W. (ed.), *The Study of Trace Fossils*. Springer-Verlag, New York, pp. 147–160.
- Savrda, C. E., 2007. Trace fossils and marine benthic oxygenation. In: Miller, W., III (ed.), *Trace Fossils. Concepts, Problems, Prospects*. Elsevier, Amsterdam, pp. 92–109.
- Savrda, C. E. & Bottjer, D. J., 1986. Trace-fossil model for reconstruction of paleoxygenation in bottom waters. *Geology*, 14: 3–6.
- Sepkoski, J. J. Jr., 1982. Flat-pebble conglomerates, storm deposits and the Cambrian bottom fauna. In: Einsele, G. & Seilacher, A. (eds), *Cyclic and Event Stratification*. Springer-Verlag, Berlin, pp. 371–385.
- Shinn, E. A., 1968. Practical significance of birdseye structures in carbonate rocks. *Journal of Sedimentary Petrology*, 38: 215–223.
- Shinn, E. A., Lloyd, R. M. & Ginsburg, R. N., 1969. Anatomy of a modern carbonate tidal flat, Andros Island, Bahamas. *Journal of Sedimentary Petrology*, 39: 1202–1228.
- Siedlecki, S., 1948. Problems of stratigraphy of marine Triassic in the Cracow area. *Rocznik Polskiego Towarzystwa Geologicznego*, 18: 191–272. [In Polish, with English summary.]
- Siedlecki, S., 1952. Utwory geologiczne obszaru pomiędzy Chrzanowem a Kwaczałą. *Biuletyn Instytutu Geologicznego*, 60: 1–230. [In Polish.]
- Swinchatt, J. P., 1969. Algal boring: a possible depth indicator in carbonate rocks and sediments. *Geological Society of America Bulletin*, 80: 1391–1396.
- Szulc, J., 1989. Shallow-water carbonate basins of seismically active zones; at the example of the Muschelkalk Basin of the Upper Silesia. *Przegląd Geologiczny*, 37: 248–252. [In Polish, with English summary.]
- Szulc, J., 1991. Stop B17 – Laryszów (Poland, Upper Silesia). In: Hagdorn, H., Simon, T. & Szulc, J. (eds), *Muschelkalk. A Field Guide*. Goldschneck-Verlag, Stuttgart, p. 74.
- Szulc, J., 1993. Early Alpine tectonics and lithofacies succession in the Silesian part of the Muschelkalk Basin. A Synopsis. In: Hagdorn, H. & Seilacher, A. (eds), *Muschelkalk. Schöntaler Symposium 1991*. Goldschneck, Stuttgart, pp. 19–28.
- Szulc, J., 1997. Middle Triassic (Muschelkalk) sponge-microbial stromatolites, diplopores and *Girvanella*-oncoids from the Silesian-Cracow Upland. In: *Proceedings of 3rd Regional Symposium of International Fossil Algae Association and 3rd International Meeting of IGCP 380, Kraków*. Institute of Geological Sciences, Jagiellonian University, Kraków, pp. 10–15.
- Szulc, J., 2000. Middle Triassic evolution of the Northern PeriTethys area as influenced by early opening of the Tethys Ocean. *Annales Societatis Geologorum Poloniae*, 70: 1–48.
- Sliwiński, S., 1961. "Olkusz" stratum. *Rudy i Metale Nieżelazne*, 12: 526–529. [In Polish, with English summary.]
- Taylor, J. C. & Illing, V. L., 1969. Holocene intertidal calcium carbonate cementation of Qatar, Persian Gulf. *Sedimentology*, 12: 69–108.
- Walker, R. G., 1982. Hummocky and swaley cross stratification. In: Walker, R. G. (ed.) *Clastic Units of the Area between Field, B. C. and Drumheller, Alberta. 11th International Congress on Sedimentology (Hamilton, Canada), Guidebook to Excursion 21A*. International Association of Sedimentologists, McMaster University, Hamilton, pp. 22–30.
- Wanless, H. R., Burton, E. A. & Dravis, J., 1981. Hydrodynamics of carbonate fecal pellets. *Journal of Sedimentary Petrology*, 51: 27–36.
- Warren, J. K., 1991. Sulfate dominated sea-marginal and platform evaporative settings: Sabkhas and salinas, mudflats and salters. In: Melvin, J. L. (ed.), *Evaporites, Petroleum and Mineral Resources*. Elsevier, Amsterdam-Oxford-New York-Tokyo, pp. 69–187.
- Warren, J. K., 2006. *Evaporites: Sediments, Resources and Hydrocarbons*. Springer-Verlag, Berlin-Heidelberg, 1035 pp.
- Winland, H. D. & Matthews, R. K., 1974. Origin and Significance of Gapestone, Bahama Islands. *Journal of Sedimentary Petrology*, 44: 921–927.
- Wood, W. W., Sanford, W. E. & Al Habshi, A. R., 2002. Source of solutes to the coastal sabkha of Abu Dhabi. *Geological Society of America Bulletin*, 114: 259–268.
- Worobiec, E. & Szulc, J., 2012. Sesja terenowa A: Góra Świętej Anny – kamieniołom w Górażdżach – kamieniołom w Tarnowie Opolskim – kamieniołom w Kamieniu Śląskim. In: Szulc, J. & Wróblewski, W. (ed.), *Materiały 46. Sympozjum Speleologiczne, Góra Św. Anny*. Sekcja Speleologiczna Polskiego Towarzystwa Przyrodników im. Kopernika, 13–

22. [In Polish.]
- Wray, J. L., 1977. *Calcareous Algae*. Elsevier, Amsterdam, 185 pp.
- Wright, V. P., 1992. A revised classification of limestones. *Sedimentary Geology*, 76: 177–186.
- Wright, V. P. & Tucker, M. E., 1991. Calcretes: an introduction. In: Wright, V. P. & Tucker, M. E. (eds), *Calcretes*. International Association of Sedimentologists, Reprint Series 2, Blackwell Scientific Publications, Oxford, pp. 1–22.
- Wyczółkowski, J., 1971. Effect of the surface morphology of the Palaeozoic substratum on the sedimentation of the Bunter Sandstone and Lower Muschelkalk. *Biuletyn Instytutu Geologicznego*, 243: 121–150. [In Polish, with English summary.]
- Wyczółkowski, J., 1982. The transgression of the Triassic Sea at the north-eastern margin of the Upper Silesian Coal Basin. *Biuletyn Instytutu Geologicznego*, 342: 39–72. [In Polish, with English summary.]
- Zawidzka, K., 1975. Conodont stratigraphy and sedimentary environment of the Muschelkalk in Upper Silesia. *Acta Geologica Polonica*, 25: 217–256.
- Ziegler, P. A., 1990. *Geological atlas of Western and Central Europe*. Shell International Petroleum Co. and the Geological Society of London, 239 pp.